Reprinted from Mechanics Today, Vol. 2,
ed. by S. Nemat-Nasser, Pergamon Press,
Chapt. I, pp. 1-93, 1975

Theory of Creep and Shrinkage in Concrete Structures: A Précis of Recent Developments

Zdeněk P. Bažant
Northwestern University, Evanston, Illinois

Contents

Summary

Although the phenomenon of creep in concrete has been known for nearly 70 years, its study has only recently gained importance because of new types of structures of higher creep sensitivity, such as nuclear reactor vessels and containers or undersea shells. This article summarizes some of the basic knowledge in this field, with emphasis on recent developments, and including some new results.

Basic experimental facts relating to creep and shrinkage are summarized first. In the simplest approximation, concrete may be regarded as an aging viscoelastic material. This yields a creep law in the form of hereditary integrals with nonconvolution kernels. Various simplified expressions for the creep function, defining these kernels, have been recommended by the engineering societies to aid the designers. To make solution of large structural systems tractable, the creep law must be converted to a rate-type form, i.e. a system of first-order differential equations involving hidden stresses or strains, with time-dependent coefficients. This is particularly advantageous for numerical time integration in conjunction with the finite element method. Maxwell and Kelvin chains with time-dependent coefficients are the two basic models.

A more realistic model requires inclusion of temperature and humidity effects. Temperature rise accelerates creep, as well as the hydration reactions that are responsible for the change of material properties (aging). These effects are formulated in terms of activation energies. A crucial role in creep, as well as shrinkage, is played by the large amount of water that is contained in concrete in the form of adsorption layers that are several molecules thick and are confined between solid cement gel particles and layers. Thermodynamics of the diffusion that takes place along such layers in response to stress and temperature changes and changes in water content of the macro-pores is discussed. It is shown that a nonlinear coupling between the flux of water molecules and the flux of solid molecules explains the basic nonlinear effects in low-stress creep, such as the drying creep effect. Further nonlinear behavior, due mainly to gradual microcracking, appears in high-stress creep. The solution of the creep and shrinkage of a concrete body depends on the solution of the macroscopic water diffusion through the body (drying or wetting), but the reverse coupling of these problems is negligible. The analysis of drying is complicated by a sharply nonlinear dependence of diffusivity upon the pore humidity, as well as upon the temperature and the degree of hydration. A mathematical formulation of these phenomena is given.

In analyzing structural problems according to a viscoelasticity theory, basic roles are played by the elastic-viscoelastic analogy and McHenry's analogy, the proofs of which are given. Various methods of numerical step-by-step methods of time integration for both linear and nonlinear stress–strain laws are also described. They may all be formulated as a sequence of elasticity problems with inelastic strains, and the latter may be replaced by equivalent applied loads. To ensure numerical stability, special new algorithms are required for the rate-type creep laws based on the Maxwell and Kelvin chains. For a number of ordinary design problems, various simplified linear creep laws that allow simple solution may be used. They are discussed in detail and one of them, serving as basis for the recently developed age-adjusted effective modulus method, is shown to yield accurate results.

The theoretical results are documented by experimental data.

1 INTRODUCTION

If concrete is subjected to sustained loads, it continues to deform further with time. This phenomenon, discovered in 1907 by Hatt[1], is now commonly referred to as creep. Concrete also exhibits stress-independent deformations which, in addition to thermal dilatation, include shrinkage (or swelling), i.e. a volumetric deformation due to changes in water content and long-time chemical processes. To distinguish these two types of time-dependent deformations, creep is usually understood as the difference in deformation between a loaded specimen and an equally old identical but unloaded companion specimen that has suffered precisely the same history of environmental conditions. The instantaneous elastic deformation produced upon stress application is often also separated from the creep deformation.

Interest in creep and shrinkage has been rising as concrete structures more susceptible to its effects have been appearing, and structural damages or failures were being experienced. The first extensive research, which came in the 1930s, was necessitated by the introduction of long-span concrete arches and large dams. Improved understanding of the phenomenon enabled the advent of prestressed concrete. Long-span prestressed bridges, shells, and tall concrete buildings provided further stimuli for research. At present, the novel uses of concrete in prestressed concrete pressure vessels for nuclear reactors réquire drastic improvement in the

present knowledge. However, in spite of the literature explosion afflicting this field, many important questions still remain unresolved, especially with regard to the constitutive equation. This is undoubtedly due to the extraordinary complexity of the material. Aside from a number of nonlinear effects, the material properties change as a result of internal chemical reactions, and the deformation problem is coupled with moisture diffusion through the material (as well as heat conduction). Consequently, for time-variable environmental conditions, it is impossible to devise creep tests in which a concrete specimen would be in a homogeneous state. This tremendously complicates the identification of material properties from test data. Furthermore, accumulation of experimental knowledge is hampered by the fact that, due to differences between regional sources of aggregates and cement, a broad range of different concretes is in use.

The purpose of the present work is to summarize and review the basic facts on the subject, with emphasis on recent developments, although some novel results are also presented; see Subsections 3.4, 4.3–4.5, and 5.3. As is clear from the preceding remarks, the central position must be allotted to the discussion of the constitutive equation. To avoid detachment from physical reality, a brief exposition of the basic experimentally observed properties of concrete is given in Section 2. In Section 3, a simplified, linearized formulation of the constitutive equation, uncoupled with diffusion processes in the material, is outlined. The nonlinear and coupled formulation then follows in Section 4. Methods of structural analysis are discussed in Section 5. Here the numerical methods are emphasized, because analytical solutions for realistic forms of the constitutive equations are unavailable at present, and those that exist are based on unacceptably oversimplified stress–strain relations. Practical problems in design are briefly examined in Section 6.

2 BASIC EXPERIMENTAL FACTS RELATING TO CREEP AND SHRINKAGE

The time-dependent deformations of concrete originate chiefly in the hardened portland cement paste[2]. This is a strongly hydrophylic porous material (of typical porosity 0.4–0.55) normally containing a large amount of evaporable (not chemically bound) water[2]. The material is formed by hydration of portland cement grains, which yields (aside from calcium hydroxide) a very fine gel-type structure consisting mainly of calcium

silicate hydrate ($3CaO \cdot 2SiO_2 \cdot 2.5H_2O$)[2]. Due to this and similar constituents, the material has an enormous internal surface (roughly 500 m^2/cm^3). The hydration process, which continues at normal temperatures for years and never becomes complete, causes a gradual change of the properties of cement paste and concrete, which in the field of mechanics is usually called aging. Furthermore, as the material has a low degree of chemical stability, its microstructure interacts with water and undergoes gradual changes in response to stress environmental conditions. These facts are responsible for the extremely complex thermomechanical behavior of this material.

To realize the various degrees of simplification in the subsequent discussions, it will be appropriate to begin with a concise (and by no means exhaustive) listing of the typical experimentally observed phenomena relevant for creep and shrinkage. Although some of the phenomena listed below will be considered in greater depth in the subsequent sections, for detailed information on experimental results, the reader would have to consult the references quoted, of which the book by Neville and Dilger[3] is most comprehensive.

1. Creep is smaller if the age at loading is higher[3–9]. This effect, called aging (or maturing), is important even for the many-year-old concrete [see Figs. 2, 3, 4, and 5(a)]. It is caused by gradual hydration of cement.

2. At constant water content w (sealed specimens) and temperature T, creep is linearly dependent on stress up to about 0.4 of the strength and obeys the principle of superposition, provided that large strain reversals (not stress reversals) and, especially, cyclic strains are excluded[3–5, 7, 10–16] [cf. also Figs. 1, 5(b), and 6].

3. Creep curves plotted in logarithm of the time from loading, $t - t'$, have a significant slope over many orders of magnitude of $t - t'$ (from 0.01 sec to several decades at least). This means that the retardation spectrum is very broad. There is no evidence of creep curves approaching some final asymptotic value. [See Figs. 2 to 4, and 5(a).]

4. In contrast with polymers and metals, the deviatoric creep and volumetric creep are about equally important[17; 3, p. 228]. At constant w and T, the Poisson ratio due to creep strains is about constant and equals its elastic value ($\nu \approx 0.18$)[18–20; 3, p. 236].

5. The tensile creep is about the same as the compressive creep [3, p. 220].

6. After unloading, creep is partly irreversible. Creep recovery of fully unloaded sealed specimens is less than that predicted when the

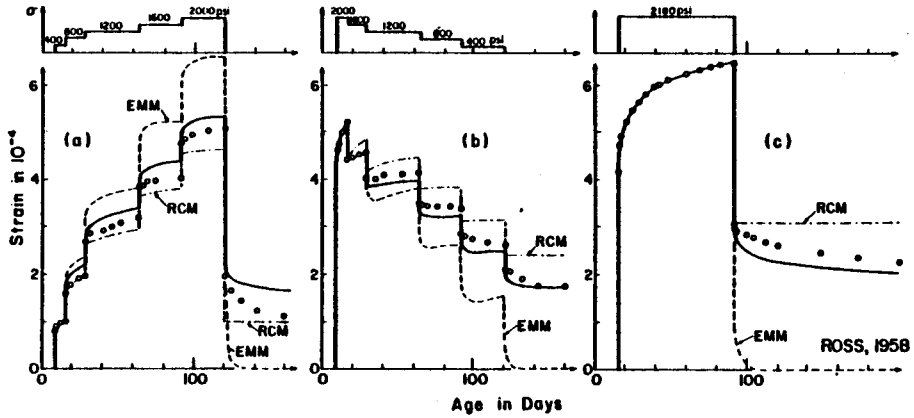

Fig. 1 Creep at variable stress compared with the prediction by principle of superposition (solid lines); cylinders $4\frac{1}{8} \times 12$ in., of 28-day strength 6720 psi; water–cement–sand–gravel ratio 0.375:1:1.6:2.8; drying at $h_a = 0.93$, 17°C; EMM and RCM are approximate predictions based on effective modulus and rate-of-creep methods from Subsection 5.5. (Adapted from Ross, A. D., "Creep of Concrete under Variable Stress," *Amer. Concrete Inst. J.* 54 (1958) 739–758, Figs. 9, 7, and 4.)

principle of superposition is applied (about $\frac{2}{3}$ of this prediction)[3, p. 95]. This is a nonlinear effect.

7. Creep recovery is almost independent of age[21–23; 3, p. 199] and is linearly dependent on the stress drop even if the previous stress has been high (0.65 of the strength[24, 14]). Creep-recovery curves tend to straight lines in the logarithmic time scale.

8. The additional creep[25, 26] and elastic strain[27] due to a stress increment after a long creep period are less than those for the same stress increment on a virgin specimen of the same age. The creep properties for such increments seem to be anisotropic.

9. At constant water content w (as well as temperature), the creep is less for smaller w[28–33]. From $h = 1.0$ to $h = 0.5$, the decrease is probably much larger than that from 0.5 to 0.0 (h = pore humidity)[28].

10. The drop of elastic modulus due to incomplete drying is only moderate[30, 31, 114] (not more than 10 percent from $h = 1.0$ to 0.1). After complete drying, a hysteresis on rewetting[34] occurs.

11. When concrete is drying simultaneously with creep, creep is accelerated (drying creep effect)[3, 4, 7, 9, 29, 34, 36, 37]. The acceleration occurs not only in compression but also in shear[3, 17] and bending[3, 34]. This effect is also manifested in the dependence of creep on the size and shape of specimen[3, 7, 38–40]. Furthermore, under simultaneous drying,

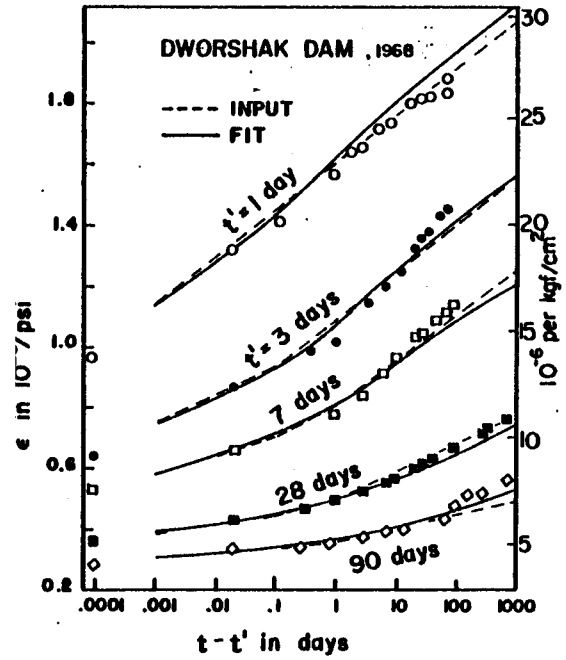

Fig. 2 Tests of D. Pirtz on creep at various ages at loading (see Ref. [26]). Cylinders 6×26 in., sealed, at 70°F; 28-day cyl. strength = 3230 psi; stress ≤ ½ strength; water–cement ratio 0.58; cement type IV; max. aggregate size 1.5 in. Solid lines show fits from Ref. [89] by Maxwell chain model with $10^6 E_{0_\mu} = 577, 233, -138, -260, 75, 62, 1120, 1520$; $10^5 E_{1_\mu} = 179, 230, 343, 469, 489, 319, -319, -378$; $10^5 E_{2_\mu} = -70, -97, -160, -242, -258, -89, 270, 626$; and $10^6 E_{3_\mu} = 81, 118, 206, 323, 349, 87, -480, -1040$; $E_{4_\mu} = 0$; for $\tau_\mu = 0.005, 0.05, \ldots, 5000, \infty (w_1 = w_2 = 0.1, w_3 = 0)$, $E_\mu = E_{0_\mu} + E_{1_\mu} t^{1/8} + E_{2_\mu} t^{1/4} + E_{3_\mu} t^{1/2} + E_{4_\mu} t^{3/4}$ in psi; ϵ is strain due to load. (Reproduced from Bažant, Z. P., and Wu, S. T., "Dirichlet Series Creep Function for Aging Concrete," *J. Engrg. Mech. Div.*, Proc. Amer. Soc. of Civil Engineers, 99 (1973) 367–387.)

the nonlinearity of creep versus stress is more pronounced[7, 28, 41], and the additional creep due to drying is irrecoverable[36].

12. Creep is considerably accelerated by any rapid change in water content, both negative and positive, and by its cycling[3, p. 156; 36].

13. In drying unsealed specimens, loading *per se* causes only a negligible loss of water, i.e. less than 3 percent of that in a companion unloaded specimen[3, p. 267; 42–44]. Also, the rise in pore humidity due to loading of a sealed specimen is negligible[44].

14. Stationary permeation of water through concrete (at constant w) does not affect creep appreciably[29].

15. When a dried specimen is rewetted (which produces swelling) and

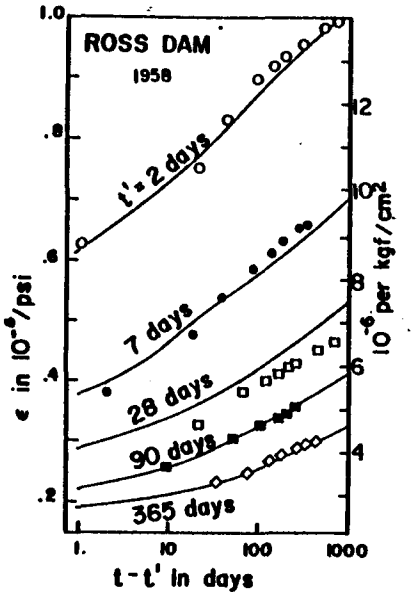

Fig. 3 Tests of creep at various ages at loading for Ross Dam (see Refs. [5, 6]). Cylinders 6 × 16 in., sealed, at 70°F; 28-day cyl. strength = 4970 psi; stress ≤ ½ strength; water–cement ratio 0.56, cement type II; max. aggregate size 1.5 in. Solid lines show fits from Ref. [89] by Maxwell chain model with $10^4 E_{0_\mu} = -115, -82, -76, -152, -143, -102, -105, -112$; $10^4 E_{1_\mu} = 196, 147, 153, 291, 273, 170, 112, 85$; $10^5 E_{2_\mu} = -729, -556, -591, 1060, -862, -332, 72, 281$; and $10^6 E_{3_\mu} = 229, 179, 190, 301, 153, -27, -105, -136$; $E_{4_\mu} = 0$; for $\tau_\mu = 0.005, 0.05, \ldots, 5000, \infty$ ($w_1 = w_2 = 0.2$, $w_3 = 0$). Formula for E_μ appears in Fig. 2 caption. ϵ is strain due to load. (Data reproduced from Bažant, Z. P., and Wu, S. T., "Dirichlet Series Creep Function for Aging Concrete," *J. Engrg. Mech. Div.*, Proc. Amer. Soc. of Civil Engineers, 99 (1973) 367–387.)

subsequently loaded in compression, the creep that follows may be substantially larger than the previous swelling[45].

16. When concrete under load is drying, the Poisson ratio due to creep strains is decreased (up to about $\nu = 0.05$)[3, p. 231; 18], and the lateral creep in a uniaxial test is unaffected by drying[3, 18].

17. As compared with the prediction of the principle superposition, pulsating loads considerably accelerate creep of concrete, even at low-stress levels (cyclic creep)[3, p. 245; 12, 36, 46–51]. When pulsation occurs after a long period under constant load, cyclic creep is negligible as compared with a virgin specimen[3, 36]. Poisson ratio decreases with the number of cycles[3, p. 248]. In cement paste at low stress, cyclic creep is not observed.

18. Aging (cement hydration) is decelerated by a drop in pore humidity[53–55] and accelerated by a rise in temperature[4].

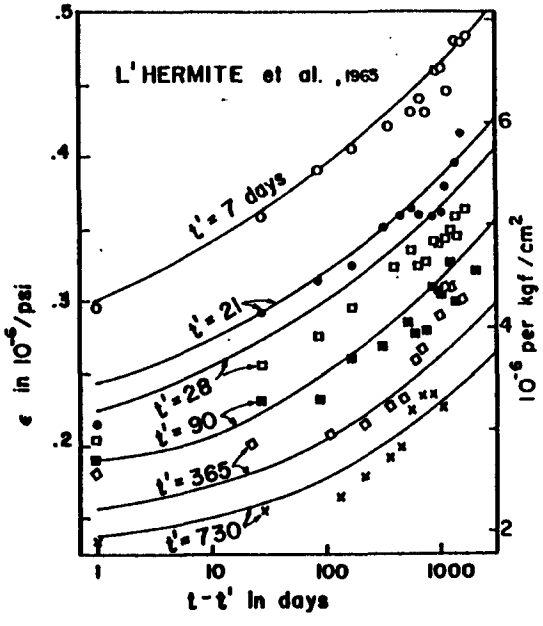

Fig. 4 L'Hermite and Mamillan's tests of creep at various ages at loading. Prisms 7 × 7 × 28 cm of 28-day strength 370 kgf/cm²; in water; at room temperature; concrete of French type 400/800; 350 kg of cement per cubic meter of concrete; stress = ½ strength; water–cement–sand–gravel ratio 0.49 : 1 : 1.75 : 3.07; Seine gravel. Solid lines show fits from Ref. [89] by Maxwell chain with $10^5 E_{0_\mu} = 562, 347, 224, 297, 331, 111, 26, 8$; $E_{1_\mu} = 117, 160, 170, 93, 59, 32, 56, 67$; $10^6 E_{2_\mu} = -421, -461, -385, -14, 378, -31, -438, -626$; $10^7 E_{4_\mu} = 266, 285, 243, -24, -441, -236, -170, 393$; for $\tau_\mu = 0.005, 0.05, \ldots, 5000, \infty$ ($w_1 = 0.1$, $w_2 = w_3 = 0$), giving E_μ in psi. Formula for E_μ appears in Fig. 2 caption. ϵ is strain due to load. (Data constructed from L'Hermite, R., Mamillan, M., and Lefèvre, C., "Nouveaux résultats de recherches sur la déformation et la rupture du béton," *Annales de l'Institut Technique du Bâtiment et des Travaux Publics* 18 (1965) 325–360; see also Int. Conf. on the Structure of Concrete, Cement and Concrete Assoc., London (1968) 423–433.) The measured J-values at $t - t' \approx 0.01$ day, for ages $t' = 7$ to 730 days shown, were 200, 165, 158, 152, 130, 119 in 10^{-6} psi^{-1}.

19. Although aging is explicable only by cement hydration, the change of creep properties is significant even in the many-years old concrete, in which the amount of cement still undergoing hydration is negligible and neither elastic modulus nor strength changes appreciably[2–9].

20. Creep rate grows with temperature[3, 44, 56–61].

21. A rapid heating as well as rapid cooling accelerates creep[3, p. 180; 61, 62].

22. First drying shrinkage from $h = 1$ to 0.5 is considerably larger than that below 0.5, while on rewetting most swelling occurs between $h = 0$ and $h = 0.5$. A substantial part of shrinkage and swelling is

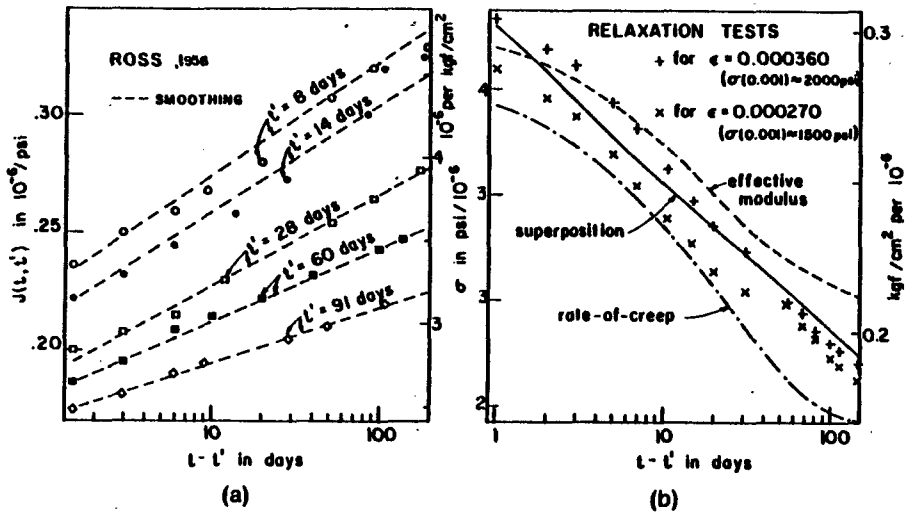

Fig. 5 Ross' tests of creep and stress relaxation (see Ref. [11]) compared with prediction [89] by principle of superposition (based on dashed smoothing of creep curves); same test series as in Fig. 1.

irreversible [63–65]. But after wetting from $h = 0$, substantial irreversibility on return to $h = 0$ occurs only if peak h has exceeded 0.5 [63–65].

23. An appreciable part of shrinkage, as well as creep acceleration due to drying, seems to be delayed with regard to the change in pore humidity [65, 129].

24. Specimens continuously immersed in water swell [4, 7, 9, 36]. Sealed specimens show autogeneous shrinkage (usually small) and also gradual self-desiccation to about $h = 0.98$ (cf. Ref. [67]) if the water–cement ratio is low.

25. Shrinkage is not affected by deviatoric stress [36].

26. Thermal dilatation strongly depends on water content, the peak occurring at about $h = 0.7$ (cf. Refs. [36, 68]).

27. Instantaneous thermal dilatation is followed by a delayed thermal dilatation. The latter is negative (i.e. a recovery) at $h = 1$ (cf. Ref. [68]).

28. Under stresses exceeding about 0.4 of the strength, creep becomes progressively nonlinear with stress [3, 7, 14, 15, 24, 28, 29, 37, 41]. The additional creep due to nonlinearity is largely irreversible and is caused mainly by gradual microcracking. The apparent Poisson ratio in the uniaxial test rises with the stress and exceeds 0.5 prior to failure, which indicates incremental anisotropy [4, 36, 50]. Failure under a long-time load exceeding about 0.8 strength occurs at a lower load than in short-time

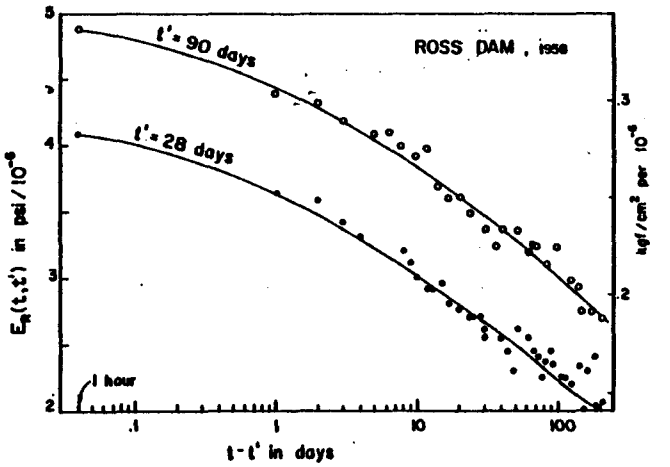

Fig. 6 Stress relaxation tests for Ross Dam (Refs. [5, 6]). The solid line fit (from Ref. [89]) is based on the same parameters as in Fig. 3; test specimens are also the same. (Reproduced from Bažant, Z. P., and Wu, S. T., "Dirichlet Series Creep Function for Aging Concrete," *J. Engrg. Mech. Div.*, Proc. Amer. Soc. of Civil Engineers, 99 (1973) 367–387.)

tests [69, 70]. This is also true of high-pulsating loads [46, 47]. Below 0.8, long-time load strengthens concrete [69, 70], and so does a low-pulsating load. Cracks heal when compressed [71].

29. Strength of concrete is higher after drying (cf. Refs. [54, 114]).

30. Water content w as a function of pore humidity h at constant T (sorption–desorption isotherm) exhibits considerable hysteresis and irreversibility [63–65]. After a wetting–drying cycle reaching above $h = 0.5$, the internal surface area of pores in cement paste is considerably decreased (and the volume of solids correspondingly increased) [35, 63, 64].

31. Diffusivity of water in concrete drops about 20 times when passing from $h = 0.85$ to $h = 0.65$ [67] (cf. Fig. 16). In saturated concrete under hydraulic overpressure, diffusivity is about 1000 times higher than that at $h = 0.999$ [67].

32. A 10 percent difference in pore humidity produces about the same flux of water as the hydraulic head of 1400 m [67].

33. Diffusivity rises with temperature and decreases with aging [67].

34. A number of further complex phenomena are observed in creep of frozen concrete, at high temperatures (over 100°C) and at very low temperatures [3, 4, 72].

3 CONCRETE APPROXIMATED AS AN AGING VISCOELASTIC MATERIAL

3.1 Integral-Type Creep Law

In the current design practice, the dependence of strains and stresses upon the histories of water content and temperature, apparent from effects 11, 12, 16, and 26 in Section 2, is disregarded. This is correct only for mass concrete at constant temperature, but is adopted in practical design, as a crude simplification, for the average behavior of the cross sections of massive beams and plates, in which the water content and temperature cannot vary substantially or rapidly. Strain (or stress) is thus considered as a functional of the previous stress (or strain) history alone. As long as no abrupt changes in the microstructure occur, this functional is logically assumed to be continuous and admitting Volterra–Fréchet series expansion[73]. Retaining only its linear term, a linear approximation results. It must be sufficiently good for sufficiently small stresses and sufficiently short-time histories. Experimentally, the linearity is found to be applicable over a broad range (see Figs. 1, 5, and 6, for example, and item 2, Section 2) and is used as the basic assumption in the current design practice. However, it should be kept in mind that, of all effects listed in Section 2, only items 1–5 can then be given proper consideration.

The linearity implies validity of the principle of superposition, due to Volterra[73]. (For nonaging materials, it was enunciated already by Boltzmann[74].) Its applicability to aging concrete was discovered by McHenry[75] and Maslov[76]. This principle states that the strain (or stress) response due to a sum of two stress (or strain) histories is the sum of the individual responses. Thus, summing the strain histories due to all small-stress increments before time t, one may write the creep law for uniaxial stress in the form

$$\epsilon(t)-\epsilon^0(t)=\int_0^t J(t,t')\,d\sigma(t'), \tag{3.1}$$

where t = time measured from casting of concrete; σ = linearized stress, ϵ = linearized strain; ϵ^0 = given stress-independent inelastic strain comprising shrinkage ϵ_{sh} and thermal dilatation; kernel $J(t,t')$ = creep function (or creep compliance) = strain at time t caused by a constant unit stress acting from time t' to time t, i.e. by Heaviside step function $\sigma(t)=H(t-t')$. Note that $1/J(t,t)=E(t)$ = Young's modulus. The hereditary integral (3.1) is written as Stieltjes integral in order to admit

discontinuous stress histories $\sigma(t)$. If $\sigma(t)$ is continuous, substitution $d\sigma(t')=[d\sigma(t')/dt']\,dt'$ yields the ordinary (Riemann) integral. All test data agree with the inequalities $\partial J(t,t')/\partial t\geqslant 0$, $\partial^2 J(t,t')/\partial t^2\leqslant 0$, $\partial J(t,t')/\partial t'\leqslant 0$, $\partial^2 J(t,t')/\partial t'^2\geqslant 0$ for any t and t'.

Under multiaxial stress, the linear behavior of concrete may be assumed as isotropic. The strain is always small. As is well known, the stress–strain relations may then be most conveniently written as separate equations for the volumetric components $\sigma^V=\sigma_{kk}/3$, $\epsilon^V=\epsilon_{kk}/3$ and the deviatoric components $\sigma_{ij}^D=\sigma_{ij}-\sigma^V\delta_{ij}$, $\epsilon_{ij}^D=\epsilon_{ij}-\epsilon^V\delta_{ij}$ of stress and strain tensors σ_{ij}, ϵ_{ij} (in Cartesian coordinates x_i, $i=1,2,3$; δ_{ij} = Kronecker delta). Thus, in analogy with Eq. (3.1),

$$\begin{aligned}3[\epsilon^V(t)-\epsilon^0(t)]&=\int_0^t J^V(t,t')\,d\sigma^V(t')\\ 2\epsilon_{ij}^D(t)&=\int_0^t J^D(t,t')\,d\sigma_{ij}^D(t'),\end{aligned} \tag{3.2}$$

where $J^V(t,t')$, $J^D(t,t')$ are the volumetric and deviatoric creep functions, defined as $\epsilon^V(t)$ and, for example, $\epsilon_{12}^D(t)$, caused by unit stresses σ^V and σ_{12}^D acting since time t'. Note that $1/J^V(t,t)=K(t)$ = bulk modulus, $1/J^D(t,t)=G(t)$ = shear modulus. The multiaxial behavior may also be characterized by the creep Poisson's ratio, which is defined as $\nu(t,t')=-\epsilon_{22}/\epsilon_{11}$ for stress $\sigma_{11}=1$ acting since time t'. Due to isotropy,

$$\begin{aligned}J(t,t')&=\tfrac{1}{9}J^V(t,t')+\tfrac{1}{3}J^D(t,t'),\\ \nu(t,t')J(t,t')&=\tfrac{1}{6}J^D(t,t')-\tfrac{1}{9}J^V(t,t'),\end{aligned} \tag{3.3}$$

which follow, e.g., from the fact that for the case of uniaxial stress $\sigma_{11}=1$ acting since time t', Eqs. (3.1) and (3.2) give $J(t,t')=\epsilon_{11}=\sigma^V J^V(t,t')/3+\sigma_{11}^D J^D(t,t')/2$ and $-\nu(t,t')J(t,t')=\epsilon_{22}=\sigma^V J^V(t,t')/3+\sigma_{22}^D J^D(t,t')/2$, where $\sigma^V=\frac{1}{3}$, $\sigma_{11}^D=\frac{2}{3}$, and $\sigma_{22}^D=-\frac{1}{3}$.

In sealed concrete specimens, ν is about constant, $\nu\approx 0.18$ (cf. item 4, Section 2). Solving Eqs. (3.3), one obtains

$$\begin{aligned}J^V(t,t')&=6(\tfrac{1}{2}-\nu)J(t,t'),\\ J^D(t,t')&=2(1+\nu)J(t,t'),\end{aligned} \tag{3.4}$$

and so creep is fully characterized by $J(t,t')$. In view of this fact and the analogy of Eq. (3.2) with Eq. (3.1), further discussions of the stress–strain relations will be restricted to the uniaxial case whenever the generalization to multiaxial stress is self-evident.

If strain history $\epsilon(t)$ is prescribed, Eqs. (3.1) and (3.2) represent

nonhomogeneous Volterra's integral equations for the stress history. The general solution (resolvent) of Eq. (3.1) may be written as

$$\sigma(t) = \int_0^t E_R(t, t')[d\epsilon(t') - d\epsilon^0(t')], \tag{3.5}$$

in which kernel $E_R(t, t')$, called relaxation function (or relaxation modulus), represents stress at time t caused by a unit constant strain introduced at time $t' \leq t$, i.e. by step function $\epsilon = H(t - t')$. Note that $E_R(t, t) = E(t)$. Integral (3.5) follows also directly from the principle of superposition as a sum of the stress responses due to all previous strain increments. When $\sigma(t)$ is specified, Eq. (3.5) represents a Volterra's integral equation for $\epsilon(t)$, and its general solution has the form of Eq. (3.1).

Creep properties are fully characterized either by $J(t, t')$ or by $E_R(t, t')$. The relation between these two functions may be obtained by considering the strain history to be a unit step function, i.e. $\epsilon = 1$ for $t > t_0$ and $\dot{\epsilon} = 0$ for $t < t_0$, in which case the response is, by definition, $\sigma(t) = E_R(t, t_0)$. Substitution into Eq. (3.1) with $\epsilon^0 = 0$ then yields

$$J(t, t_0)E(t_0) + \int_{t_0^+}^t J(t, t')\frac{\partial E_R(t, t')}{\partial t'}\,dt' = 1. \tag{3.6}$$

Similarly, by considering the stress history as a step function,

$$\frac{E_R(t, t_0)}{E(t_0)} - \int_{t_0^+}^t E_R(t, t')\frac{\partial J(t, t')}{\partial t'}\,dt' = 1. \tag{3.7}$$

Regarding the determination of $E_R(t, t')$ from $J(t, t')$ or vice versa, no analytical expression for $J(t, t')$ is known that would be sufficiently accurate and allow, at the same time, the conversion to be accomplished analytically. Therefore, a numerical method must be used (see Eqs. (5.8)–(5.12) in the sequel; a FORTRAN IV program for this purpose is listed in [146] and a more efficient one in [170]).

Stress–strain relations (3.1) are sometimes transformed by integration by parts, which gives

$$\epsilon(t) - \epsilon^0(t) = \frac{\sigma(t)}{E(t)} + \int_0^t L(t, t')\sigma(t')\,dt' \tag{3.8}$$

with $L(t, t') = -\partial J(t, t')/\partial t'$. Here $L(t, t')$ = memory function = strain at time t caused by a unit stress impulse (Dirac function) applied at time $t' \leq t$. Equation (3.5), which is based on relaxation function, may be transformed in a similar way, and the resulting memory kernel may be shown to be related to $L(t, t')$ by a Volterra integral equation similar to Eq. (3.6) or Eq. (3.7); see Ref. [77].

As a consequence of aging, the principle of fading memory [78], a fundamental postulate in classical linear viscoelasticity, is invalid for $L(t, t')$. This can be checked by evaluating the memory function $L(t, t')$ in Eq. (3.8) from an expression for $J(t, t')$ (Subsection 3.3) that fits some typical data, such as those in Figs. 2, 3, 4, and 5(a). It is found that $L(t, t')$, as function of t', attains a minimum for a certain finite t', and so the memory fades only over a sufficiently close past. Thus, concrete is like a senile man who remembers the recent events and also the events from his young age better than those from his middle age [50].

Stress relaxation data are much scarcer than creep test data because, for long testing periods, relaxation tests are less convenient. The most extensive data available are shown in Figs. 5(b) and 6, and further data of more limited range of t'-values may be found in the literature [3, 89]. The solid lines in Figs. 5(b) and 6 represent the stress relaxation curves accurately computed [according to Eqs. (5.8) to (5.11)] from the corresponding creep data in Figs. 3 and 5(a). The fact that the fit is quite close provides confirmation of the linearity of creep (principle of superposition). In fact, the fit is even better than in the original papers [6, 11] in which the relaxation curves were computed by hand with a lesser accuracy.

3.2 Creep Function in Contemporary Recommendations by Engineering Societies

The creep function is often expressed as

$$J(t, t') = \frac{1 + \phi(t, t')}{E(t')} = \frac{1}{E(t')} + C(t, t'), \tag{3.9}$$

where function $\phi(t, t')$, representing the ratio of the creep strain to the elastic (instantaneous) strain under constant stress, is called creep coefficient, and $C(t, t')$ is called specific creep. However, characterization of creep by $\phi(t, t')$ is frequently a source of confusion since all $J(t, t')$ values are thus unnecessarily made dependent upon $E(t')$, which is usually taken not as the truly instantaneous (dynamic) modulus, but as the modulus corresponding to the strain in a short time interval after load application (nonstandardized, usually 1 min, but for many older data up to

several hours). An ACI (American Concrete Institute) Committee [79] has recently recommended the approximation

$$\phi(t, t') = \phi_u(t') f(t - t'), \tag{3.10}$$

in which (Fig. 7)

$$f(t - t') = \frac{(t - t')^{0.6}}{10 + (t - t')^{0.6}}, \qquad \phi_u(t') = 2.94(t')^{-0.118} c, \tag{3.11}$$

t and t' being given in days; c is a parameter. Similar expressions of the form of Eq. (3.10) have been recommended by CEB (European Concrete

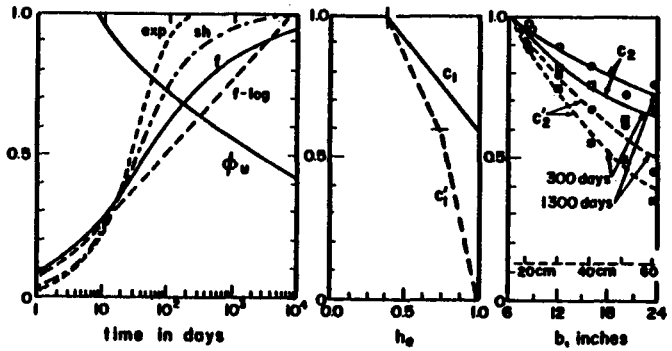

Fig. 7 Creep parameters in design recommendations. f, ϕ_u are ACI curves as given by Eqs. (3.11)[79]; sh is shrinkage curve (3.12); f-log = curve $0.113 \ln(1 + t - t')$, exp = $1 - e^{-t/\infty}$ (shown for comparison); c_1, c_1', c_2, c_2' are correction factors as functions of environmental humidity h_e and minimum thickness b of specimen [79]; 300 or 1300 days are durations of creep. [Data points after Hansen, T. C., and Mattock, A. H., "Influence of Size and Shape of Member on the Shrinkage and Creep of Concrete," *Amer. Concrete Inst. J.* 63 (1966) 267–290.]

Committee) (cf. Ref. [3]). ACI Committee [79] also gives an expression for shrinkage of concrete,

$$\epsilon_{sh}(t) = 0.0008 c' \frac{t - 7}{35 + t - 7}, \tag{3.12}$$

in which t is in days and drying is assumed to begin at $t_0 = 7$ days.

Expressions of the type (3.10) and (3.12) have the merit of simplicity, but are capable of only a crude approximation of individual test data [e.g., Figs. 2, 3, 4, and 5(a)]. Equation (3.11) giving $f(\infty) = 1$ implies boundedness of creep, whereas the actual creep curves in log $(t - t')$ scale do not approach any asymptote; but for $t - t' \leq 30$ years, Eq. (3.11) is acceptable. (Thus, the structural analyses in which the existence of an asymptotic value is assumed to allow the use of Tauberian theorems are of little relevance to concrete [80, 81].)

Parameters c in Eq. (3.11) and c' in Eq. (3.12) are correction factors to be calculated as $c = c_1 c_2 c_3 c_4 c_5 c_6$ and $c' = c_1' c_2' c_3' c_4' c_5' c_6'$. Correction factors c_3 to c_6 and c_3' to c_6' account for differences in composition of concrete, such as the cement content, water–cement ratio (of the fresh mix), percentage of fines in the aggregate, and the air content; see Ref. [79]. It is noted that the type of cement, admixtures, and especially the type of aggregate have also effect on creep [3], but corrections of ϕ are not too important because the effect on elastic strain is roughly the same. Correction factors c_1 and c_2 introduce the increase in creep caused by simultaneous drying (item 11, Section 2). The recommended values shown in Fig. 7 express the fact that drying is faster at a lower environmental humidity h_e and also in cross sections of smaller minimum thickness b. The effect of h_e and b on shrinkage is introduced through correction factors c_1' and c_2' (Fig. 7). Effect of the seasonal changes of humidity can be approximately taken into account by replacing t with a certain reduced time [77, 139, 151]. The recommendations of CEB are similar, except that CEB also gives different shapes of creep curves (function f) for different b [3]. According to ACI expressions for the relation of E to strength and the dependence of strength on age [4, 79], the elastic modulus, appearing in Eq. (3.9), approximately is (in the case of drying concrete of a thickness from 10 to 30 cm)

$$E(t') = E_{28} \sqrt{\frac{t}{4 + 0.85t}}, \tag{3.13}$$

where $E_{28} = E$ at age $t = 28$ days. For mass concrete, the increase of E from 28 days to ∞ is much larger than Eq. (3.13) predicts; a possible expression is, e.g., $E_{28}/(1 + \beta t^{-1/3})$.

Equation (3.11) has been determined as to fit the creep data from Fig. 21. Most other data are better approximated by the expression [5, 8] $f(t - t') = 0.113 \ln(1 + t - t')$. However, most tests, especially the recent, more extensive ones, are best fitted by the expression

$$J(t, t') = \frac{1 + \alpha(t')^{-n}}{E_0} + C(t, t'), \quad C(t, t') = \frac{\varphi_1}{E_0}(t')^{-m}(t - t')^n \tag{3.14a}$$

For example, the data in Fig. 2 are closely fitted with $\alpha = 0$, $m = 0.355$, $n = 0.056$, $\varphi_1 = 17.51$, $10^7/E_0 = 84.4$/psi; data in Fig. 3 with $\alpha = 0$, $m = 0.46$, $n = 0.13$, $\varphi_1 = 2.80$, $10^7/E_0 = 189$/psi; data in Fig. 4 with $\alpha = 0$, $m = 0.21$,

$n = 0.094$, $\varphi_1 = 3.74$, $10^9/E_0 = 78.8$/psi; and the low-stress curves from Fig. 25 with $\alpha = 0$, $m = 0.352$, $n = 0.22$, $\varphi_1 = 2.76$, $10^9/E_0 = 18$/psi; for nonzero α and with $p = \frac{1}{2}$ the optimum fits are not much different. The conventional values of E are obtained from Eq. (3.14a) by setting $t - t' = 0.001$ day. The material parameters in Eq. (3.14a) can be determined from test data, such as those in Fig. 2, in the following manner. First one considers the function $\bar{J} = J(t, t') - \alpha t'^{-p}/E_0$ and estimates the values of p and α/E_0. Noting that $\bar{J} = 1/E_0 + x^n \varphi_1/E_0$, where $\log x = \log(t - t') - s$, $s = (m/n)\log t'$, it is seen that after a horizontal shift by distance s all $\bar{J}$-curves plotted in $\log(t - t')$ scale must fit one common basic curve. These shifts are carried out numerically by computer and by a linear regression of the shift distances, s, the value of m/n is found. Then the common basic curve obtained by shifting is fitted by the expression $1/E_0 + x^n \varphi_1/E_0$, using an optimization method (Marquardt's algorithm). This yields n, $1/E_0$ and φ_1/E_0. Further improvement of fit is possible by simultaneously optimizing for m, n, $1/E_0$, and φ_1/E_0. Finally, several other values of α and p may be tried and the best fit selected.

For the shrinkage curves of test specimens (e.g., Fig. 16 in the sequel), the following formula has been verified:

$$\epsilon_{sh} = \epsilon_{sh}^{\infty}\left[1 + \left(\frac{\tau_{sh}}{t - t_0}\right)^{0.9}\right]^{-1/2}$$

$$\epsilon_{sh}^{\infty} = \epsilon_{sh}^{0}\frac{E(7+45)}{E(t_0+\tau_{sh})}\left\{F(0.5) + [F(h_e) - F(0.5)]\left(1 + \frac{\tau_s}{t - t_0}\right)^{-1}\right\}, \quad (3.14b)$$

$$\tau_{sh} = k_d \frac{0.3}{C_1(7)}\,45 \text{ days}, \qquad k_d = \left(\frac{k_s d}{15}\right)^2 k_T \frac{C_1(7)}{C_1(t_0)},$$

$$F(h_e) = 1 - 0.95h_e^3 - 0.25h_e^{200}$$

where d is the thickness or diameter in centimeters, $k_s = 1$ for a cylinder (1.1—prism, 0.9—cube, 1.7—slab, 0.75—sphere); C_1 is water diffusivity from Eq. (4.41) in Section 4 (normally 0.3 cm^2/day), h_e is environmental humidity (for sealed specimens, h_e is self-desiccation humidity), ϵ_{sh}^0 is the reference ultimate shrinkage (0.0011 for data in Fig. 16), t_0 is age in days at start of drying, $(t - t_0)$ is time from this start, k_T is temperature correction coefficient. The main value of expressions such as Eqs. (3.14a) and (3.14b) is to be expected in statistical evaluations and in extrapolation of short-time data available for a given construction project.

Many other expressions for functions f, ϕ_u, ϵ_{sh}, and the correction factors have also been used in the past [16, 36, 79, 82–85]. In design practice, various forms of the creep law that are an even cruder simplification than Eq. (3.10) have been widely used (rate-of-creep method, Arutyunian's law, etc.). These will be discussed in Subsection 5.5.

3.3 Dirichlet Series Expansions of Creep and Relaxation Functions

The fact that due to aging the creep function cannot be expressed as a function of a single variable, $t - t'$, causes a major complication in structural analysis problems and makes the Laplace transform methods ineffective. Therefore, numerical methods must be used. As will be shown in Subsection 5.4, for efficient numerical solutions, the integral-type creep law (3.1) must be converted into a rate-type creep law. To do this, one must approximate $J(t, t')$ [or $E_R(t, t')$] by a degenerate kernel of the form

$$\sum_{\mu} A_\mu(t')\,B_\mu(t).$$

As will be confirmed later, no loss in the generality of material representation is incurred if one restricts attention to the special case of a series of real exponentials

$$\sum_{\mu} A_\mu(t')e^{-t/\tau_\mu},$$

called Dirichlet series [86]. It may be more conveniently written in the form

$$J(t, t') = \frac{1}{E(t')} + \sum_{\mu=1}^{n} \frac{1}{\hat{E}_\mu(t')}(1 - e^{-(t-t')/\tau_\mu}), \quad (3.15)$$

where τ_μ are constants called retardation times and $\hat{E}_\mu$ are coefficients depending on t'.

Identification of material parameters $\hat{E}_\mu(t')$ or fitting of given data on $J(t, t')$ at a given fixed t' by the Dirichlet series is a difficult mathematical problem (which also arises, e.g., in connection with the numerical inversion of Laplace transform). It is notorious for unstable dependence of the series coefficients (i.e., $\hat{E}_\mu$, τ_μ upon the data [87]. Because of this instability, determination of retardation times τ_μ from the test data should not be attempted, or else an ill-conditioned equation system would result for the solution of τ_μ is not unique and substantially different τ_μ-values give equally close data fits. One may intuitively anticipate this fact, realizing that the spectrum of relaxation times is actually continuous and that any "smooth" continuous function may be characterized equally well by sets of discrete values that correspond to widely different subdivisions of time. Hence, the values of τ_μ must be appropriately selected in advance. A suitable choice is τ_μ-values uniformly distributed in a logarithmic scale,

i.e. $\tau_\mu = \tau_1 a^{\mu-1}$. Better accuracy is obtained for smaller a, but for expedience of structural analysis, the number of terms in Eq. (3.15) should be kept to a minimum. A practically sufficient accuracy is achieved with $a = 10$, i.e.

$$\tau_\mu = \tau_1 10^{\mu-1}, \qquad \mu = 1, 2, \ldots, n. \tag{3.16}$$

τ_1 must not be chosen larger than either the point at which the creep curve in $\log(t-t')$-scale begins to rise or the lower limit of the time range of interest, and τ_n must not be chosen smaller than either the point where the curve levels off or the upper limit of the range of interest. (With regard to the usually large scatter of creep data, a can be taken as large as 60, which gives about 1.5 times fewer τ_μ for the given time range to be covered. But the creep curves given by Eq. (3.15) then look "bumpy"; see Fig. 19 in Ref. [89].)

Denoting the given measured data points as $\bar{J}(t_\beta, t')$, $\beta = 1, 2, 3$, one obtains the fit of creep curve $J(t, t')$ as function of t at chosen fixed t' by the method of least squares, i.e. by minimizing the expression

$$\begin{aligned}\Phi &= \sum_\mu [J(t_\beta, t') - \bar{J}(t_\beta, t')]^2 + \Phi_1 \\ \Phi_1 &= \sum_\mu [w_1(\hat{E}_{\mu+1}^{-1} - \hat{E}_\mu^{-1})^2 + w_2(\hat{E}_{\mu+2}^{-1} - 2\hat{E}_{\mu+1}^{-1} + E_\mu^{-1})^2 \\ &\qquad + w_3(\hat{E}_{\mu+3}^{-1} - 3\hat{E}_{\mu+2}^{-1} + 3\hat{E}_{\mu+1}^{-1} - \hat{E}_\mu^{-1})^2],\end{aligned} \tag{3.17}$$

where Φ_1 is a penalty term that forces $\hat{E}_\mu$ to be a smooth function of μ, which is a physically natural property to require. The presence of the penalty term is essential; without it, coefficients $\hat{E}_\mu$ would be unstable functions of creep data (i.e. different $\hat{E}_\mu$ would give equally close fits). Thus, if $\hat{E}_\mu(t')$ were determined for various ages t', the dependence of $\hat{E}_\mu$ upon t' would be unsmooth, randomly scattered, and it would be impossible to model aging. (In classical viscoelasticity, this need does not arise, of course.) Weights w_1, w_2, w_3 should be assigned minimum values that are necessary for smoothness, which can be assessed by computing experience. (The weights must be higher for smaller a, because of a stronger tendency toward instability in identification of $\hat{E}_\mu$.)

Times t_β in which data points are specified should be distributed uniformly in $\log(t-t')$-scale. Four (or three) values per decade, $(t-t')_\beta = 10^{1/4}(t-t')_{\beta-1}$, are an expedient choice. Usually, the measured values are not so spaced, and one must first interpolate to determine $\bar{J}(t_\beta, t')$. The minimization conditions are $\partial\Phi/\partial(\hat{E}_\mu^{-1}) = 0$ ($\mu = 1, 2, \ldots, n$) and $\partial\Phi/\partial(E^{-1}) = 0$. They yield a system of $(n+1)$ linear algebraic equations for E^{-1} and $\hat{E}_\mu^{-1}$. In practical computation, the method was found to be satisfactory [88, 89, 170]. It appears that realistic smooth creep curves, characterized by a bounded slope in $\log(t-t')$-scale, can be fitted by the Dirichlet series (for small enough a) with any desired accuracy.

For nonaging materials, alternate (and in author's experience less efficient) methods, which lack the smoothing by penalty term in Eq. (3.17), were presented by Cost [90] and Schapery [91] (cf. also Ref. [92]). Other approximate methods are used to obtain continuous relaxation spectra of polymers [93]. Distefano [94, 95] studied the identification of nonaging Maxwell chain parameters from given data as a nonlinear optimization problem and applied the methods of dynamic programming.

With most creep data, one can take advantage of the fact that the creep curves in the $\log(t-t')$-scale can be closely approximated by a horizontal line segment, expressing the elastic strain, E^{-1}, followed by one or two inclined straight-line segments, with short curved transitions between the straight segments (Fig. 8). Assuming that times τ_a, τ_b shown in Fig. 8 are chosen so that $\tau_b/\tau_a = 10^m$ where m is integer, the Dirichlet series approximation is [88]:

$$E^{-1} + \sum_{\mu=-m}^{-1} k_a(1 - e^{-(t-t')/\tau_\mu}) + \sum_{\mu=0}^{n-1} k_b(1 - e^{-(t-t')/\tau_\mu}) + 1.2k_b(1 - e^{-(t-t')/\tau_n}), \tag{3.18}$$

where $\tau_\mu = (5.63\tau_a)10^\mu$, k_a, k_b slope tangents shown in Fig. 8. In the case of only one inclined straight segment, the first sum in Eq. (3.18) is left out or $k_a = m = 0$; then, evaluating expression (3.18), it can be verified that within the limits $0.22\tau_0 \leq t - t' \leq 1.5\tau_n$ the error is less than $\pm 0.03k_b$, and only $\pm 0.018k_b$ if the upper limit is reduced to τ_{n-1}. Utilizing expression (3.18), approximate fitting of creep curves by Dirichlet series can be accomplished by hand calculations.

Carrying out the fitting procedure, as just described, for various values of $t' = t'_\alpha$ ($\alpha = 1, 2, 3, \ldots$), $\hat{E}_\mu$ and E at various ages t' are obtained. For

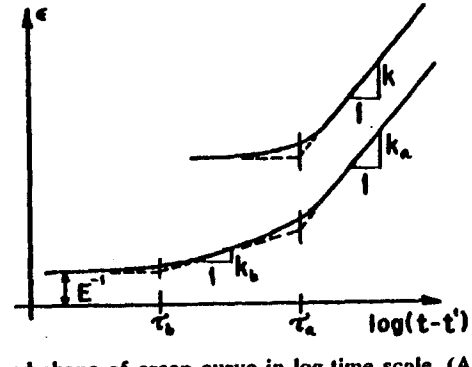

Fig. 8 Idealized shape of creep curve in log-time scale. (After Ref. [60].)

their fitting, which is best carried out by the method of least squares, functions of the type $a + b(t')^{-n}$ (where a, b, n are constants) were found to be best suited[88]. For example, it was found[88] that Eq. (3.18) fits satisfactorily the data points in Fig. 2 if $E^{-1} = 0.208 + 0.93t^{-0.5} - 0.16t^{-0.46}$, $m = n = 3$, $k_a = 0.002 + 0.16(t')^{-0.46}$, $k_b = 0.003 + 0.23(t')^{-0.25}$, $\tau_\mu = 5.63 \times 10^\mu$ days; for Fig. 3, $E^{-1} = 0.19 + 1.63(t')^{-0.75}$, $m = k_a = 0$, $k_b = 0.0025 + 0.25(t')^{-0.33}$, $J(t, t')$ being given in 10^{-6}/psi, and t, t' in days.

Conversion to a rate-type creep law is also possible if the relaxation function is expanded in Dirichlet series, which may be written as

$$E_R(t, t') = \sum_{\mu=1}^{n-1} E_\mu(t') e^{-(t-t')/\tau_\mu} + E_\infty(t'), \tag{3.19}$$

where τ_μ are constants, now called relaxation times, and E_μ, E_∞ are coefficients depending on t'. Fitting of given data points $\tilde{E}_R(t_\beta, t')$, $\beta = 1, 2, \ldots$, by expression (3.19) as function of t at a chosen fixed t' may be performed in the same manner as for Kelvin chains, minimizing the sum-of-squares expression[89, 170]:

$$\Phi = \sum_\mu [E_R(t_\beta, t') - \tilde{E}(t_\beta, t')]^2 + \Phi_1,$$

$$\Phi_1 = w_1 \sum_{\mu=1}^{n-2} (E_{\mu+1} - E_\mu)^2 + w_2 \sum_{\mu=1}^{n-3} (E_{\mu+2} - 2E_{\mu+1} + E_\mu)^2$$

$$+ w_3 \sum_{\mu=1}^{n-4} (E_{\mu+3} - 3E_{\mu+2} + 3E_{\mu+1} - E_\mu)^2, \tag{3.20}$$

where $E_R(t_\beta, t')$ are the given values of $E_R(t, t')$. The smoothing term Φ_1 does not include E_∞ because no smooth transition from E_{n-1} to E_∞ is to be expected. The reason is that E_∞ actually represents a sum of all E_μ for which τ_μ is beyond the time range of interest. For the range 1 day $\leq t' \leq$ 10,000 days, the dependence upon t' may be approximated by one of the functions

$$E_\mu = E_{0_\mu} + \sum_{i=1}^{3} \frac{E_{i_\mu}}{1 + \dfrac{t'}{3 \times 30^{(i-1)}}}, \tag{3.21a}$$

$$E_\mu = \sum_{i=0}^{3} E_{i_\mu} p^i, \quad \text{with } p = (t')^{1/6} \text{ or } p = \log(1 + t'), \tag{3.21b}$$

in which $E_{0_\mu}, \ldots, E_{3_\mu}$ are constants ($\mu = 1, 2, \ldots, n$). However, the best results have been achieved with the expression[170]

$$E_\mu = a_1 + a_2\mu + a_3 p + a_4\mu^2 + a_5\mu p + a_6 p^2$$

$$+ a_7\mu^3 + a_8\mu^2 p + a_9\mu p^2 + a_{10} p^3, \quad \mu < n \tag{3.22}$$

$$E_\infty = a_{11} + a_{12} p + a_{13} p^2 + a_{14} p^3, \quad \text{with } p = \log t',$$

in which not only the dependence upon t', but also that upon μ, is smoothed analytically. To determine $a_1, \ldots, a_{14}$, one substitutes Eqs. (3.22) into Eq. (3.19) and Eq. (3.19) into Eqs. (3.20), in which Φ_1 may be either ignored or taken as $\Sigma_i w_i a_i$, where w_i are suitably chosen weights intended to reduce curvature and slope by reducing the higher-order terms in Eqs. (3.22). The conditions $\partial\Phi/a_i = 0$ procure then a system of 14 linear algebraic equations for $a_1, \ldots, a_{14}$. A full listing of FORTRAN IV programs based on Eqs. (3.20) and (3.22) is given in Ref. [170].

Among the relaxation data available at present[5, 6, 11, 89, 96, 97], there is none that would cover sufficiently broad ranges of both $t - t'$ and t'. Therefore, relaxation data must be obtained from creep data, which can be accomplished (if the range of the latter is sufficient) numerically [see Eqs. (5.8) to (5.11) in Section 5]. The typical creep data shown in Figs. 2, 3, and 4 were converted to relaxation data and fitted by Eq. (3.19) with Eq. (3.21) or Eqs. (3.22). For the data in Fig. 2, the distributions of E_μ with $\log \tau_\mu$ (called relaxation spectra) are plotted in Fig. 9 for various t'. To check the accuracy of this fit, expression (3.19) obtained from $E_R(t, t')$ was converted [by an algorithm given by Eqs. (5.11) to (5.16) in Section 5] to creep function $J(t, t')$, which is shown by solid lines in comparison with the data points in Figs. 2, 3, and 4.

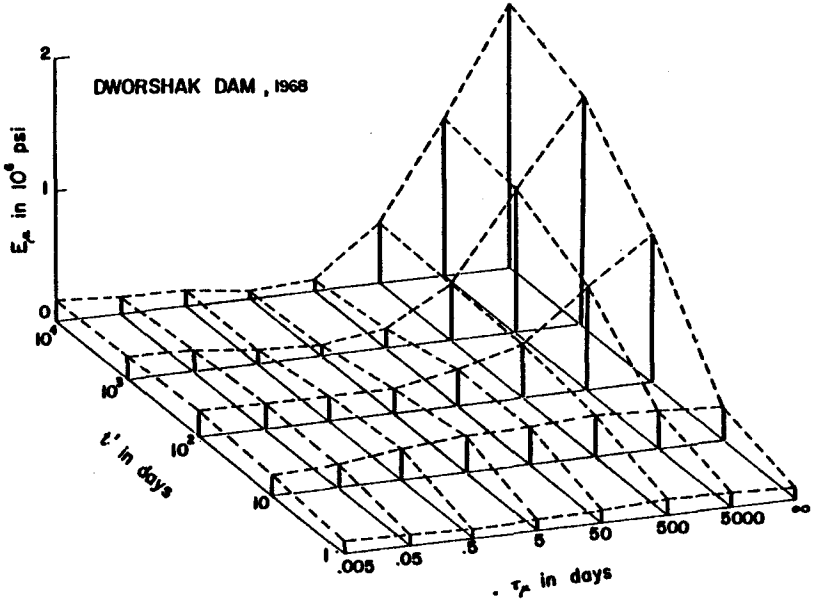

Fig. 9 Relaxation spectra at various ages for creep data in Fig. 2. (From Ref. [89].)

3.4 Rate-Type Creep Law

Upon insertion of Dirichlet series expansion (3.15), Eq. (3.1) may be written in the form

$$\epsilon(t)=\int_0^t \left[E^{-1}(t')+\sum_\mu \hat{E}_\mu^{-1}(t')\right]\, d\sigma(t')-\sum_{\mu=1}^{n}\epsilon_\mu^*(t)+\epsilon^0(t), \quad (3.23)$$

in which the quantities

$$\epsilon_\mu^*(t)=e^{-t/\tau_\mu}\int_0^t e^{t'/\tau_\mu}\hat{E}_\mu^{-1}(t')\,d\sigma\,(t'), \qquad \mu=1,2,\ldots,n \quad (3.24)$$

may be viewed as hidden material variables (internal variables [98, 99]) that, according to Eq. (3.23), characterize the past history. They satisfy differential equations

$$\dot{\epsilon}_\mu^*+\frac{\epsilon_\mu^*}{\tau_\mu}=\frac{\dot{\sigma}}{\hat{E}_\mu}, \quad (3.25)$$

and, conversely, integration of these equations may be shown to yield Eq. (3.23), so that Eqs. (3.23) and (3.25) are equivalent. The derivative of Eq. (3.23) may now be written in the form

$$\dot{\epsilon}-\dot{\epsilon}^0=\frac{\dot{\sigma}}{E(t)}+\sum_\mu \dot{\epsilon}_\mu, \quad (3.26)$$

in which

$$\dot{\epsilon}_\mu=\frac{\dot{\sigma}-\dot{\sigma}_\mu}{\hat{E}_\mu(t)}, \quad (3.27)$$

and $\dot{\sigma}_\mu=\hat{E}_\mu(t)\dot{\epsilon}_\mu^*$. Then, subtracting Eq. (3.27) from Eq. (3.25), one finds that $\dot{\epsilon}_\mu=\epsilon_\mu^*/\tau_\mu$ and

$$\dot{\sigma}_\mu=\eta_\mu(t)\ddot{\epsilon}_\mu, \qquad \mu=1,2,\ldots,n, \quad (3.28)$$

in which $\eta_\mu(t)=\hat{E}_\mu(t)\tau_\mu$. Equations (3.26) to (3.28) [88] represent a rate-type creep law, which is equivalent to creep function (3.15).

From Eqs. (3.26) to (3.28), it is readily recognized that they correspond to the well-known (generalized) Kelvin (or Kelvin–Voigt) chain model, Fig. 10(a), whose spring moduli and viscosities are given by $\hat{E}_\mu$ and η_μ, and are age dependent.

It is noteworthy that Eq. (3.27) for the springs is not equivalent to $\epsilon_\mu=(\sigma-\sigma_\mu)/\hat{E}_\mu$. The form of Eq. (3.27) is appropriate when the solid material is being added to the existing solid framework in an unstressed state [100], as is true of hydration. Furthermore, Eq. (3.28) for the dashpots differ from the usual form $\sigma_\mu=\eta_\mu\dot{\epsilon}_\mu$. For constant $\dot{\epsilon}_\mu$, this form

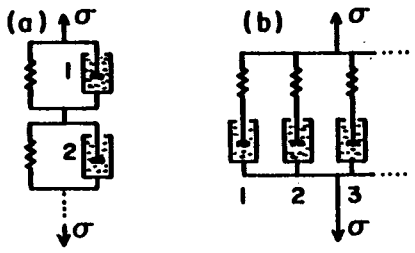

Fig. 10 (a) Kelvin chain model and (b) Maxwell chain model.

gives $\dot{\sigma}_\mu=\dot{\eta}_\mu\dot{\epsilon}_\mu$, while Eq. (3.28) yields $\dot{\sigma}_\mu=0$. However, if ϵ_μ's are interpreted as microstrains of some physical meaning on the microstructural level, then $\dot{\sigma}_\mu>0$ must hold because the solid material being added by hydration to the existing one must increase the resistance to a given deformation rate. Therefore, Eq. (3.28) lacks physical justification [88].

In view of this result, it is worthwhile to examine whether some Kelvin chain with correct dashpot relations $\sigma_\mu=\eta_\mu\dot{\epsilon}_\mu$ can also be equivalent to creep function (3.15). It can be verified [88] that this occurs for $\eta_\mu=\tau_\mu\hat{E}_\mu(t)$, $E_\mu=\hat{E}_\mu(t)-\tau_\mu d\hat{E}_\mu(t)/dt$. The latter relation, however, gives negative E_μ within some periods of time for any realistic creep function [88] (for $n=1$, see Ref. [77]), which is physically inadmissible. Another Kelvin chain representation with $\sigma_\mu=\eta_\mu\dot{\epsilon}_\mu$ can be found if E_μ in Eq. (3.15) is taken as function of t rather than t'. But incorrect elastic relations $\sigma_\mu(t)=E(t)\epsilon_\mu(t)$ then ensue.

Still another possibility is to assume *a priori* the physically correct relations [88]

$$\sigma_\mu=\eta_\mu(t)\dot{\epsilon}_\mu \qquad \text{with} \quad \frac{\eta_\mu(t)}{E_\mu(t)}=\tau_\mu=\text{constant}. \quad (3.29)$$

Then, the Kelvin chain is described by Eq. (3.26) in which $\eta_\mu\ddot{\epsilon}_\mu+(E_\mu+\dot{\eta}_\mu)\dot{\epsilon}_\mu=\ddot{\sigma}$. Integration of this differential equation for the case of stress $\sigma=1$ acting since time $t'\leq t$ and a substitution into Eq. (3.26) yield [88]:

$$\dot{\epsilon}(t)=\sum_\mu \frac{1}{\tau_\mu E_\mu(t)}e^{-(t-t')/\tau_\mu}, \qquad \text{for} \quad \sigma=H(t-t'). \quad (3.30)$$

This is a Dirichlet series, whose coefficients, however, depend on t rather than t'. To identify $E_\mu(t)$ from given creep data, one may, therefore, construct the curves of strain rate $\dot{\epsilon}$ as functions of $(t-t')$ for various constant current times t (see Fig. 10 in [88]). Nevertheless, this approach has the drawback that the derivatives of a random function (i.e. $\dot{\epsilon}$) exhibit

a much greater statistical dispersion than the function itself [i.e. $\dot{\epsilon}$ or $J(t, t')$]. Accordingly, it is desirable to integrate ϵ from Eq. (3.30). An explicit analytical expression for ϵ can be obtained only if E_μ^{-1} as function of t is also expanded in Dirichlet series, namely

$$\frac{1}{E_\mu(t)} = J_\mu + \sum_k J_{\mu k}\, e^{-t/\tau_k'}, \qquad k = 1, 2, \ldots, n_k; \quad \mu = 1, 2, \ldots, n \tag{3.31}$$

where J_μ and $J_{\mu k}$ are material constants; $\tau_k' = \tau_1' 10^{k-1}$. Integration of Eq. (3.30) then provides

$$J(t, t') = \frac{1}{E(t')} + \sum_\mu J_\mu (1 - e^{-(t-t')/\tau_\mu}) + \sum_\mu \sum_k \frac{J_{\mu k}}{1 + \frac{\tau_\mu}{\tau_k'}} e^{-t'/\tau_k'} \left\{ 1 - \exp\left[-\left(\frac{1}{\tau_\mu} + \frac{1}{\tau_k'} \right)(t - t') \right] \right\} \tag{3.32}$$

This expression can be fitted to given data on $J(t, t')$ by minimizing a sum-of-squares expression that is similar to Eq. (3.17) but has a smoothing penalty term Φ_1 in two dimensions (μ and k). (To avoid ill-conditioning of the resulting system of equations, all $J_{\mu k}$ for which $\tau_\mu \geqslant 10\tau_k'$ must be set equal to 0 because they have almost no effect on the value of $J(t, t')$.) An alternative method, which was found to work well in practice, is to put $J_{\mu k} = a_{k1} + a_{k2}\mu + a_{k3}\mu^2 + a_{k4}\mu^3$, $J_\mu = a_{01} + \cdots + a_{04}\mu^3$, and determine a_{kl} directly from the conditions $\partial\Phi/\partial a_{kl} = 0$.

It remains to decide whether all J_μ and $J_{\mu k}$ are guaranteed to be nonnegative. To this end, it is necessary, according to Eq. (3.30), that the slope of the curve of $\dot{\epsilon}$ versus $(t - t')$ at any constant t be always nonpositive, which is equivalent to the condition

$$\frac{\partial^2 J(t, t')}{\partial t\, \partial (t - t')} = -\frac{\partial^2 J(t, t')}{\partial t\, \partial t'} = \frac{\partial L(t, t')}{\partial t} \leqslant 0, \tag{3.33}$$

where L is defined below Eq. (3.8). Thus, the slope of creep recovery following a stress impulse (as well as any loading of finite duration) must be nonpositive. This agrees with all known observations, and so E_μ must always be nonnegative. Therefore, the Kelvin chain characterized by Eq. (3.29) is physically admissible. (A closer examination could reveal a connection of inequality Eq. (3.33) to the second law of thermodynamics. In Ref. [88], Eq. (3.29) was rejected because of cases of a positive slope of the curve of $\dot{\epsilon}$ versus $t - t'$ at constant t, but now it appears that this must have been caused merely by statistical scatter.)

Attention will now be shifted to the Dirichlet series expansion of the relaxation function (3.19). Inserting it into Eq. (3.5), it is possible to write

$$\sigma = \sum_{\mu=1}^{n} \sigma_\mu, \tag{3.34}$$

where

$$\sigma_\mu(t) = e^{-t/\tau_\mu} \int_0^t E_\mu(t') e^{t'/\tau_\mu} [d\epsilon(t') - d\epsilon^0(t')], \tag{3.35}$$

provided τ_μ now equals $\tau_1 10^{\mu-1}$ only for $\mu < n$, while at $\tau_n = \infty$, $E_n = E_\infty$. σ_μ are hidden stresses (internal variables) characterizing the past history. They satisfy (and follow from) the differential equations

$$\frac{\dot{\sigma}_\mu}{E_\mu(t)} + \frac{\sigma_\mu}{\eta_\mu(t)} = \dot{\epsilon} - \dot{\epsilon}^0, \qquad \mu = 1, 2, \ldots, n, \tag{3.36}$$

with the notation

$$\eta_\mu(t) = \tau_\mu E_\mu(t). \tag{3.37}$$

It is now readily seen that Eqs. (3.34) and (3.36)[89] correspond to the (generalized) Maxwell chain model, Fig. 10(b), whose spring moduli and viscosities are given by E_μ and η_μ, and are age dependent. In contrast with some of the previous cases of Kelvin chains, Eq. (3.36) indicates the correct form of the equations for time-variable dashpots and springs, as mentioned before. Also, E_μ and η_μ are, according to Eq. (3.19), always nonnegative, because the relaxation curves have always nonpositive slope.

In conclusion, both the Maxwell chain and the Kelvin chain (with a proportionate age dependence of η_μ and E_μ) can represent the material behavior as closely as desired. Thus, they are mutually equivalent, and they must also be equivalent to any other possible spring-dashpot model, similarly as in classical viscoelasticity [93, 101]. The identification of material parameters from test data is simpler for the Maxwell chain, and therefore this model will be used as the basis for the ramifications in the subsequent section, despite the fact that the use of Kelvin chain is conceptually more convenient for interpretation of creep tests. In the case of Kelvin chain, the identification is, unfortunately, simple only for such forms of spring and dashpot relations that cannot be brought in correspondence with the physical processes in the microstructure [88, 89]. However, such Kelvin chains are admissible only when water content and temperature are constant.

4 ENVIRONMENTAL FACTORS AND NONLINEAR EFFECTS IN CREEP AND SHRINKAGE

4.1 Effect of Temperature and Humidity on Aging

The rate of hydration or aging depends on temperature T and pore humidity h (relative vapor pressure). This effect may be expressed in terms of a change of the time scale, considering that all material parameters [e.g., E_μ and η_μ from Eq. (3.36)], rather than being functions of actual time t, are functions of the so-called equivalent hydration period t_e defined as [67, 100, 115]

$$t_e = \int \beta \, dt = \int \beta_T \beta_h \, dt, \tag{4.1}$$

where β_T is a coefficient depending on T, β_h is a coefficient depending on h, and β is the relative hydration rate.

Since hydration is a thermally activated process, β_T may naturally be assumed to obey the Arrhenius equation [102], i.e.

$$\beta_T = \exp\left[\frac{U_h}{R}\left(\frac{1}{T_0} - \frac{1}{T}\right)\right], \tag{4.2}$$

where U_h is the activation energy of hydration, R = gas constant = 1.986 cal/°K, T is absolute temperature, and T_0 is the chosen reference value of T. Equation (4.2) is only approximate because, strictly speaking, hydration consists of several chemical reactions, each of which probably has a different activation energy. Nevertheless, Verbeck [104] found that the rates at which the hydration heat is evolved at various temperatures conform to the Arrhenius equation with $U_h/R = 2700$°K between 0°C and 100°C and up to 90 days of age. This value has been assumed, with success, in fitting the data on creep at various temperatures [60] [including Fig. 12(a), (b), (c)].

An estimate of the dependence of β_h upon h, based on the observation [53] that hydration slows considerably below $h = 0.8$ and other data [54, 55], is shown in Fig. 11 and may be expressed [67, 115] as $\beta_h \approx [1 + (3.5 - 3.5h)^4]^{-1}$.

4.2 Creep Law of Mass Concrete at Variable Temperature

Mass concrete (a term used for concrete inside massive structures) can never lose an appreciable amount of water and remains nearly saturated, and so the variability of water content need not be considered, i.e.

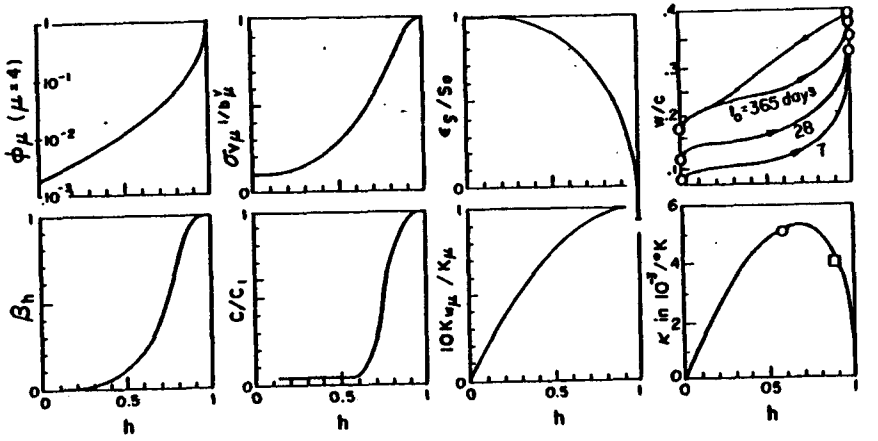

Fig. 11 Typical dependence of some material parameters on pore humidity h. w/c = water mass per unit mass of cement (after Powers, T. C., and Brownyard, T. C., "Studies of Physical Properties of Hardened Portland Cement Paste," *Amer. Concrete Inst. J.* 42 (1946)). Data points on κ after Monfore's and Jensen's tests. (See Bažant, Z. P., "Thermodynamics Theory of Concrete Deformation at Variable Temperature and Humidity," Report 69-11, Div. of Struct. Engrg. and Struct. Mech., Uni. of Calif., Berkeley, Aug. 1969.) Curve C/C_1 from Bažant, Z. P., and Najjar, L. J., "Nonlinear Water Diffusion in Nonsaturated Concrete," *Materials and Structures* (RILEM) 5 (1972) 3–20.

$h \approx 1.0$, $\beta_h = 1$. The main difficulty in formulating a creep law of mass concrete at variable temperature is due to the fact that temperature rise accelerates not only creep (effect 20, Section 2) but also aging [effect 18, Eq. (4.1)]. Mukaddam and Bresler [106] have considered both of these effects, replacing time t in Eq. (3.1) with reduced time

$$t_{red} = \int \psi_1(T)\psi_2(t^*) \, dt,$$

in which ψ_1 is the usual shift function as used for thermorheologically simple materials [78] and proposed for concrete by Sackman [107], and t^* is the corrected age, defined for constant temperature T as $t^* = t_0 + (t' - t_0)e^{-A(T-T_0)}$, where T_0 and t_0 are chosen reference temperature and reference age; A is a constant. A modified form of reduced time,

$$t_{red} = \int \psi_1(T)\psi_3(t - t') \, dt,$$

in which $\psi_3(t - t') = d \log (1 + t - t')/dt$, was later proposed by Rashid [108]. These approaches, however, do not allow the creep law at variable temperature to be converted to a rate-type form. This form is

unavoidable for creep analysis of large structural systems and is also necessary to enable the use of the well-founded concept of activation energy of thermally activated processes [102, 103]. Without attempting the formulation of a creep law that would reflect aging, the activation energy was used in the discussions of concrete creep by Polivka and Best (cf. Ref. [60]), Hansen [44], Ruetz [29], Wittmann [28, 51, 97], Maréchal [59], and others (cf. Ref. [60]).

Considering rate-type creep law (3.34), (3.36), one may regard viscosities η_μ in Eq. (3.36) as characteristics of various sorts of thermally activated processes involved in creep deformation. Thus, in view of Eq. (3.16) [60, 100],

$$\frac{1}{\eta_\mu} = \frac{1}{\eta_{\mu_0}} \exp\left[\frac{U_\mu}{R}\left(\frac{1}{T_0}-\frac{1}{T}\right)\right] = \frac{10^{1-\mu}}{E_\mu(t_e)\tau_1} \exp\left[\frac{U_\mu}{R}\left(\frac{1}{T_0}-\frac{1}{T}\right)\right], \quad (4.3),$$

in which U_μ are activation energies of creep deformation ($\mu = 1, 2, \ldots, n$). They need not be all equal, and then the simplest distribution is a linear one [60],

$$U_\mu = U_1 + (\mu - 1)\Delta U, \quad (4.4)$$

where U_1 and ΔU are constants. Substitution in Eq. (4.2) gives

$$\eta_\mu = a^{\mu-1}\tau_T E_\mu(t_e), \quad (4.5)$$

in which

$$\tau_T = \tau_1 \exp\left[-\frac{U_1}{R}\left(\frac{1}{T_0}-\frac{1}{T}\right)\right],$$
$$a = 10 \exp\left[-\frac{\Delta U}{R}\left(\frac{1}{T_0}-\frac{1}{T}\right)\right]. \quad (4.6)$$

From Eqs. (4.5) and (4.6), it may be easily deduced [60] that U_1 causes a shift of the creep curve in the log time to the left and ΔU causes an increase in its slope if U_1 and ΔU are considered independently of aging. On the other hand, the acceleration of aging, considered independently of U_1 and ΔU, causes a decrease of the ordinates of the creep curve.

The dependence of elastic modulus E, as well as E_μ, upon T is neglected because its change between 25°C and 100°C is not too large [8, 60, 109]. Equations (4.1) to (4.6) do not apply above 80–100°C because the chemical composition of cement is altered, and below 0°C because freezing of water changes the material, and probably also for rapid changes of temperature (effect 21, Section 2) because certain nonlinear terms are neglected; see Subsection 4.5.

Identification of the material parameters from given test data at various constant temperatures may be carried out combining the Dirichlet series expansions at reference temperature, as discussed previously, with the determination of U_1 and ΔU by trials of various values according to the *regula falsi* method [60]. Some of the fits of the best data available, as obtained in Ref. [60] for the creep law characterized by Eqs. (3.34), (3.36), and (4.4) to (4.6), are shown in Fig. 12(a), (b), (c). (The average value for U_μ is about 10,000 cal.) Unfortunately, it is found that the data presently available are insufficient in scope for unique determination of U_μ. In fact, equally good fits were obtained [60] with either constant or variable U. Close fits would also be possible with other (more general) dependence of η_μ and t_e upon T, and so the fits of the test data presently known may not be interpreted as a proof that creep is a thermally activated process. But if the activation energy concept were not imposed, the degree of arbitrariness in material identification would be even higher. Thus, the purpose of the activation energy concept, as introduced here and in Refs. [60, 100], should be seen in the reduction of the number of unknown material parameters.

4.3 Microdiffusion Mechanism of Creep and Its Thermodynamics

At variable water content w (per unit volume of material), the strain history depends not only upon the stress history, but also upon the histories of water content w and temperature T (as is apparent from effects 9, 11, 12, 16, 17, 21–23, 26, 29, Section 2). As this functional dependence cannot be assumed to be linear, the number of unknown material parameters that would have to be introduced in formulating the constitutive equation becomes so large that, in addition to the limited creep and shrinkage data presently available, further information on the constitutive equation must be deduced from a material science type theory of the processes in the microstructure.

The walls of the pores in cement paste restrict the motion of adjacent water molecules and retain them in a fixed position for a certain "lingering time" (from 10^{-12} sec up), forming thus absorbed water layers. Their maximum thickness reaches 5 molecules [43, 110], so that a pore in cement paste must be at least 10 molecules (or 26.3 Å) thick to accommodate the complete adsorbed layers on two opposite walls. Such pores, called macropores, usually contain air with water vapor and, at a higher saturation, also capillary water if they are large enough to accommodate the capillary meniscus. Pores that are less than 10

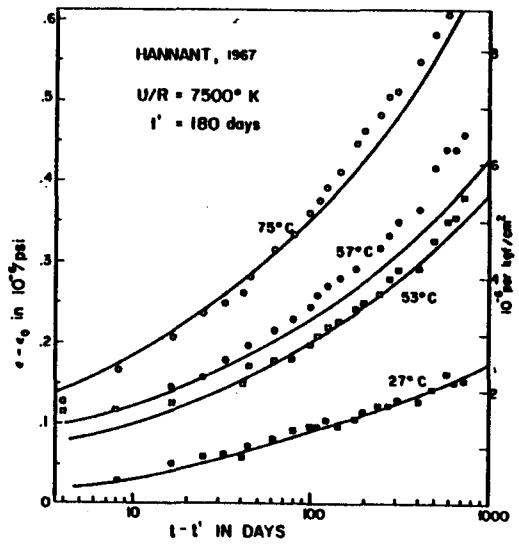

(a)

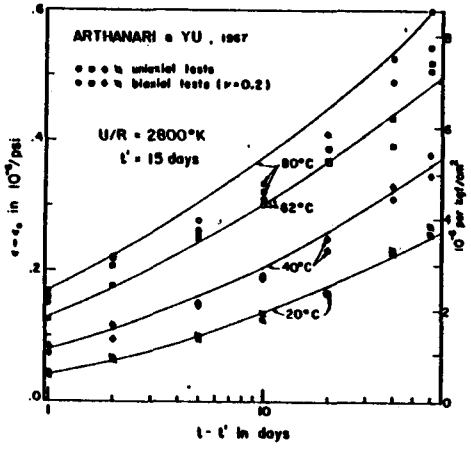

(b)

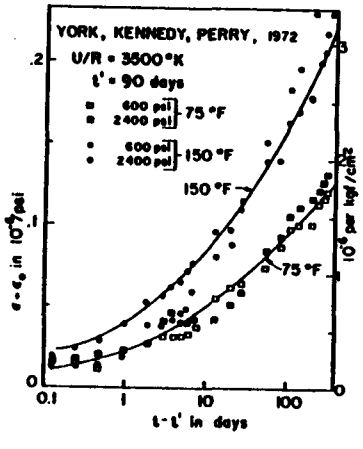

(c)

Fig. 12 (a) Hannant's tests of creep at various temperatures. Cylinders cured 5 months in water at 20°C, then sealed by copperfoil; 28-day cyl. strength 7800 psi; water–cement ratio 0.47; Oldbury limestone aggregate, stress $< \frac{1}{3}$ strength; ϵ_0 is instantaneous strain; solid lines show fits from Ref. [60] by Maxwell chain. (Data extracted from Hannant, D. J., "Strain Behavior of Concrete up to 95°C under Compressive Stresses," *Conf. on Prestressed Concrete Pressure Vessels*, Group C, Paper 17, Institution of Civil Engineers, London (1967) 57–71.) (b) Arthanari and Yu's biaxial tests of creep at various temperatures. Specimens sealed by epoxy coats; raised to test temperature 1 day before loading; cube strength

molecules thick will be called micropores. From the enormous internal surface of hardened cement paste (Section 2), it has been estimated that the solid particles of cement gel, believed to be essentially laminar in shape, are typically 30 Å thick and are separated by pores of average thickness 15 Å[43]. Hence micropores must constitute the major part of pore volume in cement gel. At a high enough degree of saturation by water, the micropores are completely filled by adsorbed water layers that cannot develop their full thickness, and are therefore called hindered adsorbed water layers. (These are assumed to include not only the physically adsorbed water[41, 110], i.e. molecules bound by van der Waals forces, but also the chemically bound interlayer hydrate water[35, 64] not more than 2 molecules in thickness; see Fig. 13.) Molecules in adsorbed layers are not held permanently and can diffuse along the solid surface. Such surface diffusion processes, also involving diffusion of some components of the adsorbent solids (Ca ions), cause a change of mass and thickness of the hindered adsorbed layers and are now widely believed to be the dominant mechanism of the time-dependent deformations of concrete under moderate stress levels.

Without solids diffusion, the aforementioned micromechanism was first proposed and thermodynamically discussed in 1965 and 1966 by Powers[43, 110], although a nonthermodynamic quantitative analysis had been made already in 1959 by Hrennikoff[111] and vague suggestions had been given by others in the 1930s[112, 113]. Partly different or even rival views of the creep and shrinkage mechanism were advanced by Feldman and Sereda[63, 64] and Wittmann[54, 114], without attempting to set up a constitutive equation (cf. also Ref. [116]). Powers' ideas were extended and translated into mathematical forms, which include solids diffusion, and the appropriate macroscopic constitutive equation was derived in

6000 psi; water–cement ratio 0.564; max. aggregate size $\frac{3}{4}$ in.; biaxial creep converted to uniaxial data using $\nu = 0.2$; ϵ_0 is initial instantaneous strain; solid lines show fits from Ref. [60] by Maxwell chain. (Data extracted from Arthanari, S., and Yu, C. W., "Creep of Concrete under Uniaxial and Biaxial Stresses at Elevated Temperature, *Mag. Concrete Res.* 19 (1967) 149–156.) (c) Creep tests at various temperatures and stress levels by York, Kennedy, and Perry (data on tests F-33, E-39, B-4, B-7). Specimens cured 83 days, sealed by epoxy and copper jackets, at 73°F; then raised to test temperature and tested; 28-day cyl. strength 6000 psi; water–cement ratio 0.425, limestone aggregate of max. size $\frac{3}{4}$ inch; stress ≤ 0.4 strength; ϵ_0 is initial instantaneous strain; solid lines how fits from [60] by Maxwell chain. (Extracted from York, G. P., Kennedy, T. W., and Perry, E. S., "Experimental Investigation of Creep in Concrete Subjected to Multiaxial Compressive Stresses and Elevated Temperatures," Research Report 2864-2, University of Texas, Austin (1970).)

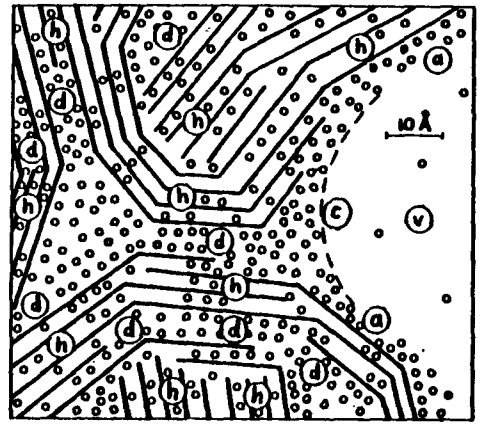

Fig. 13 Idealized microstructure of hardened Portland cement paste. *d*—physically adsorbed water; *h*—interlayer hydrate water; *a*—free adsorbed water; c—capillary water; *v*—vapor; thickness-to-length ratio of particles is strongly exaggerated (after Ref. [116].)

1968 (cf. Ref. [100]) and further refined in subsequent years [68, 115, 116]. This formulation serves as the basis of the exposition in the sequel. For the sake of brevity, only a simplified and abridged sketch will be given; for a detailed treatment see Ref. [116].

Alternative constitutive equations for porous materials with variable water content have also been studied in the spirit of modern continuum mechanics (but without quantitative relation to micromechanism of creep) by Creus and Onat [117] and Stouffer and Wineman [118, 119]. Their equations, however, have been linear and capable of modeling only very few of the effects listed in Section 2. In a very general context, concrete belongs to the class of interacting continua or mixtures whose thermodynamics was discussed by Bowen [120] and others, without any reference to concrete.

The usual formulation of surface thermodynamics [121, 122] due to Gibbs (dealing only with surface excess quantities) cannot be applied to hindered adsorbed layers (Fig. 14) because it implies zero thickness of the surface phase and prevents thus consideration of the changes in thickness $2l_d$ of the layer. Whereas extension to finite thickness [123] is useless for sorption studies concerned with pores that are not filled by adsorbed water (and is also dubious in view of the ambiguity in defining the thickness of the adsorbed layer), it is requisite [116] in the case of adsorption between two solid surfaces (whose change in distance can be defined rigorously).

The total energy $\bar{U}_w$ per unit mass of water in the hindered adsorbed layer (Fig. 14) is defined by the total differential $d\bar{U}_w = T\,d\bar{S}_w + dW$, where $T\,d\bar{S}_w$ is heat supplied to the unit mass of water, $\bar{S}_w$ is entropy per unit mass of water, $dW = -\pi'_w d(\Gamma_w^{-1}) + p_w\,dl_d/\Gamma_w =$ work done on the unit mass, l_d is half-thickness of the layer (Fig. 14), Γ_w^{-1} is the area covered by the unit mass of water, Γ_w is surface mass concentration, i.e., mass of water per unit area of layer and half-thickness; p_w is transversal pressure due to water (force per unit area of layer), called disjoining pressure; π'_w is total spreading pressure, i.e., resultant (over half-thickness l_d) of the compressive stresses in water along the layer. To deal with systems of variable mass, it is expedient to introduce a new potential that depends on T and π'_w instead of $\bar{S}_w$ and Γ_w^{-1}. This is achieved by Legendre transformation $\mu_w = \bar{U}_w - T\bar{S}_w + \pi'_w\Gamma_w^{-1}$. Differentiation and substitution of the previous expression for $d\bar{U}_w$ yields the total differential $d\mu_w = -\bar{S}_w\,dT + \Gamma_w^{-1}\,d\pi'_w + p_w\Gamma_w^{-1}\,dl_d$; μ_w is called Gibbs free energy per unit mass of water, or chemical potential. Similar relations can be written for solids in the layer, labeled by s instead of w. Thus, realizing

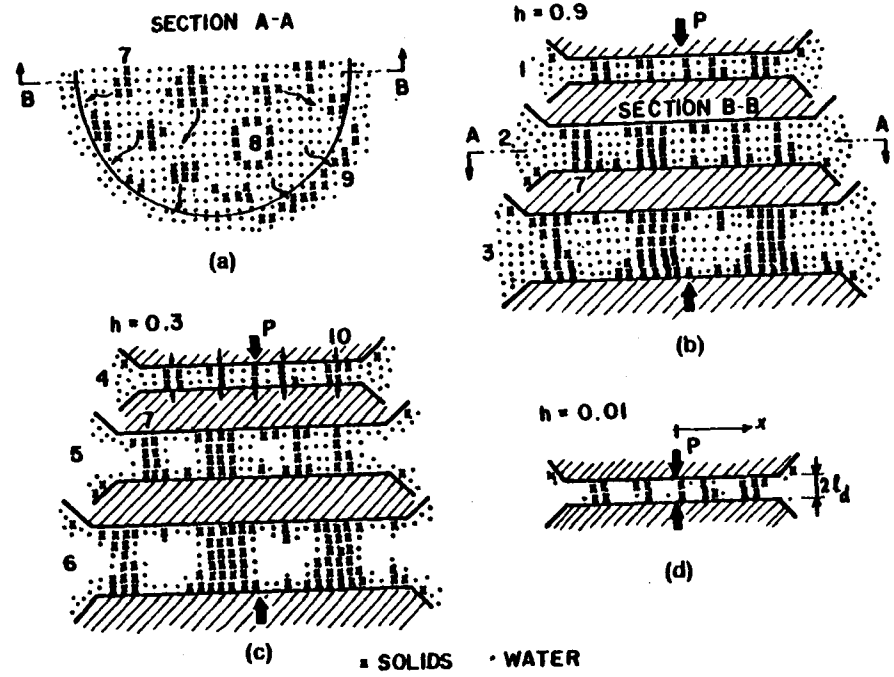

Fig. 14 Idealized hindered adsorbed water layers of various thicknesses. (a), (b) near saturation humidity; (c) at medium humidity; (d) at very low humidity. (Adapted from Ref. [125].)

that chemical potential must also depend on the relative surface concentration of solids, defined as $\xi = \Gamma_s/(\Gamma_s + \Gamma_w)$, one may write

$$d\mu_w = -\bar{S}_w\,dT + \Gamma_w^{-1}\,d\pi'_w - p_w\Gamma_w^{-1}\,dl_d + \frac{\partial\mu_w}{\partial\xi}\,d\xi$$
$$d\mu_s = -\bar{S}_s\,dT + \Gamma_s^{-1}\,d\pi'_s - p_s\Gamma_s^{-1}\,dl_d + \frac{\partial\mu_s}{\partial\xi}\,d\xi. \qquad (4.7)$$

However, the terms with $d\xi$ will be omitted in the subsequent analysis because changes in ξ are unessential for explanation of the effects from Section 2 to be considered in this section. (The present formulation also neglects electric phenomena arising from the fact that the diffusing solids are probably mainly calcium ions.)

Consider now a specified region α of the layer (referred to by superscript α) to be in equilibrium with its surroundings. Imagine an infinitesimal deviation from equilibrium in which mass dN_w^α is transferred into region α from some region β, which may represent another region of the hindered layer or some phase of water in the adjacent macropore (water adsorbed on its walls, capillary water or water vapor). The change of the Gibbs free energy of water in the regions α and β combined is $d\mathcal{G} = \mu_w^\alpha\,dN_w^\alpha + \mu_w^\beta(-dN_w^\alpha) = (\mu_w^\alpha - \mu_w^\beta)\,dN_w^\alpha$. According to the second law of thermodynamics, $d\mathcal{G} < 0$ for any finite change toward equilibrium, and $d\mathcal{G} = 0$ for any equilibrium (i.e. reversible) change and for an infinitesimal deviation from equilibrium. Hence $\mu_w^\alpha - \mu_w^\beta = 0$. Thus, in equilibrium the chemical potential of one component (e.g., water) must have the same value in all parts of the system that can exchange mass (a result well known in general from chemical thermodynamics[123]). (Rigorously, the chemical potential represents a tensor[116, 120], but for the present discussion this complication is unnecessary.)

Thus, thermodynamic equilibrium is characterized by zero gradients of μ_w and μ_s within the layer and, consequently, the isothermic diffusion fluxes $\mathbf{J}_w$, $\mathbf{J}_s$ of water and solids along the layer depend on these gradients. For sufficiently small gradients, the dependence must be linear, i.e.

$$\begin{Bmatrix}\mathbf{J}_w\\ \mathbf{J}_s\end{Bmatrix} = -\begin{bmatrix}a_{ww} & a_{ws}\\ a_{sw} & a_{ss}\end{bmatrix}\begin{Bmatrix}\operatorname{grad}\mu_w\\ \operatorname{grad}\mu_s\end{Bmatrix}, \qquad (4.8)$$

where $a_{ww}, \ldots$ are diffusion coefficients. Their dependence on temperature ought to obey the activation energy concept, i.e. be similar to Eq. (4.3). (By Onsager relations[124], $a_{ws} = a_{sw}$.) Conservation of mass

requires that

$$\frac{\partial\Gamma_w}{\partial t} = -\operatorname{div}\mathbf{J}_w, \qquad \frac{\partial\Gamma_s}{\partial t} = -\operatorname{div}\mathbf{J}_s. \qquad (4.9)$$

The equation of state of the hindered adsorbed layer is analogous to Hooke's law and can be shown[116] to have (for $d\xi \approx 0$) the form

$$\begin{Bmatrix}dp_w\\ d\pi'_w/l_d\end{Bmatrix} = \begin{bmatrix}C_{1w} & C_w\\ C_w & C_{2w}\end{bmatrix}\begin{Bmatrix}-dl_d/l_d + \alpha'_w\,dT\\ d\Gamma_w/\Gamma_w + \alpha''_w\,dT\end{Bmatrix}, \qquad (4.10)$$

in which C_{1w}, C_{2w}, C_w can be regarded as elastic moduli and α'_w, α''_w as linear thermal dilatation coefficients. (They can all be expressed as second partial derivatives of Helmholtz free energy $\bar{F}_w$ per unit mass of water ($\bar{F}_w = \bar{U}_w - T\bar{S}_w$) with respect to l_d, Γ_d and T[116].) A similar equation of state may be written for solids in the layer.

In thermodynamic equilibrium, the thickness, l_a, of the (unhindered) adsorbed water layer on the walls of a macropore is larger, the higher is humidity h (relative vapor pressure) of the vapor in the macropore. (Thicknesses of 1, 2, and 5 molecules occur, at 25°C, for $h = 0.12, 0.51, 1.0$, and $\frac{1}{2}$ of monomolecular layer occurs at $h = 0.03$[43].) A pore of given thickness becomes filled by adsorbed water at a certain humidity $h = h_f$ for which $l_a \approx l_d$ (actually even earlier, because of the formation of surface meniscus). The corresponding transversal pressure $p_w = p_f$ is probably small, $p_f \approx 0$. But for $h > h_f$, when full thickness l_a cannot be accommodated on both surfaces confining the layer, p_w becomes very large. Imagine an equilibrium process in which h is gradually changed at constant T while l_d is kept constant. The change of chemical potential of vapor in the macropore μ_v may be expressed assuming the vapor to obey the ideal gas equation, $p_v/\rho_v = RT/M$, where p_v is vapor pressure, ρ_v is its mass density, $M = 18.02$ g/mole = molecular weight of water, $R = 82.06\ \text{cm}^3\,\text{atm}\ (\text{deg K} \times \text{mole})^{-1}$ = gas constant. Then, at constant T, $d\mu_v = \rho_v^{-1}\,dp_v = RM^{-1}T\,dp_v/p_v = RM^{-1}T\,d(\ln h)$. The equilibrium change of chemical potential in the layer must be the same, i.e. $d\mu_w = d\mu_v$. Integrating, one shows that the chemical potential of water in any phase that is in equilibrium with vapor of humidity h equals

$$\mu_w = RM^{-1}T\ln h + \mu_{vs}(T), \qquad (4.11)$$

where μ_{vs} is the value of μ_w at $h = 1$. Furthermore, eliminating $d\Gamma_w$ from Eq. (4.10)[116], one obtains

$$dp_w = \frac{\nu_w}{l_d}\,d\pi'_d, \qquad \text{at } dl_d = dT = 0, \qquad (4.12)$$

and so

$$dp_w = \nu_w\rho_w RM^{-1}T\,d(\ln h), \qquad \text{at } dl_d = dT = 0, \qquad (4.13)$$

in which $\nu_w = C_w/C_{2w}$, $\rho_w = \Gamma_w'/l_d$. Equation (4.13) is valid for both completely and partially filled pores. If the pore is filled, ν_w and ρ_w are probably almost constant, and Eq. (4.13) can be integrated, furnishing the equilibrium value:

$$p_w = p_w(h, T) = \nu_w \rho_w R M^{-1} T \ln h + p_1(T), \tag{4.14}$$

in which $p_1(T) = p_f(h, T) - p_w(h_f, T)$. For example, for a pore of two molecules in thickness ($h_f = 0.12$), and with $\rho_w = 1\ \mathrm{g/cm^3}$, $\nu_w \approx 0.6$[125], and $p_1 \approx 0$, Eq. (4.8) yields $p_w = 1720$ atm at 25°C and $h = 1.0$. This huge pressure is resisted by the solid framework in the material. It explains, in part, the small tensile strength and also the increase of strength due to drying (effect 28, Section 2), because p_w drops with h.

For a hindered adsorbed layer of specified geometry, the time variation of thickness l_d due to a given history of the resultant of pressure p_w at a given history of T and h can be solved from differential equations (4.8), (4.9), (4.7), and (4.10) with appropriate boundary conditions for p_w [see Eq. (4.14)]. Numerical studies of this initial boundary-value problem[125] confirm that several effects in creep due to variable humidity (effects 11, 12, 16, 21, Section 2) can indeed be modeled, provided a_{ss} and a_{ww} are considered to be dependent upon grad μ_w and grad μ_s (which makes the problem nonlinear). Two types of hindered layers are considered: a layer of uniform thickness l_d filled over the whole area and a layer of variable thickness between two spherical surfaces in which the filled region varies its area. It is found that for modeling the main phenomena in creep, the simpler model of a layer of uniform thickness is sufficient. (In the unfilled region, the dependence of C_w, C_{1w}, C_{2w} upon Γ_w, derived in Ref. [125], is quite strong and adds to nonlinearity of the problem. A simplified statistical–mechanical theory is available for the equilibrium states in this case[116, 126].)

4.4 Constitutive Equation at Variable Temperature and Humidity

The creep mechanism outlined in the previous section is only a hypothesis. However, as later discussions will show, it allows for modeling and explanation of most of the effects listed in Section 2, which speaks strongly in its support.

To relate the equations for the diffusion in the micropores to the macroscopic stress–strain relations, a hindered adsorbed layer of uniform thickness $2l_d$ will now be treated in a rather simplified manner, using solely quantities averaged over the whole layer. Because the creep strains

observed are always small, the average change of l_d must also be small. On this basis, the term with dl_d may be neglected in Eq. (4.7)[116], and relation (4.7) may be utilized. If the layer is assumed to be initially in thermodynamic equilibrium (characterized by $T = T_0$, $p_w = p_{w_0}$, $\mu_w = \mu_{w_0}$, $h = h_0$, etc.), then Eq. (4.7) with Eq. (4.12) yields, for a sufficiently small deviation from the initial state,

$$\begin{aligned} \mu_w - \mu_{w_0} &= -\bar{S}_w(T - T_0) + l_d \nu_w^{-1}(p_w - p_{w_0}), \\ \mu_s - \mu_{s_0} &= -\bar{S}_s(T - T_0) + \Gamma_s^{-1} l_d \nu_s^{-1}(p_s - p_{s_0}). \end{aligned} \tag{4.15}$$

Within the adjacent macropore, migration of water molecules is relatively very fast, so that the water adsorbed on its walls, as well as the capillary water, may be assumed to remain in equilibrium with water vapor of humidity h at any time. Thus, according to Eq. (4.11), the values of μ_w, μ_s at the boundary B between the hindered layer and the macropore are

$$\begin{aligned} \mu_w^B - \mu_{w_0} &= -\bar{S}_w^B(T - T_0) + \frac{RT}{M} \ln \frac{h}{h_0}, \\ \mu_s^B - \mu_{s_0} &= -\bar{S}_s^B(T - T_0), \end{aligned} \tag{4.16}$$

in which the transverse pressure in solids in the (unhindered) adsorbed layer is taken as $p_s^B \approx p_{s_0}^B \approx 0$. The average mass fluxes into the layer are $f_d \dot{\Gamma}_w / L_d$ and $f_d \dot{\Gamma}_s / L_d$, where f_d is the area of the layer, L_d is length of its boundary with the macropore. Thus, in analogy with Eq. (4.8),

$$\begin{Bmatrix} f_d \dot{\Gamma}_w / L_d \\ f_d \dot{\Gamma}_s / L_d \end{Bmatrix} = \begin{bmatrix} a_{ww} & a_{sw} \\ a_{ws} & a_{ss} \end{bmatrix} \begin{Bmatrix} (\mu_w^B - \mu_w)/D \\ (\mu_s^B - \mu_s)/D \end{Bmatrix}, \tag{4.17}$$

where D is a certain average distance of flow. From Eq. (4.10),

$$\frac{\dot{\Gamma}_w}{\Gamma_w} = c_w \frac{\dot{l}_d}{l_d} + \frac{\dot{p}_w}{C_w} - \bar{\alpha}_w \dot{T}, \tag{4.18}$$

where $c_w = C_{1w}/C_w$, $\bar{\alpha}_w = \alpha_w'' + c_w \alpha_w'$. To correlate the microscopic quantities with macroscopic (uniaxial) strain ϵ and the macroscopic stresses, it will be assumed that

$$l_d = \frac{\dot{\epsilon} - \dot{\epsilon}_S(h) - \alpha_1 \dot{T}}{n_d}, \qquad p_s - p_{s_0} = \frac{-\sigma_\mu^s}{f_d}, \qquad p_w - p_{w_0} = \frac{-\sigma_\mu^w}{f_d}, \tag{4.19}$$

where n_d may be visualized as double the number of hindered adsorbed layers of a similar type intersecting a unit length in the material and f_d as the total area occupied by these layers per unit area of the material; σ_μ^s and σ_μ^w are macroscopic hidden stresses due to solids and water in layers

of a similar type; $\epsilon_S(h)$ and $\alpha_1\dot{T}$ are shrinkage strain and thermal dilatation due to solid particles between the hindered layers. Now, if Eqs. (4.19), (4.15), (4.16), and (4.18) with a similar relation for $\dot{\Gamma}$, are substituted into Eq. (4.17), one obtains

$$\begin{aligned}\dot{\sigma}_{s_\mu} + \phi_{ss_\mu}\sigma_{s_\mu} + \phi_{sw_\mu}[\sigma_{w_\mu} - f_\mu(h, T)] &= E_\mu^{\,s}(\dot{\epsilon} - \dot{\epsilon}_S(h) - \alpha_\mu^{\,s}\dot{T}),\\ \dot{\sigma}_{w_\mu} + \phi_{ws_\mu}\sigma_{s_\mu} + \phi_{ww_\mu}[\sigma_{w_\mu} - f_\mu(h, T)] &= E_\mu^{\,w}(\dot{\epsilon} - \dot{\epsilon}_S(h) - \alpha_\mu^{\,w}\dot{T}),\end{aligned} \tag{4.20}$$

where

$$E_\mu^{\,s} = \frac{f_d^2 c_s \Gamma_s C_s}{n_d L_d l_d}, \qquad E_\mu^{\,w} = \frac{f_d^2 c_w \Gamma_w C_w}{n_d L_d l_d}, \tag{4.21}$$

$$\phi_{ss_\mu} = \frac{C_s l_d a_{ss}}{\nu_s D}, \qquad \phi_{ww_\mu} = \frac{C_w l_d a_{ww}}{\nu_w D}, \tag{4.22}$$

$$\phi_{sw_\mu} = \frac{C_s l_d a_{sw}}{\nu_w D}, \qquad \phi_{ws_\mu} = \frac{C_w l_d a_{ws}}{\nu_s D},$$

$$\alpha_\mu^{\,s} = \frac{n_d L_d l_d \bar{\alpha}_s}{c_s \Gamma_s f_d} + \alpha_1, \qquad \alpha_\mu^{\,w} = \frac{n_d L_d l_d \bar{\alpha}_w}{c_w \Gamma_w f_d} + \alpha_1, \tag{4.23}$$

$$\begin{aligned} f_\mu(h, T) &= \sigma_\mu^{\,h} + \nu_d \frac{f_d}{l_d}(\bar{S}_w^{\,B} - \bar{S}_w)(T - T_0),\\ \sigma_\mu^{\,h} &= \nu_w \frac{f_d}{l_d}\frac{RT}{M}\ln\left(\frac{h_0}{h}\right).\end{aligned} \tag{4.24}$$

The difference in entropies of solids, $\bar{S}_s^{\,B} - S_s$, has been considered here as negligible for lack of any evidence to the contrary. Subscript $\mu = 1, 2, \ldots, n$ is appended to all coefficients in order to distinguish between hindered adsorbed layers of various types (in area, thickness, for example) characterized by different rates of the diffusion processes. The condition of equilibrium of hidden stresses may be written as

$$\sum_{\mu=1}^{n}(\sigma_{s_\mu} + \sigma_{w_\mu}) = \sigma. \tag{4.25}$$

In a more rigorous approach, Eqs. (4.20) can be derived from the principle of minimum entropy production [98] introducing assumed distributions instead of averaged quantities (cf. Ref. [115]). But expressions (4.21) to (4.24) would then be more complicated.

For lack of experimental information on the microstructure, it should not be expected that the material parameters could be predicted from Eqs. (4.21) to (4.24). The merit of the foregoing considerations is to be seen mainly in the fact that a rational form of the constitutive equation has been deduced.

The temperature dependence of the diffusion coefficients $a_{ww}, \ldots$ in Eq. (4.8) may logically be assumed to obey the activation energy concept. Thus, in view of Eq. (4.22),

$$\phi_{ww_\mu} = \phi^{\,h}_{ww_\mu}\phi_T, \qquad \phi_{ss_\mu} = \phi^{\,h}_{ss_\mu}\phi_T, \qquad \phi_{sw_\mu} = \ldots,$$

with

$$\phi_T = \exp\left[\frac{U_\mu}{R}\left(\frac{1}{T_0} - \frac{1}{T}\right)\right], \tag{4.26}$$

where $\phi^{\,h}_{ww_\mu}, \ldots$ are coefficients that depend on h, approximately in the form indicated in Fig. 11, and also on the stress level. Equation (4.3), introduced previously for creep at variable T and constant water content, is thus a special case of the present formulation.

Adding Eqs. (4.20), we see that the rate-type creep equation (3.36) for constant h and T is a special case of Eqs. (4.20) if $\phi_{ss_\mu} + \phi_{ws_\mu} = \phi_{sw_\mu} + \phi_{ww_\mu} = E_\mu/\eta_\mu = 1/\tau_\mu$, $E_\mu^{\,s} + E_\mu^{\,w} = E_\mu$, $\sigma_{s_\mu} + \sigma_{w_\mu} = \sigma_\mu$. Thus, Eqs. (4.20), along with Eq. (4.25), may be viewed as a generalization of the creep law based on Maxwell chain, which was previously found to be a suitable model and may be visualized as is shown in Fig. 15, in which moduli $E_\mu^{\,s}$, $E_\mu^{\,w}$ are interpreted by the springs, and the diffusion processes of various speeds, corresponding to rate coefficients $\phi_{ss_\mu}, \ldots$, are depicted by the layer-shaped diffusion elements. In view of this result and the discussion of the data fitting by Dirichlet series in Section 3, it is no infringement on generality to assume that, at low-stress levels,

$$\phi^{\,h}_{ss_\mu} = \phi^{\,h}_{ww_\mu} = \frac{1}{\tau_\mu}, \qquad \phi^{\,h}_{sw_\mu} = \phi^{\,h}_{ws_\mu} = \frac{c_\mu}{\tau_\mu} \qquad \text{for} \quad h = 1, \tag{4.27}$$

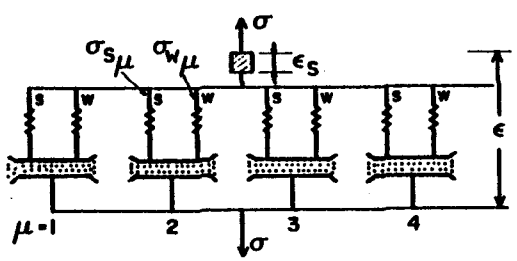

Fig. 15 Idealized model of the interaction of water and solids with diffusion elements of various relaxation times. (Generalization of Maxwell chain from Fig. 10(a).)

where c_μ is a function of μ, and τ_μ is given by Eq. (3.16). Equality of $\phi^h_{s_\mu}$ and $\phi^h_{w_\mu}$ is also justified by the fact that significant coupling can exist only between diffusion processes of roughly equal rates.

Equations (4.20) and (4.25) interpret creep alone when all stress-independent terms are neglected, i.e. $\dot{\epsilon}_{s_\mu}{}^0 = \dot{\epsilon}_{w_\mu}{}^0 = f_\mu = 0$. The mechanism of creep may be imagined as follows. As macroscopic compressive stress σ is applied, transversal pressures p_s, p_w and, according to Eq. (4.10) or Eq. (4.12), spreading pressures π'_s and π'_w are increased. This alters μ_s and μ_w [Eqs. (4.15) and (4.7)] and destroys thermodynamic equilibrium because $\mu_s{}^B$, $\mu_w{}^B$ in the adjacent macropore is not affected. As a result, solids and water begin migrating out of the hindered adsorbed layers, and their thickness l_d is thus decreased. If tension is applied, the reverse process is set off.

Drying shrinkage (Fig. 16) is interpreted by Eqs. (4.20) and (4.25) as the strain at $\sigma = \dot{T} = 0$ that is due to $\epsilon_S(h)$ and $\sigma_\mu{}^h$. (Their approximate dependence on h is shown in Fig. 11.) Thermodynamic equilibrium between the hindered layer and the macropore is characterized by the condition $\sigma_{w_\mu} = f_\mu(h, T)$. If pore humidity h drops down, $\mu_w{}^B$ is decreased [Eq. (4.11) or Eq. (4.16)], and the initial thermodynamic equilibrium is destroyed. In Eq. (4.20) this is manifested by creation of a nonzero difference $\sigma_{w_\mu} - f_\mu(h, T)$. As a result, water molecules start flowing out of the hindered layers and drag some solids in the layer with them. The inherent gradual loss of solid mass per unit area of the layer causes a gradual decrease of the thickness. This type of shrinkage, reflected by terms $\sigma_\mu{}^h$, is always delayed with regard to the drop in h. (In contrast with creep, the delays probably do not exceed one month; effect 23, Section 2.) Noteworthy is the fact that the delayed shrinkage is governed by the same hidden stresses as the creep. This conforms with the identity of their physical mechanisms.

In addition, a drop in h also results in higher surface tension (or lower spreading pressure) on the walls of nonsaturated pores. To equilibrate the surface tension, compression stress is immediately generated within the solid particles, giving rise to elastic compression, manifested as shrinkage. This type of shrinkage, reflected by the term $\epsilon_S(h)$, appears immediately with the drop in pore humidity.

Shrinkage stress is the stress induced by shrinkage when some deformation component is prevented, e.g., $\epsilon = 0$. It is instructive to realize that, for the simplified case $\phi_{sw_\mu} = \phi_{ws_\mu} = \epsilon_S = 0$, and for $h(t)$ in the form of a step function with step at t_0 (which can occur only in infinitely thin specimens), integration of Eq. (4.20) leads to the Dirichlet series:

$$\sigma(t) = \sum_\mu \sigma_{w_\mu}(t) = \sum_\mu \sigma_\mu{}^h(t_0)(1 - e^{\phi_{ww_\mu}(t-t_0)}). \tag{4.28}$$

This is only that part of shrinkage stress that is due to delayed shrinkage, and it is noteworthy that it varies monotonously in time because all $\sigma_\mu{}^h$ are of the same sign. Superimposed upon it is the part due to instantaneous shrinkage $\epsilon_S(t)$, which may reach a maximum at a finite time (and so may the total shrinkage stress; cf. Fig. 27).

If a phenomenological approach were taken, then the Dirichlet series expansion of the stress induced by delayed shrinkage would show, without reference to any physical model, that terms of the type of f_μ should appear in Eq. (4.20).

Thermal dilatations of concrete are known from experiments to be an extremely complicated phenomenon (cf. Ref. [68]). They depend strongly on water content and exhibit an aftereffect, i.e. continue after the temperature change has ceased. By physical source, three different components can be distinguished [68, 116].

1. Pure thermal dilatation, which is due to the thermal dilatation coefficients $\alpha_\mu{}^s$, $\alpha_\mu{}^w$ for solids and water. Because probably $\alpha_\mu{}^s > \alpha_\mu{}^w$, warming creates disjoining pressure in water, which, in turn, induces a flow out of the hindered layer and leads to some recovery of thermal dilatation. This effect must be smaller, the lower the water content.

2. Thermal shrinkage or swelling, which is introduced through the terms $f_\mu(h, T)$ in Eqs. (4.20) and is caused by the difference in entropy densities, $\bar{S}_w{}^B - \bar{S}_w$, in Eqs. (4.24). Considering that $\bar{S}^V = \bar{S}_w{}^B + Q_w{}^B/T_0 = \bar{S}_w + Q_w/T_0$, where $\bar{S}^V$ is the entropy per unit mass of vapor in the macropore, and Q_w, $\bar{S}_w$, $Q_w{}^B$, $\bar{S}_w{}^B$ are latent heats and entropies per unit mass of adsorbed water within the hindered layer and on its boundary, i.e. on the walls of the macropore, one obtains

$$\bar{S}_w{}^B - \bar{S}_w = \frac{Q_w - Q_w{}^B}{T_0}. \tag{4.29}$$

Here always $Q_w > Q_w{}^B$ and $\bar{S}_w{}^B > \bar{S}_w$ because the water molecules within the hindered layers must be held stronger than those at the walls of macropore (and must also exhibit less disorder). Thus, according to Eq. (4.7), warming destroys initial equilibrium $\mu_w = \mu_w{}^B$ and produces a difference $\mu_w - \mu_w{}^B > 0$, setting off a flow out of the hindered layers and causing some of the dilatation to recover with a certain delay. This effect also must be less at a smaller water content.

3. Hygrothermic dilatation, which is introduced through the terms f_μ and $\sigma_\mu{}^h$. It is due to the rise in h that is produced by a rise in T at constant

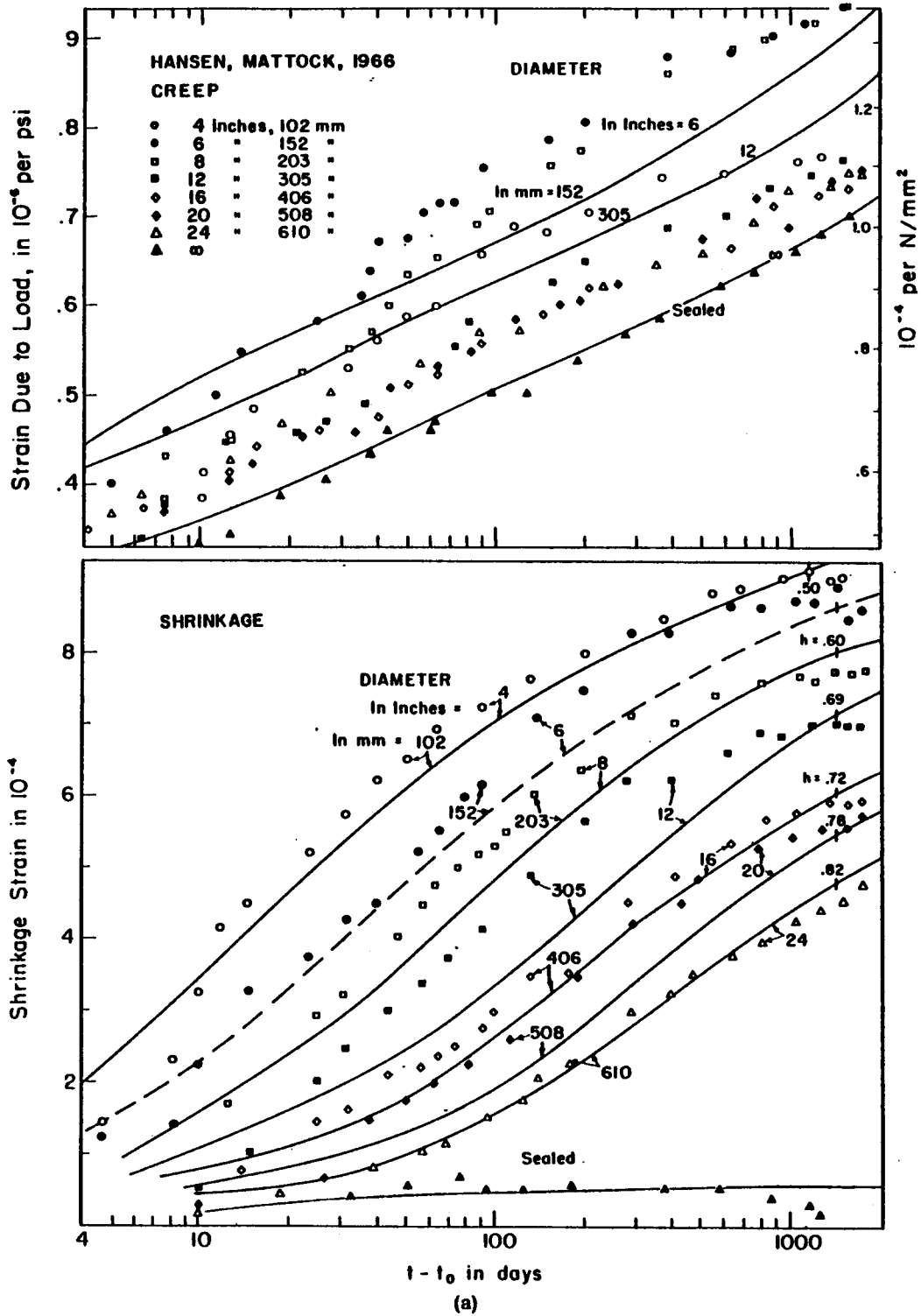

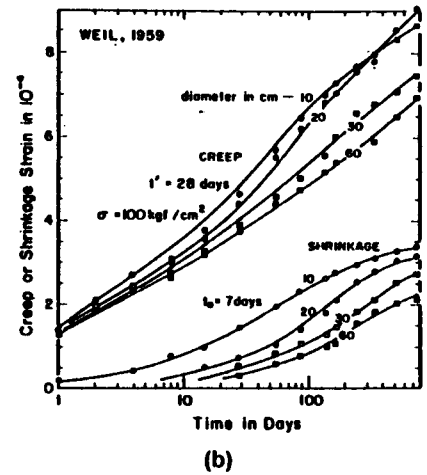

Fig. 16 (a) Hansen and Mattock's data on the effect of size on shrinkage and creep of specimens drying at $h_e = 0.50$. Cylinders sealed at ends; 28-day cyl. strength ≈ 6000 psi; Elgin gravel (92 percent calcite, 8 percent quartz) max. size ¾ in., 500 lb of ASTM type III cement per cubic yard of concrete; cured 2 days in mold and 6 days in fog at 70°F; tested at 70°F; loaded and exposed to drying at 8 days of age; stress ≈ ½ of 8-day strength; Young's modulus at loading $\approx 3.7 \times 10^6$ psi; h-values in the figure indicate measured h in the axis of cylinder. The solid lines are the fits[166] obtained for $f'_c = 500$ psi, $S_t = 260$ psi, $S_\infty = 0.0011$, $C_\infty = 0.032$ in.²/day, and $B = 0$, according to Eqs. (4.34a) to (4.34c). (Data for 1777 psi are out of range of the theory and are not fitted.) (Data points constructed after Hansen, T. C., and Mattock, A. H., "Influence of Size and Shape of Member on the Shrinkage and Creep of Concrete," *Amer. Concrete Inst. J.* 63 (1966) 267–290.) (b) Weil's data on the effect of size on shrinkage and creep of specimens drying at $h_e = 0.65$. Cylinders, 4 diameters long; concrete of 246 kgf/cm² cyl. strength and 306 kgf/cm² cube strength, 28-day el. modulus at 10th loading 269,000 kgf/cm²; water–cement–aggregate ratio 0.52:1:5.4; Rhine sand and gravel (mostly quartz); 7 days of moist curing, then exposed to drying ($t_0 = 7$); loading at $t' = 28$ days; 20°C; shrinkage or creep time shown is measured from instant t_0 or t', respectively; creep strain does not include instantaneous strain; measured on the middle half-length, on the surface. (Data adapted from Weil, G., "Influence des Dimensions et des Tensions sur le Retrait et le Fluage de Béton," *RILEM Bull.*, No. 3 (1959) 4–14, Figs. 5, 6.)

w and is characterized by the hygrothermic coefficient $\kappa = (\partial h/\partial T)_w \geq 0$ [cf. Eq. (4.38) below]. This causes an increase of $\mu_w{}^B$ and generates flow of water into the hindered layers, which causes them to expand. This dilatation is also delayed. It represents continued dilatation rather than recovery. It is zero at $h = 0$ and reaches maximum at $h \approx 0.7$, as is indicated by the diagram of κ in Fig. 11. At $h = 1$, it is negligible (except at temperatures above 100°C, at which it can be large because the high pressure of the steam in the macropores is no longer negligible as a loading of the material).

As a result of this complex picture, thermal dilatation depends on h and on time, as is qualitatively indicated in Fig. 17[68]. Existing test data (cf. Ref. [68]) support this qualitative picture, but are probably insufficient to formulate the phenomenon quantitatively.

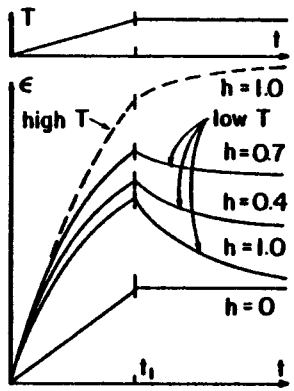

Fig. 17 Typical delayed thermal dilatations at various humidities h (after Ref. [68]).

Imposing the condition of isotropy, one can generalize Eqs. (4.20) and (4.25) to multiaxial stress as follows:

$$\begin{aligned}\dot{\sigma}_{s_\mu}{}^V + \phi^V_{ss_\mu}\sigma_{s_\mu}{}^V + \phi^V_{sw_\mu}[\sigma_{w_\mu}{}^V - f_\mu{}^V(h,T)] &= 3K_\mu{}^s(\dot{\epsilon}^V - \dot{\epsilon}_S(h) - \alpha_\mu{}^s\dot{T}),\\ \dot{\sigma}_{w_\mu}{}^V + \phi^V_{ws_\mu}\sigma_{s_\mu}{}^V + \phi^V_{ww_\mu}[\sigma_{w_\mu}{}^V - f_\mu{}^V(h,T)] &= 3K_\mu{}^w(\dot{\epsilon}^V - \dot{\epsilon}_S(h) - \alpha_\mu{}^w\dot{T}),\end{aligned} \tag{4.30}$$

$$\begin{aligned}\dot{\sigma}_{s_\mu}{}^D + \phi^D_{ss_\mu}\sigma_{s_\mu}{}^D + \phi^D_{sw_\mu}\sigma_{w_\mu}{}^D &= 2G_\mu{}^s\dot{\epsilon}^D\\ \dot{\sigma}_{w_\mu}{}^D + \phi^D_{ws_\mu}\sigma_{s_\mu}{}^D + \phi^D_{ww_\mu}\sigma_{w_\mu}{}^D &= 2G_\mu{}^w\dot{\epsilon}^D,\end{aligned} \tag{4.31}$$

$$\begin{aligned}\sum_\mu(\sigma_{s_\mu}{}^V + \sigma_{w_\mu}{}^V) &= \sigma^V,\\ \sum_\mu(\sigma_{s_\mu}{}^D + \sigma_{w_\mu}{}^D) &= \sigma^D, \qquad \mu = 1,2,\ldots,n,\end{aligned} \tag{4.32}$$

where superscripts V and D distinguish between the volumetric and the deviatoric components of stress and strain tensors $\sigma = [\sigma_{ij}]$ and $\epsilon = [\epsilon_{ij}]$ and label the corresponding coefficients. Note that, because of isotropy, no stress-independent terms analogous to f_μ and ϵ_S can appear in Eqs. (4.31). [Actually, the incremental creep properties at high stress seem to be distinctly anisotropic, but experimental information is insufficient for a realistic generalization of Eqs. (4.30) to (4.32).]

Recalling the discussion that justified Eq. (4.27), one may assume that, at $h = 1$ and low-stress levels, $\phi^V_{ss_\mu} = \phi^D_{ss_\mu}$, $\phi^V_{ww_\mu} = \phi^D_{ww_\mu}$, etc.

According to the present model, the deviatoric creep is not mainly controlled by a slip but by diffusion from compressed layers normal to one principal direction of stress deviator into expanding layers normal to another principal direction[100, 115], while the volumetric creep corresponds to equal compression of layers of all directions and diffusion into the macropores. A slip may also be involved in creep deformation, but seems not to be the rate-controlling process, since otherwise, for one reason, it would be hard to explain that, in contrast with metals, polymers, and (highly porous) clays, the volumetric creep is equally pronounced as the deviatoric creep (effect 4, Section 2). (Furthermore, slip could not account for the similarities between shrinkage and creep, apparent from effects 11, 14, and 16, Section 2).

The fact that at constant pore humidity h the creep rate is greater, the higher is h (effect 9, Section 2) (Fig. 18) [28–33] may be explained by considering that hindered adsorbed layers of different thicknesses and areas (Fig. 14) contribute to creep. The mobility of solids must be contingent upon the presence of water since in a perfectly dry state the creep is very small[28–33]. Thus, as thicker and thicker layers become filled at increasing h, more and more solids become mobile, and the creep rate must grow. The main increase should occur at higher humidities (effect 9, Section 2), at which the thicker pores with weaker held and potentially more mobile solids [Fig. 14(b), (c)] become filled.

Extending the original Powers' ideas on adsorbed water[43, 110], the diffusion of solids including dissolution of solids from the solid surfaces and their reprecipitation at different locations has been proposed as an essential part of the creep mechanism[100, 115, 116]. This mechanism, which has not been previously included in the mathematical formulation, should be regarded as a hypothesis. Though it has not been experimentally confirmed (and could hardly be, because of the extremely small amounts of solids that need be involved to account for the small creep strains), it is plausible because hydration, as any chemical reaction, may be reversed when the sign of the free energy difference is altered due to a change in σ or h, and because the solid microstructure is rather mobile, as is evidenced by the fact that cracks heal under compression[71] and hydrated cement powder can be compacted into a solid body by pressure at room temperature[63]. The hypothesis of solids diffusion is inevitable if one should explain phenomena 1 to 7 listed below.

1. If there were no solids connecting the opposite surfaces in the

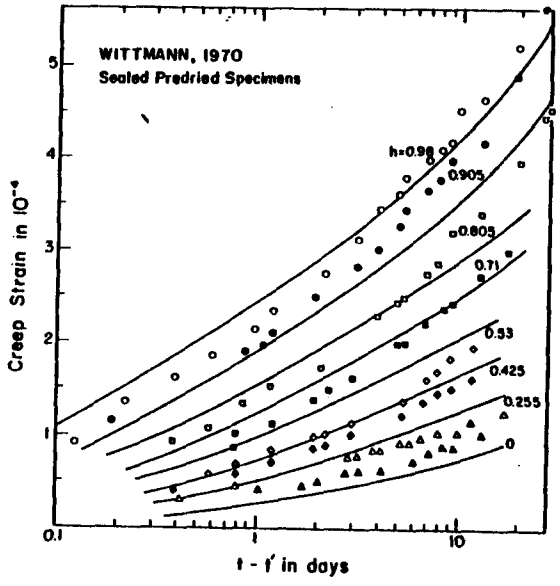

Fig. 18 Wittmann's tests of creep at various constant water contents. Solid cement paste cylinders 18 × 60 mm; water–cement ratio 0.4; cured sealed for 28 days at 20°C; then dried in oven at 105°C for 2 days, resaturated for 3 months at various constant humidities h shown, at 20°C. Then tested for creep in the same environment under stress 150 kgf/cm² equal 0.2 of failure stress before test; $E \approx 210{,}000$ kgf/cm² for 1 min loading; strain at 1 hour under load is subtracted from values shown. The solid lines are fits[166] for $S_t = 240$ psi, $S_0 = 0.0004$, $C_0 = 0.025$ in.²/day, and $B = 0.4$, obtained according to Eqs. (4.34a) to (4.34c). (Data points constructed after Wittmann, F., "Einfluss des Feuchtigkeitsgehaltes auf das Kriechen des Zementsteines," *Rheol. Acta* 9 (1970) 282–287, Fig. 1.)

hindered layer, either the surfaces would collapse together on complete drying, which would yield a large shrinkage strain (of the order of 0.1), or a sharp elastic modulus drop would occur, none of which is true (effect 10).

2. If the solid particles confining the hindered layer actually came to contact on full drying, the creep that follows rewetting could not be greater than the previous swelling, which contradicts effect 16, Section 2. On the other hand, creep must be unbounded if solids can dissolve from the surfaces confining the layer, diffuse out, and precipitate near the entrance of the layer [2 in Fig. 19(b)].

3. The substantial decrease of the internal surface area (accessible to water), which is caused by wetting–drying cycles (effect 30, Section 2) can be explained only by assuming that the diffusing water molecules knock out some of the solid molecules over their activation energy barriers, exerting thus a drag on the solids and driving some of them toward the

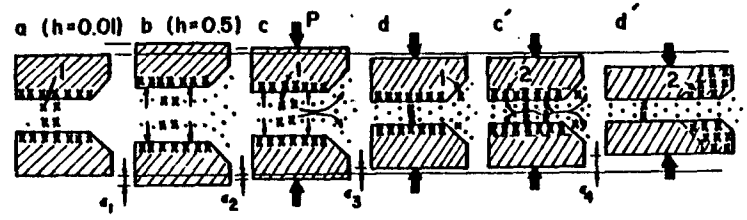

Fig. 19 Various hypothetical stages in relative displacement of two solid adsorbent particles of cement paste at swelling followed by creep; crosses = solids, dots = water (after Ref. [125]).

entrances to the micropores, where they precipitate and block the access into the pore [9 in Fig. 14(a)] or create inaccessible enclaves [8 in Fig. 14(a)]. This effect should be again more pronounced when the wetting–drying cycle reaches into higher h (as observed in Ref. [63]) because thicker pores with more mobile solids become involved. The changes of pore structure due to diffusion of solids also explain the significant hysteresis of desorption–sorption isotherms (effect 30, Section 2) and other irreversibility (effects 22, 10, Section 2).

4. Blocking of the micropores by the diffusing and reprecipitating solids (Fig. 14) can be caused by only a minute amount of solids. This can explain why creep properties continue changing with age long after the growth of elastic modulus with age has ceased (effect 19, Section 2).

5. The aforementioned blocking, together with an increase in area and transverse stiffness of the hindered layer due to solids reprecipitating near its boundary [Fig. 14(d)], can explain why, after a long period of creep, the elastic and creep compliances for subsequent load increments decrease (effect 8, Section 2), and probably also gain anisotropic form.

6. On reaching full saturation, creep does not drop, even though water transfer to macropores becomes hindered; see p. 49.

7. Finally, it appeared impossible to model the drying creep effect (item 11, Section 2) (Figs. 20 and 21) without diffusion of solids[125, 166].

The smallness of the drop in elastic modulus on drying (effect 10, Section 2) implies that the stiffness of solids across the layers must be much higher than that of water, or $E_\mu^s \gg E_\mu^w$ (roughly $E_\mu^w \approx 0.1 E_\mu^s$). This is further supported by the fact that the volume compressibility of water is much higher than that of concrete[100]. Thus, the applied load is carried across the layer essentially by solids; i.e. water is not important as a load-bearing component, contrary to a previous hypothesis[43, 110]. However, by means of the disjoining pressure caused by a change in h [Eq. (4.14)], water can introduce into the microstructure large forces.

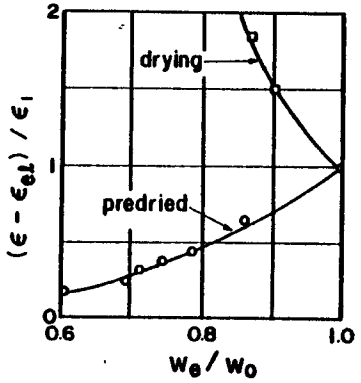

Fig. 20 Ruetz's data on creep of drying and predried specimens. Solid cement paste cylinders 17×60 mm, 28 days old; moist cured; water–cement ratio 0.5; stress σ = 100 kfg/cm², at 20°C; ϵ, ϵ_1 = 6-day creep strain at evaporable water content w_e and at saturation value $w_e = w_0$; ϵ_{el} = instantaneous (elastic) strain on loading; approximately $w_e/w_0 \approx h$; drying specimens were exposed from the moment of loading to air of h yielding equilibrium water content w_e; predried specimens were deprived of evaporable water before the test in oven at 105°C and then saturated to equilibrium at w_e prior to loading. (From Ruetz, W., "An Hypothesis for the Creep of Hardened Cement Paste and the Influence of Simultaneous Shrinkage," *Int. Conf. on the Structure of Concrete*, held in London, 1965, Cement and Concrete Assoc. (1968) 365–387.)

In view of the smallness of creep strains, the amount of water expelled during creep from the micropores into the macropores (or vice versa) must also be small, probably much less than 0.1 percent of the volume of concrete (since typically creep strains do not exceed 0.001, and even this is not due entirely to water but also to expelled solids). From sorption–desorption isotherms (Fig. 11), it is evident that a small change in water content of unsaturated concrete cannot cause a large change in pore humidity h. Consequently, assuming the same to be true for the water content of the macropores taken separately, one concludes that pore humidity h is not seriously affected by loading. Comparisons in measured h between loaded and unloaded sealed specimens[44], as well as in the water loss between loaded and unloaded unsealed specimens[3, 42–44] (item 13, Section 2), confirm this conclusion. Furthermore, no effect of load upon the macroscopic diffusivity of water [C in Eq. (4.40)] has been observed.

Thus, fortunately, the problem of macroscopic water diffusion in concrete (the drying problem), discussed in Subsection 4.6, may be considered as independent of the stress and strain problem. But the

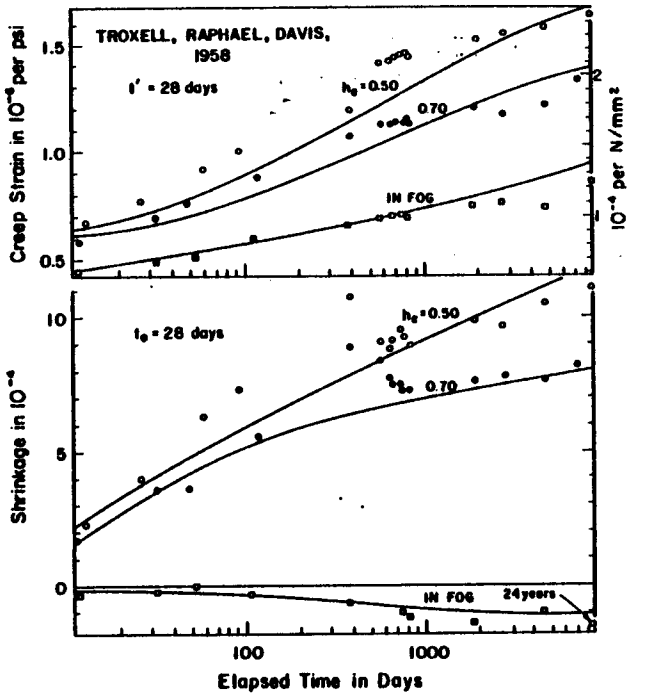

Fig. 21 Troxell, Raphael, and Davis' data on creep and shrinkage at various humidities. Tests of longest duration known; 28-day cyl. strength ≈ 2500 psi; stress = ½ strength; 70°F; cement type I; water–cement–aggregate ratio 0.59:1:5.67; granite aggregate; 1.5 in. max. size; 4×14 in. cylinders, unsealed. The solid lines are fits[166] for f'_c = 400 psi, S_1 = 300 psi, S_∞ = 0.0008, C_∞ = 0.025 in.²/day, and B = 0.4, obtained according to Eqs. (4.34a) to (4.34c). (From Troxell, G. E., Raphael, J. M., and Davis, R. W., "Long Time Creep and Shrinkage Tests of Plain and Reinforced Concrete," *Proc. ASTM* 58 (1958) 1101–1120.)

reverse is not true at all, and so the drying problem must be solved prior to analyzing stresses and strains.

A fully saturated concrete containing no water vapor (which can occur, in view of self-desiccation, only under hydraulic overpressure) does not seem to creep less than concrete at $h = 0.99$, despite the fact that at saturation the transfer of water from micropores to macropores requires volume compression of liquid water rather than vapor. This may be explained in part by the fact that the volume compressibility of cement paste particles is probably an order of magnitude less than that of capillary water. But more important, perhaps, this is explained by the fact that creep is mainly due to diffusion of solids (and so the fact that the

transfer of water is much less extensive in case of a filled macropore is inessential).

4.5 Nonlinear Effects in Creep and Shrinkage

First, attention will be given to nonlinear effects at moderate stress levels. Of these, the most important one is the drying creep effect (item 11, Section 2; Figs. 20 to 22), also called "Pickett effect," after its

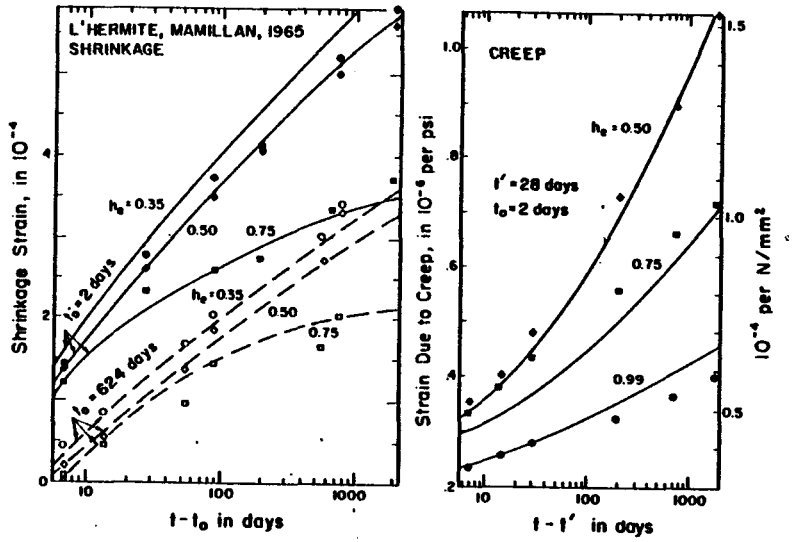

Fig. 22 Tests of creep and shrinkage at various humidities by L'Hermite and Mamillan. Same test series as in Fig. 4. The solid lines are fits[166] for $f_c' = 600$ psi, $S_s = 260$ psi, $S_\infty = 0.0003$, $C_\infty = 0.025$ in.²/day, and $B = 0.4$, obtained according to Eqs. (4.34a) to (4.34c). (Data adapted from L'Hermite, R., Mamillan, M., and Lefèvre, C., "Nouveaux résultats de recherches sur la déformation et la rupture du béton," *Annales de l'Institut Technique du Bâtiment et des Travaux Publics* **18** (1965) 325–360.)

discoverer[34]. He has linked it to the shrinkage stresses assuming them to be superimposed on the stresses due to applied load and thus cause the total stress to reach into the nonlinear range, in which the specific creep rate is higher. However, some later obtained experimental results are at variance with this explanation[125]. Within the framework of the theory expounded in previous paragraphs, modeling of the drying creep effect requires a nonlinear dependence of the mass fluxes upon the gradients in Eq. (4.8) to be introduced[125]. Thus,

$$a_{ss} = a_s^0 + a_s^w |\text{grad}\,\mu_w|^2 + a_s^s |\text{grad}\,\mu_s|^2, \quad a_{ww} = \cdots, \quad a_{sw} = \cdots, \tag{4.33}$$

or

$$\phi^h_{ss_\mu} = \phi_{s_\mu}{}^0 + \phi_s^w (\sigma_{w_\mu} - f_\mu)^2 + \phi_s^s \sigma_{s_\mu}{}^2, \quad \phi^h_{ww_\mu} = \cdots, \quad \phi^h_{sw_\mu} = \cdots,$$

in which a_s^0, $\phi_{s_\mu}{}^0$, a_s^w, ... are functions of h. (Note that the gradient vector appears only in the form of its invariant.) The dependence of a_{ww}, ϕ_{ww_μ}, a_{ws}, ϕ_{ws_μ}, etc., upon the gradients is probably inessential since creep is mainly due to the diffusion of solids. In absence of drying, grad μ_w and $(\sigma_{w_\mu} - f_\mu)$ are very small, and $a_s^s \ll a_s^w$ or $\phi_s^s \ll \phi_s^w$ must hold because creep is nearly linear with stress, while at simultaneous drying creep is distinctly nonlinear with stress[7, 41].

In a physical sense, coefficient a_s^w or $\phi_{s_\mu}{}^w$ represents a nonlinear coupling between the two diffusions of solids and water, whereas coefficient a_{sw} or ϕ_{sw_μ} from Eq. (4.8) or Eq. (4.20) represents a linear coupling. Coefficient a_{sw} reflects a drag of the diffusing water molecules upon the molecules (ions) of solids; water molecules when hit by the solid molecules are knocked from their equilibrium positions over their activation energy barriers. Obviously, this must occur in the direction of grad μ_w. On the other hand, a_s^w reflects an excitation (increase in mobility) of solids rather than a drag; the impinging water molecules do not knock out the solid molecules, but merely impart them energy, which makes their later escapes over the activation energy barriers more probable, i.e. more frequent. In contrast with the case of a drag, these escapes are actually caused by thermal fluctuations in energies and occur therefore in random directions, so that the subsequent movement of solids can be influenced only by grad μ_s, and not by grad μ_w. The frequency of these escapes must grow nonlinearly with the imparted energy, or with flux $\mathbf{J}_w$ (as can be shown from Maxwell–Boltzmann's distribution law of thermal energies[103]). This again justifies that "grad" appears in Eq. (4.33) in square. Since excitation and thermal escape require less imparted energy than direct knocking out the molecule, and is thus more frequent, coefficient a_{sw} or ϕ_{sw_μ} is probably of much lesser significance than a_s^w or $\phi_{s_\mu}{}^w$.

This conclusion is supported by the experimental facts that acceleration of compression creep occurs not only at drying, but also at wetting or humidity cycling[3, p. 156; 36], i.e. for either sign of humidity change (or either sign of grad), and that drying accelerates not only creep in compression, but also in shear[3, 17] and in bending[3, 34]. In the case of compression creep at wetting, the flux of solids due to creep, $\mathbf{J}_s$ in Eq.

(4.8), is opposite to the flux of water, J_w, induced by the change in pore humidity. In the cases of shear and bending at drying or wetting, opposite fluxes occur for half of all layers. If the drag (coefficients a_{sw}, ϕ_{sw_μ}) were decisive, either deceleration of creep (in the former case) or no change in rate (in the latter cases) would have to occur, which is at variance with experiments (effects 11, 12, Section 2). By contrast, if the excitation and thermal escapes prevail (coefficients a_s^w, $\phi_{s_\mu}^w$), the signs of fluxes J_w, J_s are immaterial, and acceleration must always occur, as is actually observed. Thus, probably, $a_{sw} \approx a_{ws} \approx \phi_{sw_\mu} \approx \phi_{ws_\mu} \approx 0$ can be assumed.

(The drying creep has already been discussed as a nonlinear effect by Pickett[34] and by Wittmann[37]. They assume that a certain stress σ^h due to shrinkage superimposes its effect upon stress σ due to load, and results, because of the nonlinear dependence of creep rate upon σ, in a higher creep per unit stress. However, this hypothesis would predict deceleration of creep on wetting, while the opposite seems to be true. Also, it would not predict any change for creep due to shear or bending.)

Identification of the material parameters in constitutive law (4.20) from the given test data represents an inverse (nonlinear initial boundary-value) problem, because coefficients of differential equations have to be determined from prescribed solutions. This is a mathematical problem of great complexity, compounded by the fact that all test data for variable water content refer to specimens that were not in a homogeneous state. Using step-by-step time integration combined with finite elements over the specimen (Subsection 5.3), the identification can be accomplished by an optimization algorithm[105, 166] based on quasi-linearization and a least-square criterion[166]. However, this succeeds only if a sufficiently good guess of the starting values of the material parameters is made, for which the thermodynamic theory outlined before is indispensable. Also, the data set analyzed must be sufficiently extensive to permit unambiguous identification of the material parameters. For this reason, it is necessary to fit the creep and shrinkage data obtained in different laboratories on different concretes simultaneously, and assume that, whereas the parameters for reference (constant humidity) conditions are different, those that modify them for humidity effects are nearly the same. It has been found[166] that the known test data for variable humidity conditions (at $T = T_0$) are sufficiently well fitted by the following expressions (the fits by these expressions appear as the solid curves in Figs. 16, 18, 21, 22, 25):

$$\phi_{ss_\mu}^{\,v} = \frac{1}{\tau_\mu}\phi_\mu \psi_\mu^{\,v} \rho_\mu^{\,v}, \qquad \phi_{ww_\mu}^{\,v} = \frac{1}{\tau_\mu}\phi_\mu \psi_\mu^{\,v} \qquad \mu = 1, \ldots, n \quad (n = 7)$$

$$\phi_{ss_\mu}^{\,D} = \frac{1}{\tau_\mu}\phi_\mu \psi_\mu^{\,D} \rho_\mu^{\,D}, \qquad \phi_{ww_\mu}^{\,D} = \frac{1}{\tau_\mu}\phi_\mu \psi_\mu^{\,D}, \qquad \tau_\mu = 0.05 \times 10^{\mu-1}\ \text{days}$$

$$\phi_{sw_\mu}^{\,v} = \phi_{ws_\mu}^{\,v} = \phi_{sw_\mu}^{\,D} = \phi_{ws_\mu}^{\,D} \approx 0, \tag{4.34a}$$

in which (see also the graphs in Fig. 11)

$$\phi_\mu = 10^{-a_\mu\sqrt{1-h}}, \qquad \psi_\mu^{\,v} = 1 + \left(\frac{\sigma_{w_\mu}^{\,v} - \sigma_\mu^{\,h}}{\sigma_{V_\mu}}\right)^2, \qquad \psi_\mu^{\,D} = 1 + \left(\frac{\sigma_{w_\mu}^{\,v} - \sigma_\mu^{\,h}}{\sigma_{D_\mu}}\right)^2$$

$$\rho_\mu^{\,v} = \rho_\mu^{\,D} = 1 + \left(\frac{\sigma_{s_\mu}^{\,v}}{\sigma_{a_\mu}}\right)^2 + \frac{J_2(\sigma_{s_\mu}^{\,D})}{\sigma_{b_\mu}^2}$$

$$\sigma_{V_\mu} = 10^{-b_\mu^{\,v}(1-h^2)^2}\sigma_C, \qquad \sigma_{D_\mu} = 10^{-b_\mu^{\,D}(1-h^2)^2}\sigma_C \tag{4.34b}$$

$$a_\mu = 3.6 - 0.095(\mu - 1)^2, \qquad \sigma_C = 6\ \text{psi}$$

$$b_\mu^{\,D} = 0.3 \times 10^{B_\mu}, \qquad b_\mu^{\,v} = 1.2 b_\mu^{\,D}, \qquad B_\mu = 1.4 + B(\mu - 1)$$

$$\sigma_{b_\mu} = \sigma_{a_\mu} = (1.1 + 0.2\mu)\sigma_B; \qquad \sigma_B = 1\ \text{psi}$$

and $J_2(\sigma_{s_\mu})$ is second invariant of the deviatoric tensor $\sigma_{s_\mu}^{\,D}$. The terms causing shrinkage [and the (tangent) elastic moduli] are (cf. Fig. 2):

$$\epsilon_S = S_0(1 - 0.95h^3 - 0.25h^{200}),$$

$$\dot{\sigma}_\mu^{\,h} = S_1 \frac{\tau_S}{\tau_S + \tau_\mu}\frac{\dot{\epsilon}_S}{S_0}, \qquad \tau_S = 20\ \text{days}, \tag{4.34c}$$

$$K_{s_\mu} = 0.9K_\mu, \qquad K_{w_\mu} = 0.1h(2-h)K_\mu,$$

$$G_{s_\mu} = 0.9G_\mu, \qquad G_{w_\mu} = 0.1h(2-h)G_\mu,$$

where K_μ, G_μ are determined from $E_\mu(t_\epsilon)$ using $\nu = 0.18$. In the above expressions, functions ϕ_μ account for the fact that concrete with constan h creeps less for lower h. Functions $\psi_\mu^{\,v}$, $\psi_D^{\,v}$ override this dependenc when sufficiently strong simultaneous drying occurs. Coefficient 1.2 in Eq (4.34b) causes the acceleration of creep by drying to be more intense in volumetric than in deviatoric deformations. (This accounts for the drop of the apparent creep Poisson's ratio with the duration of the drying creep test, and could be explained by the plausible hypothesis that the increase of diffusion rate due to drying in layers of one orientation should not affect much the rate in layers of another orientation.) All of these functions depend on μ because the intensity of humidity influences varies with creep duration. (Note that $\sigma_\mu^{\,h}$, introducing delayed shrinkage, becomes negligible for $\tau_\mu > 20$ days.) Term h^{200} in (4.34c) is needed to model swelling at $h = 1$ and, at the same time, autogeneous shrinkage of mass concrete

self-desiccating to $h = 0.98$. The age dependence of shrinkage is obtained through that of E_μ [and of C, in Eq. (4.41)]. Coefficients 0.1 and 0.9 in (4.34b) correspond to the fact that solids probably are relatively much less compressible than water and give only a mild decrease of elastic moduli with h. Functions $\rho_\mu{}^V$ and $\rho_\mu{}^D$ express the nonlinear dependence of creep upon stress, and are taken in a form that assumes the incremental properties to remain isotropic. (This is certainly a simplification.) The nonlinear diffusion or rate coefficients [Eq. (4.33)], other effects (item 8, cracking) has been considered [166] by replacing all E_μ with $E_\mu/(1+6\sigma^2/f_t'^2)$, where f_t' is the uniaxial tensile failure stress, and σ is the maximum principal stress.

While the foregoing nonlinear effects are all explicable in terms of nonlinear diffusion or rate coefficients [Eq. (4.33)], other effects (item 8, Section 2, or item 3, Subsection 4.4) require a formulation that characterizes the change of solid structure due to diffusion. For example, the solids diffused under uniaxial compression from the hindered layers perpendicular to σ probably precipitate near the boundary of the layer, extending thus its area (Fig. 14) and increasing the stiffness across the layer. In the simplest approach, this may be modeled by relations of the type $dE_{s_\mu} = -k_\mu \phi_{ss_\mu} \sigma_{s_\mu}\, dt$ [115]. But existing test data are insufficient to develop such relations quantitatively.

Attention will now be turned to nonlinear effects characteristic of the high-stress range (stress exceeding about 0.4 strength). Because stress is a tensor, it can be logically expected to affect the material properties in a nonisotropic fashion, except when the stress itself is isotropic (i.e. hydrostatic). Therefore, if a nonlinear dependence of creep upon stress is considered, stress-induced anisotropy of incremental properties intervenes and should be taken into account in both the short-time and the time-dependent deformations. The incremental anisotropy must, of course, be formulated in a special form that satisfies the condition of isotropy with regard to the initial (unstressed) state. Stress–strain laws of this type are studied in nonlinear viscoelasticity, and their special case is Truesdell's theory of hypoelasticity, which has already been applied to short-time deformations of concrete [168]. However, material identification methods have not yet advanced enough to yield formulations relevant to concrete; they will have to be if a nonlinear structural analysis for concrete in multiaxial stress (even for short-time deformations) should ever be made realistic. (A recent formulation of nonlinear behavior, developed in viscoplasticity [169, 171], might be applicable to concrete; it promises a simplification of the identification problem because the stress-induced incremental anisotropy is modeled indirectly, by postulating that the deformation increments depend on a certain scalar measure of deformation, or "intrinsic time," which is an isotropic function of strain.)

By contrast, the nonlinear effects in drying creep and shrinkage are due mainly to pore humidity which is a scalar, and so incremental anistropy is probably inessential. Nevertheless, some anisotropy must certainly result from the differences in solid rearrangements due to diffusion in layers of various orientations. In Eqs. (4.30) to (4.32), incremental anisotropy has been neglected, and accordingly the material parameters [in Eq. (4.34b), for example] have been considered dependent only upon the invariants of tensors σ_{s_μ}, σ_{w_μ}, and σ. To introduce incremental anisotropy in these equations, one could perhaps use some sort of a flow rule with a normality structure, because the rate of state variables (J_s, for example) is here assumed to depend only upon its associated thermodynamic force (grad μ_s, for example) and no other variables (p_s, for example)—conditions that were shown to suffice, in general [99].

The existence of a very strong incremental anisotropy is evidenced by the facts that in uniaxial compression, the apparent Poisson's ratio grows to and beyond 0.5 prior to failure [128], and that the velocity of sound in the transverse direction becomes much less than that in the longitudinal direction. Physically, the incremental anisotropy is explained by the fact that, in the high-stress range, the nonlinear dependence of creep (as well as instantaneous deformation [36, 128]; Fig. 24) upon stress is caused predominantly by microcracking, which follows a preferred orientation determined by the principal stress directions [36, 128]. (Microcracking is, of course, gradual in the case of creep.) This nonlinearity due to microcracking is important beyond roughly 0.4 strength. (For low-strength concrete, the fraction is less, and the effect is more pronounced.) Microcracks occur chiefly in the interface between the aggregate and the cement mortar or cement paste (bond cracks) (cf. Ref. [128] with further reference). Accordingly, the neat cement paste (when free of shrinkage stress) exhibits no nonlinearity due to microcracking and behaves in a perfectly linear viscoelastic manner almost up to failure (except for deformations affected by humidity), and even perfectly reversibly in case of short-time deformations in a perfectly dry state [129].

At moderately high stress levels (around 0.5 strength), the inelastic strain due to microcracking is significant only under cyclic or pulsating loads and is called cyclic creep [3, 12, 36, 46–52]. This effect is absent in neat cement paste (because microcracking is absent) and is especially large in low-strength concrete (and in reinforced structures because it is

augmented by the slip in bond reinforcement). Consider cyclic stress $\sigma = \sigma_0 + \sigma_1 \sin \omega t$, where σ_0, σ_1, ω are constants. According to a linear creep law (or principle of superposition), the cyclic creep strain ϵ_c after many cycles should roughly equal creep due to constant stress $\sigma = \sigma_0$. But in reality, the creep strain is usually larger than static creep under stress $\sigma_{max} = \sigma_0 + \sigma_1$ for the same period of time (Fig. 23). Most data indicate that ϵ_c is little dependent on $\sigma_{min} = \sigma_0 - \sigma_1$ and on frequency ω and is proportional to σ_{max} in the moderate-stress range[46]. Thus, $\epsilon_c(N) \approx \phi_N \sigma_{max}/E$, provided number N of cycles is large, $\omega > 1$ cycle/hr and $\sigma_{min} < 0.85\sigma_{max}$; ϕ_N is the cyclic creep coefficient, which depends on N similarly as ϕ depends on t (Section 3). According to Ref. [49], ϕ_c for 2×10^6 cycles roughly equals ϕ for 20-year load duration. Gaede's data[46] can be acceptably fitted assuming that ϕ_N equals creep coefficient (Section 3) $\phi(t_r, t')$ for $t_r = t' + (N/f)(1 + f/20{,}000)$, where f is the number of cycles per day. [Thus, cyclic creep can be introduced through the rate coefficients

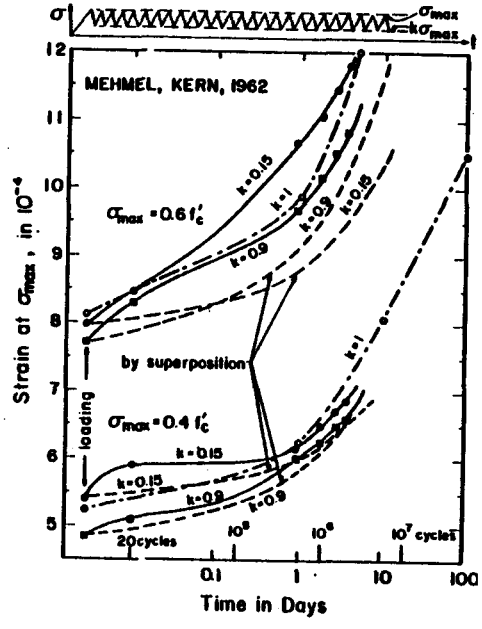

Fig. 23 Cyclic creep tests by Mehmel and Kern. After 20 slow cycles (completed within minutes after first loading), stress σ was pulsating as shown at 380 cycles/min; cylinders 15 × 60 cm; water–cement–aggregate ratio 0.44 : 1 : 4.5; cube strength 498 kgf/cm²; drying in laboratory atmosphere. Dashed lines—prediction by principle of superposition; f'_c = strength of specimen at loading. (Data extracted from Mehmel, A., and Kern, E., "Elastische und Plastische Stauchungen von Beton infolge Druckschwell- und Standbelastung," *Deutscher Ausschuss für Stahlbeton* Heft 153, Berlin (1962), Figs. 25, 28, 31.)

$\phi_{s_\mu}, \ldots$ in (4.30) to (4.32).] However, data in Fig. 23 indicate that at ow stress levels, only the short-time creep is accelerated by pulsation, while the long-time creep is unaffected. [Then among coefficients ϕ_{s_μ} $\mu = 1, 2, \ldots, n$) only those for small μ would be increased by pulsation.]

Attempts have been made to generalize the uniaxial integral-type creep aw into the high-stress range, replacing $L(t, t')$ in Eq. (3.8) with a function $L(t, t') + L_1(t, t')f_1[\sigma(t')]$[24, 130, 131], which has been compared with est data in Ref. [24].

For the sake of simplification, all nonlinear creep is frequently onsidered as irrecoverable (similarly as in rate-of-creep method, Subsection 5.5), which is somewhat closer to reality than in the linear range[83, 132]. Then the stress–strain law has the form

$$\dot{\epsilon} - \dot{\epsilon}^0 = \frac{\dot{\sigma}}{E} + \dot{\bar{\phi}}(t)F(\sigma, t), \tag{4.35}$$

which can be interpreted as a nonlinear age-dependent Maxwell type creep law; $\phi(t)$ is a given function of one variable which is taken so as to describe correctly the shape of the creep curve at low stress and a chosen reference age t_0 at loading, i.e. $\bar{\phi}(t) = \phi(t, t_0)$. In accordance with the rate process theory[102, 103], F as a function of σ may be considered as $E^{-1} \sinh(\sigma/\sigma_1)$, where σ_1 is a constant[29, 37, 115]; E may be taken as the instantaneous elastic modulus at low stress.

Equation (4.35) is a special case of the rate-of-creep method; and it similarly (see Subsection 5.5) underestimates creep due to later stress changes. This may be avoided if Eq. (4.35) is, alternatively, regarded as a derivative of the relation $\epsilon(t) = f\{\sigma(t), t\}$, in which case $f(\sigma, t)$ is a function describing, at constant σ, the creep isochrones (Fig. 24). Then, in Eq. (4.35), $1/E = \partial f(\sigma, t)/\partial\sigma$ and $\dot{\bar{\phi}}(t)F(\sigma, t) = \partial f(\sigma, t)/\partial t$. These relations correspond, in fact, to the methods used in [133–135]. They somewhat overestimate creep due to later stress changes and include the recoverable creep component, as is clear from the fact that for low stress, they coincide with the effective modulus method (Subsection 5.5).

However, Eq. (4.35), as well as the preceding integral formulation with $L_1(t, t')$, has an inherent limitation in that it cannot fit data involving a broad range of response delays. As is well known from Volterra–Fréchet series expansion of a functional[73, 78], the creep law for a broad range must include multiple integrals of the type

$$\int_\tau^t \int_\theta^t L(t, \tau, \theta)\sigma(\tau)\sigma(\theta)\, d\tau\, d\theta,$$

but the identification of material parameters would then be hardly

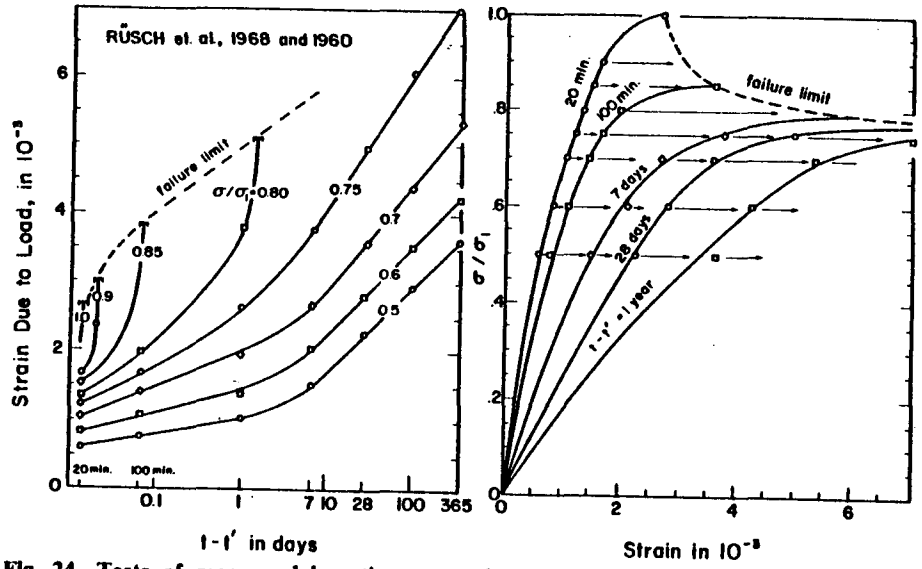

Fig. 24 Tests of creep and long-time strength at high stress by Rüsch *et al.* Prisms 10 × 15 × 60 cm with widened ends; water–cement–aggregate ratio 0.55 : 1 : 4.9; Rhine gravel (mostly quartz); 28-day cube strength 350 kgf/cm²; moist cured for 7 days at 20°C, then drying at $h_e = 0.65$ and 20°C. Load applied at a strain rate 0.003/20 min; σ_f is failure stress of the specimen. Data points are interpolated and smoothed. Note that creep isochrones (ϵ versus σ at constant t) are constructed from creep data at constant ϵ. (Adapted from Rüsch, H., *et al.* "Festigkeit und Verformung von unbewehrtem Beton unter konstanter Dauerlast," *Deutscher Ausschuss für Stahlbeton* Heft 198, W. Ernst, Berlin (1968).)

tractable. Thus, development of a nonlinear rate-type creep law seems to be inevitable again.

The incomplete recovery at and after unloading is certainly due in part to changes of solid microstructure mentioned before, and also to micro-cracking, in the case of high stress. However, the fact that the unloading branch immediately after first short-time loading of a virgin concrete has a higher slope than the first loading branch, even if both are nearly linear, can be explained only by closing of voids (similar to "locking materials") and by formation of new bonds upon the first loading, combined with micro-cracking. Mathematical formulation of these phenomena will probably be possible with the help of endochronic theory and deformation measure of the type proposed for metals by Valanis [169].

4.6 Drying and Wetting of Concrete

Assuming grad T to be negligible and grad μ_w to be sufficiently small in magnitude, one can write

$$\mathbf{J} = -\bar{c}\ \text{grad}\ \mu_w, \tag{4.36}$$

where grad is the macroscopic gradient and J is the macroscopic mass flux of water. If possible differences in solute concentrations (i.e. osmotic pressures) are neglected, substitution of expression (4.11) for water in the macropores of nonsaturated concrete yields

$$\mathbf{J} = -c\ \text{grad}\ h \qquad \text{with } c = \bar{c}\left(\frac{R}{M}\right)\frac{T}{h}, \tag{4.37}$$

where c is the permeability. Because exchange of molecules between various states of water within each macropore is much faster than drying of the specimen, thermodynamic equilibrium may be assumed to exist within each macropore. Then pore humidity h can depend only on temperature T, water content w (the mass of water per unit volume of material, including both the evaporable water w_e and the chemically combined nonevaporable water w_n), and the size and shape of pores as affected by the degree of hydration or t_e. Thus,

$$dh = k\,dw + \kappa\,dT + dh_s \tag{4.38}$$

in which $k = (\partial h/\partial w)_{T,t_e}$ is the cotangent of slope of the desorption or sorption isotherm (Fig. 11); $dh_s = h_s(t_e + dt_e) - h_s(t_e)$, where $h_s(t_e) = h$ at constant w and T at progressing hydration; $\kappa = (\partial h/\partial T)_{w,t_e}$ = hygrothermic coefficient ($\kappa \geq 0$). It depends strongly on h (Fig. 11), which may be approximately predicted from the Brunauer–Emmett–Teller theory, a statistical-mechanical theory of multilayer adsorption, as applied to the walls of macropores; see Refs. [67, 100]. The sorption isotherms exhibit a pronounced irreversibility (hysteresis, Fig. 11 [63–65, 136]). This is attributable to changes in pore structure due to solid diffusion (cf. preceding item 3 in Subsection 4.4), and in the range $h \geq 0.7$, in which a significant part of w is capillary water, also to the fact that in pores of a given geometry, more than one equilibrium shape of capillary menisci exists [100, 136]. Function $h_s(t_e)$ represents the so-called self-desiccation of sealed specimens, a gradual drop in h approaching an asymptotic value in a few months (cf. Ref. [67]). It is weaker for higher water–cement ratios and is caused by consumption of evaporable water for hydration, whose effect on h is, however, mostly offset by the decrease in pore volume, so that the drop in h_s is relatively feeble. (For water–cement ratio 0.5, $h_s(\infty) \approx 0.97$.) Thus, dh_s may approximately be neglected. (Anyhow, if drying causes h to drop below 0.5, $dh_s \approx 0$ because $\beta_h \approx 0$.)

Recalling the condition of conservation of mass, $\partial w/\partial t = -\text{div}\,\mathbf{J}$, we

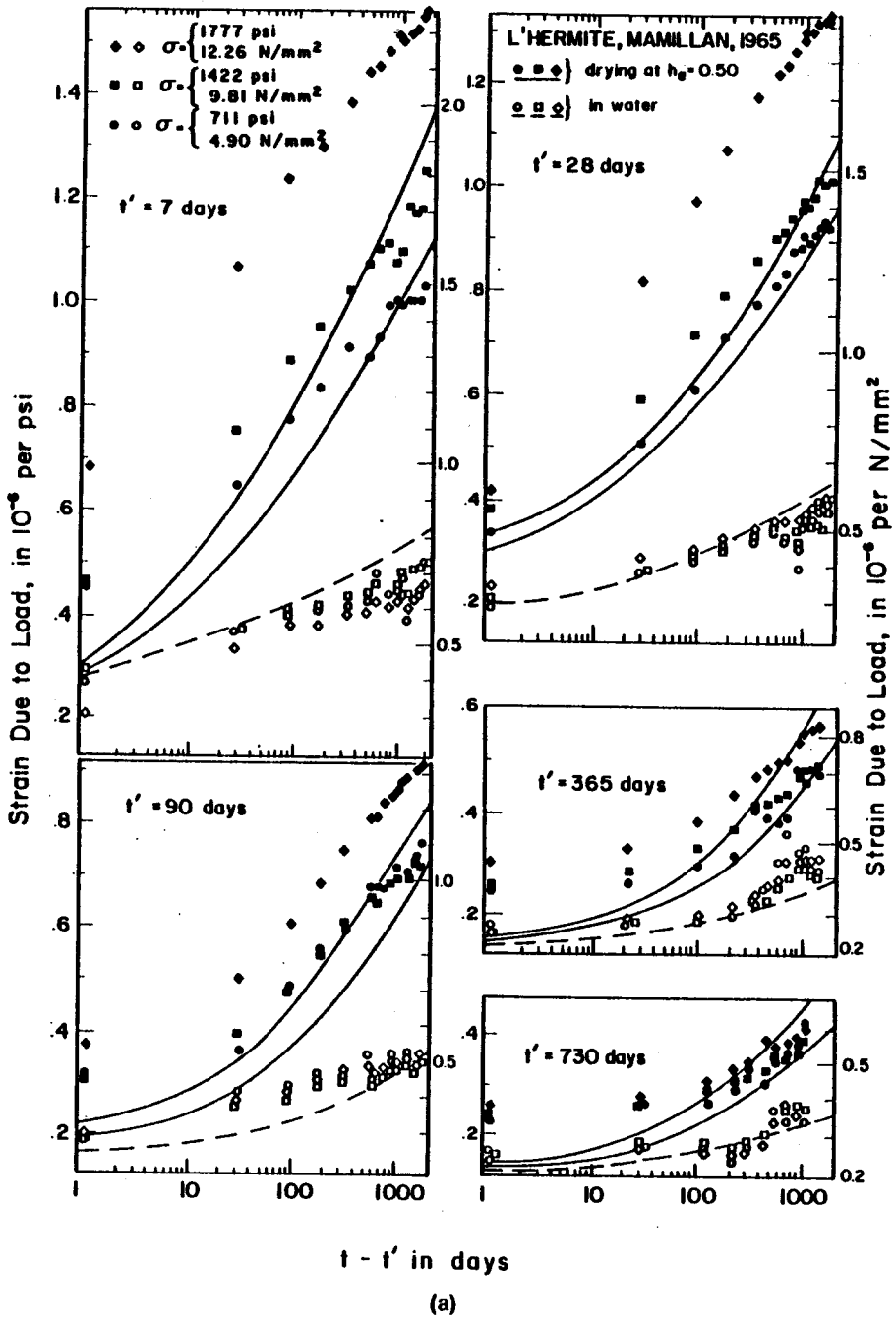

(a)

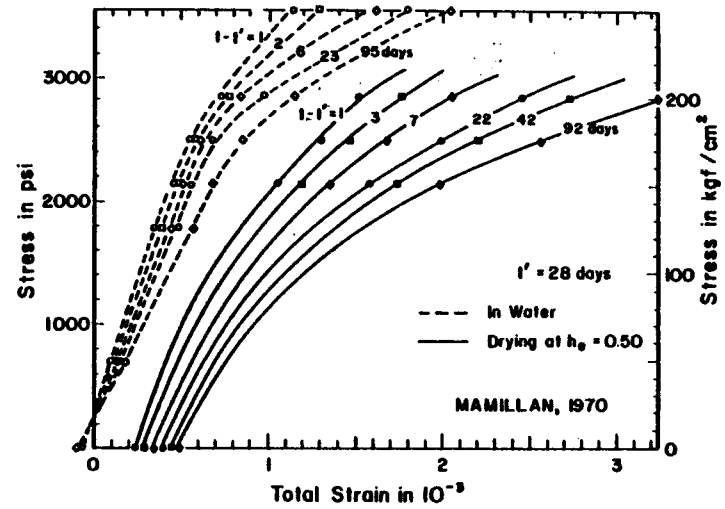

(b)

Fig. 25 (a) L'Hermite and Mamillan's tests of creep at various stress levels, ages, and humidities. Same test series as in Fig. 4. The solid lines are fits[166] for the same material parameters as in Fig. 22. (Data extracted from a private communication and from L'Hermite, R., Mamillan, M., and Lefèvre, C., "Nouveaux résultats de recherches sur la déformation et la rupture du béton," *Annales de l'Institut Technique du Bâtiment et des Travaux Publics* 18 (1965) 325–360.) The measured J-values at $t - t' \approx 0.01$ day, for ages $t' = 7$ to 730 days shown, were 248, 196, 190, 172, 144 in 10^{-6}/psi. (b) Mamillan's tests of saturated and drying specimens at various stress levels. Prisms $7 \times 7 \times 28$ cm; short-time failure stress 250–300 kgf/cm², 28 days old when loaded; cured 2 days in mold, 5 days in water, then drying in air of $h_e = 0.50$ at 20°C; other factors probably same as in Fig. 4. (After Mamillan, M., and Lelan, M., "Le Fluage de Béton," *Annales de l'Institut Technique du Bâtiment et des Travaux Publics* (Supplément) 23 (1970) and (1968), Figs. 13, 14.)

note that from Eqs. (4.37) and (4.38)

$$\frac{\partial h}{\partial t} = k \operatorname{div}(c \operatorname{grad} h) + \frac{\partial h_s}{\partial t} + \kappa \frac{\partial T}{\partial t}. \tag{4.39}$$

Here k may approximately be taken as constant (especially for desorption from $h = 1$ to $h = 0.3$ and for low water–cement ratios). Then k can be combined with c, setting $kc = C$ = diffusivity. Fitting of extensive data on drying and water permeation, some of which is shown in Fig. 26, has revealed[67] that C drops about 20 times when passing from $h = 0.85$ to $h = 0.65$ (Fig. 11). Approximately,

$$C = kc = C_1(T, t_e)\left\{\alpha_0 + \frac{1-\alpha_0}{1+\left(\frac{1-h}{1-h_c}\right)^n}\right\}, \tag{4.40}$$

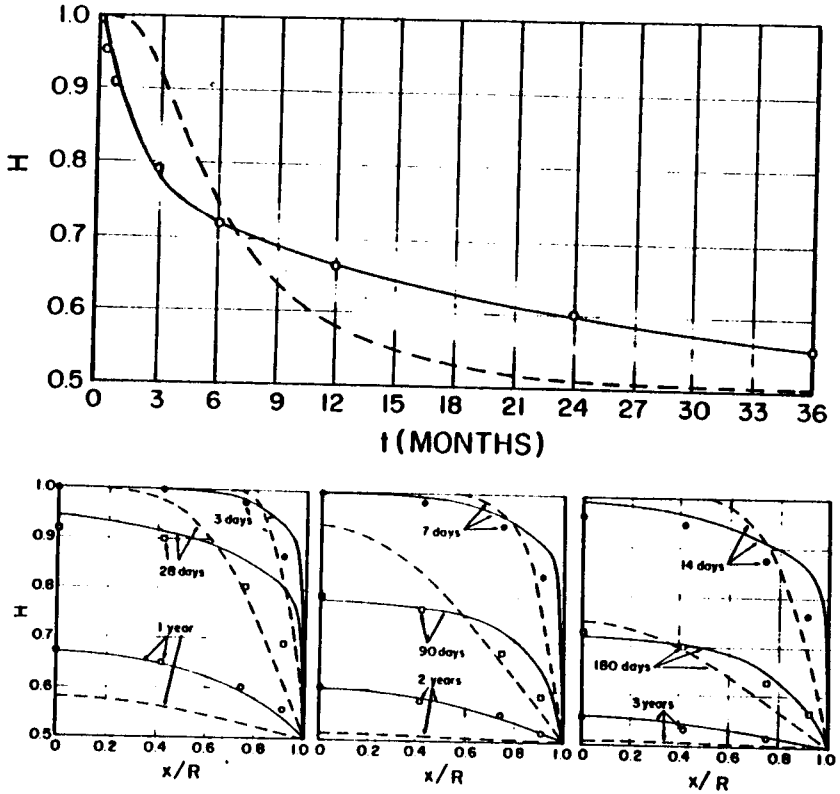

Fig. 26 Hanson's data on center-point humidity and humidity distributions of dryin cylinders. Diameter 6 in., environment of $h_e = 0.50$, 73°F; water–cement–sand–gravel rati 0.657 : 1 : 3.26 : 3.69; Elgin gravel; 7 days old specimen at the start of drying; solid lines shov fits from Ref. [67] for $a_0 = \frac{1}{30}$, $h_c = 0.792$, $n = 6$, $C_1 = 0.239\ \text{cm}^2/\text{day}$. Dashed lines are the bes possible fit with a linear theory. (For fits of many other data, see Ref. [67].) (After Hanson, J A., "Effects of Curing and Drying Environments on Splitting Tensile Strength," *Amer Concrete Inst. J.* 65 (1968) 535–543.)

where $\alpha_0 \approx 0.05$, $n \approx 10$, $h_c \approx 0.75$. Dependence of C_1 on temperature T may be deduced from the assumption that $\tilde{c}$ in Eq. (4.36) obeys the activation energy concept. Thus, taking Eq. (4.37) into account and denoting the chosen reference temperature by T_0, one obtains

$$C_1(T, t_e) = C_0(0.3 + 3.6t_e^{-1/2})\frac{T}{T_0}\exp\left(\frac{Q}{RT_0} - \frac{Q}{RT}\right), \tag{4.41}$$

where $C_0 = \text{constant} = C$ for $T = T_0$, 298°K, $t_e = 28$ days and $h = 1$; $Q \approx 9300$ cal according to the test data analyzed in Ref. [67]. The

dependence on age t_e was deduced by fitting Wierig's data (cf. Ref. [166]) on the drop of permeability c with curing period. Charts for prediction of drying of simple bodies are given in Ref. [67].

The boundary condition of moisture transfer at the surface relates the normal flux $\mathbf{n} \cdot \mathbf{J}$ to the difference in μ_w between the concrete surface and the ambient atmosphere ($\mathbf{n}$ is the unit outward normal of the surface). Then, because of Eq. (4.11), $\mathbf{n} \cdot \mathbf{J} = B(\ln h - \ln h_e)$, where h_e is the environmental humidity and B is the surface emissivity depending on T and the circulation of air. Thus, expressing $\mathbf{J}$ from Eq. (4.36),

$$\mathbf{n} \cdot \text{grad}\, h = \frac{c}{B}\ln\frac{h}{h_e}. \tag{4.42}$$

As a very crude estimate, $c/B \approx 1$ mm in room environment. For bodies thicker than about 5 cm, the drying is so slow that $B \approx 0$ may be assumed, so that $h \approx h_e$, on the surface. The boundary condition of perfectly sealed surface is obtained for $B \to \infty$.

The strong dependence of C upon h makes the diffusion problem highly nonlinear. This complicates analysis, and it is best to use numerical methods. Solutions shown by solid lines in Fig. 26 have been obtained by the finite-difference method.

The dependence of C upon h has implications for the mechanism of the macroscopic diffusion. If water transport occurred mainly in the form of vapor, C would have to be essentially independent of h. On the other hand, migration of molecules along the layers adsorbed at the walls of macropores must be slower, the thinner the layer. Consequently, the latter must be the dominant mechanism. [This conclusion has also been made [43] realizing that the mean free path of water molecules in vapor (about 800 Å at 25°C) is many times greater than the probable minimum cross section encountered along the continuous passages through the cement paste, so that the probability of a vaporized molecule passing through is extremely low.] The sharp drop in C (Fig. 11; item 31, Section 2) probably corresponds to transition of the flow from the third to the second molecular layer adsorbed on macropore walls.

Diffusion of water through saturated concrete under hydraulic overpressure p leads to the differential equation $\partial p/\partial t = C_{sat}\nabla^2 p$. It has been deduced from plausible physical hypotheses [67] that $C_{sat} \approx 1000C$, where C corresponds to $h = 0.999$ [Eq. (4.41); item 31, Section 2]. For a continuous mass flux, the gradients normal to the interface between a saturated and a nonsaturated zone are related as [67] $\text{grad}_n\, p = k_1\, \text{grad}_n\, h$, where $k_1 = 1360$ atm (T/298°K). Thus, at 25°C, a difference 0.1 in h

produces about the same flux as the hydraulic head of 1400 m (item 32, Section 2). This is confirmed [67] by Carlson's observation that a wall of thickness L exposed on one side to an atmosphere of $h_e = 0.5$ and on the other side to water of 70.3 m hydraulic head is not, in a stationary state, saturated deeper than $0.04L$ from the wet face. The initial speeds of propagation of a front of hydraulic pressure and a front of drying at $h = 1$ can be shown to be about in the ratio 30: 1 [67].

5 METHODS OF STRUCTURAL ANALYSIS

5.1 Elastic–Viscoelastic Analogy for Aging Materials

The linear stress–strain relations studied in Section 3, e.g., the integral-type creep laws (3.1), (3.2), (3.5), and (3.8), can be written in the operator form

$$\epsilon - \epsilon^0 = E^{-1}\sigma \quad \text{or} \quad \sigma = E(\epsilon - \epsilon^0) \qquad \text{uniaxial stress,} \tag{5.1}$$

$$\left.\begin{aligned} 3(\epsilon^V - \epsilon^0) &= K^{-1}\sigma^V \quad \text{or} \quad \sigma^V = 3K(\epsilon^V - \epsilon^0) \\ 2\epsilon_{ij}^D &= G^{-1}\sigma_{ij}^D \quad \text{or} \quad \sigma_{ij}^D = 2G\,\epsilon_{ij}^D \end{aligned}\right\} \qquad \text{multiaxial stress,} \tag{5.2}$$

where E^{-1}, K^{-1}, G^{-1} are uniaxial, volumetric, and deviatoric creep operators, E, K, G are corresponding inverse operators (relaxation operators). They all represent linear Volterra's integral operators and obey the same rules as linear algebra, except that a product is not commutative. Thus, any of the equations of elasticity in which only linear combinations of elastic constants appear may be generalized to creep by replacing them with the corresponding operators. This correspondence is called elastic–viscoelastic analogy. It was stated in the operator form (for aging materials) first by Mandel [137], although for the special case of homogeneous structures, an equivalent analogy given in Subsection 5.2 was discovered earlier. (Caution is needed when a product of elastic constants appears; it is necessary to go over the derivation of the equation in elasticity to determine what the order of operators in the product is.)

To give an example, the equation for bending of a homogeneous beam in presence of creep is readily obtained in the form

$$Ik(t) = E^{-1}M(t) = \int_0^t J(t, t')\, dM(t'),$$

where k is bending curvature, M is bending moment, and I is moment of inertia of the cross section.

The linear rate-type creep laws can also be written in the form of Eq. (5.1) or Eq. (5.2). Then, if all hidden variables are eliminated, operators E, E^{-1}, G, ... represent quotients of two linear differential operators with time-dependent coefficients. For this formulation, the elastic–viscoelastic analogy was stated in Refs. [77, 138, 139]. In the case when hidden stresses or strains are used, a set of hidden variables must first be associated with each force or displacement variable before the analogy can be applied. To give an example, associate M with a system of hidden bending moments M_μ, $\mu = 1, \ldots, n$. Creep law (3.34), (3.36) is then immediately generalized for bending of a homogeneous beam as

$$M = \sum\nolimits_\mu M_\mu, \qquad \dot{M}_\mu/E_\mu + M_\mu/\eta_\mu = \dot{k}I.$$

For the linear creep problem, uniqueness of solution can be proved [140–142] in an analogous manner as in elasticity, and similar variational principles can also be stated [138, 139, 140, 141, 172].

5.2 Homogeneous Structures and McHenry's Analogy

McHenry's Analogy. *Consider a structure (body) which has the following properties:*

(i) homogeneity, i.e. *creep properties are the same in all points, which requires the differences in age, water content or temperature, and the presence of reinforcement to be neglected;*

(ii) constancy of creep Poisson ratio ν (Section 2);

(iii) absence of deformable supports;

(iv) linearity of the associated elasticity problem, which implies small displacements.

Denote further by $\sigma_{ij}^{el}(t)$, $u_i^{el}(t)$ the stresses and displacements (with t as a parameter) for an elastic structure of time-constant modulus $E = E_0$, caused by surface loads $p_i(t)$, volume forces $f_i(t)$ $(i = 1, 2, 3)$, prescribed boundary displacements $u_i^0(t)$ and inelastic strains $\epsilon^0(t)$ as given functions of time. Then, if $\epsilon^0 = u_i^0 = 0$,

$$\sigma_{ij}(t) = \sigma_{ij}^{el}(t), \qquad u_i(t) = E_0E^{-1}u_i^{el}(t). \tag{5.3}$$

If, instead, $p_i = f_i = 0$, then

$$\sigma_{ij}(t) = E_0^{-1}E\sigma_{ij}^{el}(t), \qquad u_i(t) = u_i^{el}(t). \tag{5.4}$$

Proof. Regard Eqs. (5.3) and (5.4) as chosen substitutions without specifying the meaning of σ_{ij}^{el} and u_i^{el}. Insert Eq. (5.3) or Eq. (5.4) in Eq. (5.2) and, in accordance with condition (ii), put $K = K_0E/E_0$, $G = G_0E/E_0$. Furthermore, substitute Eq. (5.3) or Eq. (5.4) for σ_{ij} and u_i into the

linearized strain definition, the equilibrium conditions and the boundary conditions, i.e. into

$$\epsilon_{ij} = \tfrac{1}{2}(u_{i,j} + u_{j,i}), \qquad \sigma_{ij,j} + f_i = 0 \qquad \text{in } \mathcal{V}, \tag{5.5}$$

$$\sigma_{ij} n_j = p_i \qquad \text{on } \Gamma_1, \qquad u_i = u_i^0 \qquad \text{on } \Gamma_2, \tag{5.6}$$

in which $\mathcal{V}$ is the domain of the structure, Γ_1 is part of the surface on which surface loads p_i are prescribed, Γ_2 is part of the surface on which displacements u_i^0 are enforced, n_j is unit outward normal at the surface, and subscripts following a comma denote partial derivatives. After this substitution, Eqs. (5.5), (5.6), and (5.2) are recognized to represent formulation of the linear elasticity problem for σ_{ij}^{el}, u_i^{el}. Since its solution is unique and σ_{ij}^{el}, u_i^{el} could not be the elastic solutions if Eq. (5.3) or Eq. (5.4) were inequalities, the proof is completed.

Equivalently, it may be stated that $\sigma_{ij}(t)$ and $u_i(t)$ equal the elastic solution due to the fictitious loads $E_0E^{-1}p_i(t)$, $E_0E^{-1}f_i(t)$, plus the elastic solution due the fictitious prescribed displacements $E_0^{-1}Eu_i(t)$ and inelastic strains $E_0^{-1}E\epsilon^0(t)$. In this form, the analogy was discovered in 1943 by McHenry[75], although for the special case of statically indeterminate framed structures (in which constancy of ν need not be required due to neglect of shear strains), the essence of the analogy was deduced already in 1937 by Dischinger[143]. A rigorous mathematical proof, though much lengthier than the present one, was first given in 1951 by Arutyunian[144].

Equations (5.3) and (5.4) indicate that, under the conditions specified, all displacements and stresses in the structure vary in the same proportion as in a homogeneously stressed specimen.

With the aid of the principle of superposition, McHenry's analogy also enables analysis of the practically important cases (cf. Section 6), in which the statical system of a loaded and creeping structure (satisfying the conditions mentioned) is changed at time t_1 by introducing a new constraint, capable of providing new reaction force X. Assume that $X(t_1) = 0$ and denote by t_0 the time of application of the constant loads, $t_0 \leq t_1$. Further, denote by σ_{ij}^{II}, ϵ_{ij}^{II}, and u_i^{II} the stresses, strains, and displacements obtained for modulus $E(t_0)$ according to the theory of elasticity for the new system of constraints (statical system), existing after time t_1, and by σ_{ij}^{I}, ϵ_{ij}^{I}, and u_i^{I} similar values for the original system of constraints, existing prior to time t_1. Let u_X denote the displacement in the direction of X; obviously, $u_X^{II} = 0$, but $u_X^{I} \neq 0$.

According to Eq. (5.3), $\sigma_{ij} = \sigma_{ij}^{I}$ and $u_i = u_i^{I}[1 + \varphi(t, t_0)]$ for any $t < t_1$. If no new constraints were introduced, displacement increments $\Delta u_X = u_X^{I}\,\Delta\varphi\,(t)$, where $\Delta\varphi\,(t) = \varphi(t, t_0) - \varphi(t, t_1)$ would arise after time t_1. To cancel Δu_X, it may be imagined that enforced displacements $-u_X^{I}\,\Delta\varphi\,(t)$ or $(u_X^{II} - u_X^{I})\,\Delta\varphi\,(t)$ in the direction of X are superimposed. By virtue of Eq. (5.4), this produces additional strains $\Delta\varphi\,(t)(\sigma_{ij}^{II} - \sigma_{ij}^{I})/E(t_0)$. Thus, the total strains at $t \geq t_1$ are

$$\epsilon_{ij}(t) = \sigma_{ij}^{I}\frac{1 + \varphi(t, t_0)}{E(t_0)} + (\sigma_{ij}^{II} - \sigma_{ij}^{I})\frac{\varphi(t, t_0) - \varphi(t_1, t_0)}{E(t_0)}. \tag{5.7}$$

Knowing the strain history, one can easily compute (cf. Subsection 5.3) the stress changes $\sigma_{ij}(t) - \sigma_{ij}^{I}$, which are affected solely by the second term in Eq. (5.7). An approximate formula for these changes (which is exact for $t_1 = t_0$) follows from Eqs. (5.28) to (5.32) in the sequel.

If a constraint of a structure that creeps at constant stress state (e.g., a temporary construction support) is removed, load $(-X)$ is in fact superimposed in the sense of the previous reaction X. Thus, according to Eq. (5.3), merely an elastic change of stress (without any delayed response) occurs.

5.3 Numerical Step-by-Step Methods

The realistic forms of creep law of concrete do not admit analytical solutions of creep problems, and so numerical techniques must be employed. Of these, the step-by-step integration schemes, in which time t is subdivided by discrete times t_r, $(r = 0, 1, 2, \ldots)$ in time steps $\Delta t_r = t_r - t_{r-1}$, are most convenient. Time t_0 coincides with the time the first stress is introduced into the structure. If the loading is steady, the rate of change of all variables decays with time [approximately as $(t - t_0)^{-1}$]. Therefore, times $t_0, t_1, \ldots$ are best chosen in the form of a geometric progression, i.e. the time steps appear as constant in the $\log(t - t_0)$-scale. A high accuracy is usually achieved with $\Delta t_1 = 0.01$ day and $(t_r - t_0)/(t_{r-1} - t_0) = 10^{1/8}$, although even quotient $10^{1/2}$ is sufficient for practical purposes.

Consider that an instantaneous stress change $\Delta\sigma_1$ occurs immediately after time t_0, while subsequently $\sigma(t)$ varies smoothly at a decaying rate. Then the Stieltjes integral in Eq. (3.1) may be approximated, with an error of the order of Δt^3, by the sum

$$\epsilon_r - \epsilon_r^0 = \sum_{q=1}^{r} J(t_r, t_{q-(1/2)})\,\Delta\sigma_q \qquad \text{for} \quad r \geq 1, \tag{5.8}$$

where $\epsilon_r = \epsilon(t_r)$, $\Delta\sigma_q = \sigma(t_q) - \sigma(t_{q-1})$, etc., and

$$t_{q-(1/2)} = t_0 + \sqrt{(t_{q-1} - t_0)(t_q - t_0)} \quad \text{for} \quad q > 1,$$
$$t_{1-(1/2)} = t_0 \quad \text{for} \quad q = 1. \tag{5.9}$$

This is justified by the fact that, under steady load, σ varies within each time step about linearly with $\log(t - t_0)$ and $t_{q-(1/2)}$ is the *middle* of the interval in the $\log(t - t_0)$-scale. Replacing r by $r-1$, Eq. (5.8) becomes

$$\epsilon_{r-1} - \epsilon^0_{r-1} = \sum_{q=1}^{r-1} J(t_{r-1}, t_{q-(1/2)})\,\Delta\sigma_q \quad \text{for} \quad r \geq 2. \tag{5.10}$$

Subtracting Eq. (5.10) from Eq. (5.8), one obtains

$$\Delta\epsilon_r = \frac{\Delta\sigma_r}{E''_r} + \Delta\epsilon''_r, \tag{5.11}$$

where

$$\begin{aligned}
E''_r &= \frac{1}{J(t_r, t_{r-(1/2)})} && \text{for} \quad r \geq 1 \\
\Delta\epsilon''_r &= \sum_{q=1}^{r-1} \Delta J_{r,q}\,\Delta\sigma_q + \Delta\epsilon_r{}^0 && \text{for} \quad r > 1, \\
\Delta\epsilon''_1 &= \Delta\epsilon_1{}^0 && \text{for} \quad r = 1 \\
\Delta J_{r,q} &= J(t_r, t_{q-(1/2)}) - J(t_{r-1}, t_{q-(1/2)}) && \text{for} \quad r > 1,\ q \geq 1.
\end{aligned} \tag{5.12}$$

The above equations also hold for an instantaneous change of load at time t_r, i.e. $t_r = t_{r-1}$; however, in such a case, the subsequent time interval must be so small that $J(t_{r+1}, t_r)$ very nearly equals $J(t_r, t_r)$. (This is practically inconvenient, so that the effect of the response to an instantaneous load change is better computed separately and is then superimposed.) Alternatively, $J(t_r, t_{q-(1/2)})$ in the expressions for $\Delta\epsilon''_r$ and $\Delta J_{r,q}$ may be replaced by $\frac{1}{2}[J(t_r, t_q) + J(t_r, t_{q-1})]$, maintaining the same order of accuracy, and the intermediate times $t_{q-(1/2)}$ may be dispensed with.

Equation (5.8) has the form of an elastic stress–strain relation with modulus E''_r and inelastic strain $\Delta\epsilon''_r$. Their values are fully determined by stress increments prior to time step Δt_r under consideration, and so the solution of $\Delta\epsilon_r$ and $\Delta\sigma_r$ in any time step is an elasticity problem with inelastic strains. Analogous results may be obtained for the multiaxial stress states and for creep law (3.5) based on the relaxation function [145].

Equations (5.8) to (5.11) were first introduced in Ref. [146], in which practical convergence was also studied. Similar expressions based on evaluating the integral in Eq. (3.1) or Eq. (3.8) with a rectangle rule were used in [108, 147, 155]. A general solution in terms of a series of elasticity problems seems to have been first formulated in Ref. [145] using Eq. (3.8) rather than Eq. (3.1). But for this form of creep law, it is impossible to increase the time step beyond a certain small value without causing numerical instability [131, 148, 149]. The method can be easily extended to nonlinear creep law analogous to Eq. (3.8) [131]. For simplified creep laws (Subsection 5.4), this type of method was used in Refs. [138, 150, 151].

Equations (5.8) to (5.11) are also very efficient for conversion of creep function $J(t, t')$ into the relaxation function $E_R(t, t')$ and vice versa [146].

As is clear from Eq. (5.11), the values of stress (or strain) increments in all previous time steps must be stored, and long sums of the type (5.10) must be evaluated in each time step. Considering that about 100 time steps are needed in a typical problem, the storage requirements become about 100-fold of those in the corresponding elastic problem, which presents formidable difficulties in case of large finite-element systems. This may be avoided by using some of the rate-type creep laws. Here another difficulty arises, however, when the standard step-by-step algorithms, e.g., the Euler and Runge–Kutta methods or predictor–corrector methods, are applied. Namely, numerical instability occurs if the time step exceeds a certain value roughly equal to the shortest relaxation or retardation time, so that an overwhelming number of steps would be required to reach the long-term solution. Fortunately, it was found that the time step can be arbitrarily increased if σ_r or ϵ_r are determined from σ_{r-1}, ϵ_{r-1} according to the exact integral of the creep law under the assumption that all material parameters (i.e. E_μ, η_μ) and all rates of prescribed inelastic strains are constant during the time step.

The exact integral of Eq. (3.36) based on Maxwell chain is already given by Eq. (3.35). Simplifying it for constant E_μ, η_μ, $\dot\epsilon$, $\dot\epsilon^0$, one obtains the following recurrent formula for the hidden stress [89]:

$$\sigma_{\mu_r} = \sigma_{\mu_{r-1}} e^{-\Delta t_r/\bar\tau_\mu} + \lambda_{\mu_r} E_{\mu_{r-(1/2)}}(\Delta\epsilon_r - \Delta\epsilon_r{}^0) \qquad \mu = 1, 2, \ldots, n, \tag{5.13}$$

where

$$\lambda_{\mu_r} = (1 - e^{-\Delta t_r/\bar\tau_\mu})\frac{\bar\tau_\mu}{\Delta t_r}, \qquad \bar\tau_\mu = \frac{\eta_{\mu_{r-(1/2)}}}{E_{\mu_{r-(1/2)}}}. \tag{5.14}$$

Expressing $\Delta\sigma_{\mu_r}$ from Eq. (5.13) and writing $\Delta\sigma_r = \Sigma_\mu\,\Delta\sigma_{\mu_r}$, one arrives at the pseudoelastic stress–strain law (5.11) in which [89]

$$\begin{aligned}
E''_r &= \sum_{\mu=1}^{n} \lambda_\mu E_{\mu_{r-(1/2)}}, \\
E''_r\,\Delta\epsilon''_r &= \sum_{\mu=1}^{n} (1 - e^{-\Delta t_r/\bar\tau_\mu})\sigma_{\mu_{r-1}} + E''_r\,\Delta\epsilon_r{}^0.
\end{aligned} \tag{5.15}$$

The exact integral of rate-type creep law (3.26), (3.27), (3.28) corresponding to the Dirichlet series creep function (3.15) is composed of expressions (3.24) for hidden variables ϵ^*_μ, from which it can be similarly derived [88, 152] that

$$\epsilon^*_{\mu_r} = \frac{\lambda_{\mu_r}\Delta\sigma_{\mu_r}}{\hat{E}_{\mu_{r-(1/2)}}} + \epsilon^*_{\mu_{r-1}} e^{-\Delta t_r/\bar{\tau}_\mu} \qquad \mu = 1, 2, \ldots, n, \tag{5.16}$$

where λ_{μ_r}, $\bar{\tau}_\mu$ are given again by expressions of the form of Eq. (5.15). Expressing $\Delta\epsilon^*_{\mu_r}$ from Eq. (5.16) and $\Delta\epsilon$ from Eq. (3.23), one again obtains the pseudoelastic stress–strain law (5.8), in which [88, 152]

$$\frac{1}{E''_r} = \frac{1}{E_{r-(1/2)}} + \sum_{\mu=1}^{n} \frac{1-\lambda_{\mu_r}}{\hat{E}_{\mu_{r-(1/2)}}},$$
$$\Delta\epsilon''_r = \sum_{\mu=1}^{n} (1 - e^{-\Delta t_r/\bar{\tau}_\mu})\epsilon^*_{\mu_{r-1}} + \Delta\epsilon^0_r. \tag{5.17}$$

Differential equations (4.20) expressing the nonlinear constitutive equation based on microdiffusion mechanism can also be integrated exactly under the assumption that all coefficients as well as prescribed rates are constant within the step. This involves solution of two simultaneous linear differential equations with constant coefficients. After some tedious manipulations, it is found that the hidden stresses in solids and water obey the recurrent relations

$$\sigma_{s_{\mu_r}} = f_\mu + f'_\mu(\Delta\epsilon - \Delta\epsilon^0), \qquad \sigma_{w_{\mu_r}} = g_\mu + g'_\mu(\Delta\epsilon - \Delta\epsilon^0), \tag{5.18}$$

with

$$f_\mu = A_1(\gamma_1 + \phi_{ww_\mu})e^{\gamma_1\Delta t_r} - A_2\phi_{sw_\mu}e^{\gamma_2\Delta t_r},$$
$$f'_\mu = S - B_1(\gamma_1 + \phi_{ww_\mu})e^{\gamma_1\Delta t_r} + B_2\phi_{sw_\mu}e^{\gamma_2\Delta t_r},$$
$$g_\mu = f_\mu - A_1\phi_{ws_\mu}e^{\gamma_1\Delta t_r} + A_2(\gamma_2 + \phi_{ss_\mu})e^{\gamma_2\Delta t_r}, \tag{5.19}$$
$$g'_\mu = W + B_1\phi_{ws_\mu}e^{\gamma_1\Delta t_r} - B_2(\gamma_2 + \phi_{ss_\mu})e^{\gamma_2\Delta t_r},$$

in which

$$A_1 = \frac{\sigma_{s_{\mu_{r-1}}}(\gamma_2 + \phi_{ss_\mu}) + (\sigma_{w_{\mu_{r-1}}} - f_\mu)\phi_{sw_\mu}}{D'},$$
$$B_1 = \frac{S(\gamma_2 + \phi_{ss_\mu}) + W\phi_{sw_\mu}}{D'},$$
$$A_2 = \frac{\sigma_{s_{\mu_{r-1}}}\phi_{ws_\mu} - (\sigma_{w_{\mu_{r-1}}} - f_\mu)(\gamma_1 + \phi_{ww_\mu})}{D'}, \tag{5.20a}$$
$$B_2 = \frac{S\phi_{ws_\mu} + W(\gamma_1 + \phi_{ww_\mu})}{D'},$$

$$\gamma_1 = -\phi_0 + \sqrt{\phi_0^2 - D},$$
$$\gamma_2 = -\phi_0 - \sqrt{\phi_0^2 - D},$$
$$\phi_0 = \tfrac{1}{2}(\phi_{ss_\mu} + \phi_{ww_\mu}),$$
$$D = \phi_{ss_\mu}\phi_{ww_\mu} - \phi_{sw_\mu}\phi_{ws_\mu},$$
$$D' = (\gamma_1 + \phi_{ww_\mu})(\gamma_2 + \phi_{ss_\mu}) - \phi_{sw_\mu}\phi_{ws_\mu}, \tag{5.20b}$$
$$S = \frac{\phi_{ww_\mu}E_\mu^s - \phi_{sw_\mu}E_\mu^w}{D\,\Delta t_r},$$
$$W = \frac{\phi_{ss}E_\mu^w - \phi_{ws_\mu}E_\mu^s}{D\,\Delta t_r}.$$

Expressing $\Delta\sigma = \Sigma_\mu\,(\Delta\sigma_{s_\mu} + \Delta\sigma_{w_\mu})$ from Eq. (5.19), one again finds the pseudoelastic stress–strain law (5.8) with

$$E''_r = \sum_\mu (f'_\mu + g'_\mu),$$
$$E''_r\Delta\epsilon'' = \sum_\mu (\sigma_{s_{\mu_{r-1}}} + \sigma_{w_{\mu_{r-1}}} - f_\mu - g_\mu). \tag{5.21}$$

Equations (5.19) to (5.21) are valid for $D \neq 0$ or $\gamma_1 \neq \gamma_2$; otherwise, they must be modified. For $\phi_{sw_\mu} = \phi_{ws_\mu} = 0$ (probably a typical case; Section 4.5), the two simultaneous differential equations (4.20) split in two independent equations, and formulas (5.19) to (5.21) considerably simplify; see Ref. [166]. Coefficients $\phi_{ss_\mu}, \ldots, \phi_{ws_\mu}$, f_μ in Eqs. (5.19) and (5.20) should all be evaluated for the mid-step, $t_{r-(1/2)}$. The generalization of Eqs. (5.13) to (5.21) to multiaxial stress is straightforward [152].

The algorithm given by Eqs. (5.16) to (5.17) was first presented in Refs. [88, 152] and algorithm (5.13) to (5.15) in Ref. [89]. A similar algorithm for Kelvin chain was given in Ref. [116]. Special cases of these algorithms for nonaging thermorheologically simple materials were developed by Taylor *et al.* [153] and Zienkiewicz *et al.* [154], respectively. A partly similar algorithm for aging concrete, which also eliminates storage of stress history but does not allow an arbitrary increase of time step, was given in [131, 155]. Numerical stability for cases of prescribed stress or strain history was proved in [88, 89, 152], and excellent convergence was demonstrated by an example in Ref. [152].

In each time step Δt_r, the analysis proceeds in the following sequence. (1) Elastic moduli E''_r (or analogous bulk and shear moduli) and inelastic strains $\Delta\epsilon''_r$ are evaluated (for all elements of the structure). (2) Then, solving an elasticity problem (by finite-element method, for example), displacement increments Δu_i and increments $\Delta\sigma$, $\Delta\epsilon$ (for all elements) are

determined. (3) Finally, the values of hidden stresses or strains at the end t_r of the time step are computed from Eq. (5.13), Eq. (5.16), or Eq. (5.18), and their values at t_{r-1} may be discarded from computer memory.

If the constitutive law is nonlinear, as is the case for Eqs. (5.19) to (5.21), E_r'' and $\Delta\epsilon_r''$ in step (1) above are first evaluated for $\sigma = \sigma_{r-1}$. Then, after solving the elasticity problem, step (2), and the hidden variables, step (3), one returns to step (1) to compute improved values of E_r'' and $\Delta\epsilon_r''$ on the basis of the average values of stresses and hidden variables in the time step, as obtained previously (i.e. $\sigma = \sigma_{r-1} + \frac{1}{2}\Delta\sigma$, etc.). Steps (2) and (3) are then iterated to get improved values of $\Delta\sigma$, $\Delta\epsilon$, Δu_i, $\Delta\sigma_\mu$, etc. More than two iterations are usually not appropriate, because a decrease of Δt_r is for improvement of accuracy more efficient than further iterations.

Structural analysis for any other nonlinear creep law may also be converted to a series of linear elasticity problems[131]. As an example, consider the nonlinear Maxwell type law (4.35). First, it must be linearized within each time step considered, which is achieved by $F(\sigma, t) = [F]_{r-1} + (\sigma - \sigma_{r-1})/\bar{E}$, where $1/\bar{E} = [\partial F/\partial\sigma]_{r-(1/2)}$. The best integration formula is obtained when σ is solved exactly from the differential equation (4.35) under the assumption that $d\epsilon/d\bar{\phi}$, $d\epsilon^0/d\bar{\phi}$, and E are constant during the step. After rearrangement, this leads to the pseudoelastic law (5.8), in which

$$E_r'' = E_{r-(1/2)}\frac{1 - e^{-\Delta\varphi_r^*}}{\Delta\varphi_r^*}$$
$$\Delta\epsilon_r'' = \Delta\bar{\phi}_r F(\sigma_{r-1}, t_{r-1}) + \Delta\epsilon_r^0, \tag{5.22}$$

and $\Delta\phi_r^* = \Delta\bar{\phi}_r E_{r-(1/2)}/\bar{E}$. Because of nonlinearity, the analysis of each step should be iterated; in the first run, all coefficients depending on σ are evaluated for $\sigma = \sigma_{r-1}$, and in the repeated run, they are evaluated for $\sigma = \sigma_{r-1} + \frac{1}{2}\Delta\sigma_r$, where $\Delta\sigma_r$ is taken according to the first run. The high accuracy of formula (5.22) is due to the fact that in the linear case with constant E (which coincides with the rate of creep method; Subsection 5.4), Eq. (5.22) gives the exact expressions for both the creep at constant σ and the stress relaxation at constant ϵ.

5.4 Conversion of Inelastic Strains to Applied Loads

As has been shown, the solution of a linear elasticity problem with general inelastic strains (or, equivalently, inelastic stresses) is the basis for integration of the creep problem in space coordinates. The handling of general inelastic strains is easily incorporated into the finite-element method. This can be expediently implemented, in the most general formulation, according to the following theorem, also applicable for the finite-difference or other methods.

THEOREM. *Consider the general (anisotropic) elastic stress–strain relations*

$$\sigma_{ij} = C_{ijkl}(\epsilon_{kl} - \epsilon_{kl}''), \tag{5.23}$$

where C_{ijkl} is elastic moduli, ϵ_{kl} is linearized strain tensor, and ϵ_{kl}'' is prescribed inelastic strain tensor. Define further

$$\sigma_{ij}'' = C_{ijkl}\epsilon_{kl}'', \qquad \tilde{f}_i = -\sigma_{ij,j}'' \quad \text{in } \mathcal{V},$$
$$\tilde{p}_i = n_j\sigma_{ij}'' \quad \text{on } \Gamma_1, \qquad \tilde{p}\dagger = n\dagger(\sigma_{ij}''^{+} - \sigma_{ij}''^{-}) \quad \text{on } \Gamma^*, \tag{5.24}$$

where σ_{ij}'' is inelastic stress tensor, $\tilde{f}_i$ and $\tilde{p}_i$, $\tilde{p}\dagger$ are (fictitious) volume and surface loads equilibrating σ_{ij}'', Γ^* is surface with unit normal $n\dagger$ across which σ_{ij}'' changes discontinuously from $\sigma_{ij}''^{-}$ to $\sigma_{ij}''^{+}$. Then the stresses, strains, and displacements caused by ϵ_{ij}'' are

$$\sigma_{ij} = \tilde{\sigma}_{ij} - \sigma_{ij}'', \qquad \epsilon_{ij} = \tilde{\epsilon}_{ij}, \qquad u_i = \tilde{u}_i, \tag{5.25}$$

where $\tilde{\sigma}_{ij}$, $\tilde{\epsilon}_{ij}$, and $\tilde{u}_i$ are the solutions corresponding to loads $\tilde{f}_i$, $\tilde{p}_i$, $\tilde{p}\dagger$, with no inelastic strains, and to given boundary displacements u_i^0 (if any).

Proof. Assuming uniqueness of solutions, it needs to be shown that

$$\tilde{\sigma}_{ij} = C_{ijkl}\tilde{\epsilon}_{kl},$$
$$\tilde{\epsilon}_{ij} = \tfrac{1}{2}(\tilde{u}_{i,j} + \tilde{u}_{j,i}),$$
$$\tilde{\sigma}_{ij,j} + \tilde{f}_i = 0 \quad \text{in } \mathcal{V},$$
$$\tilde{n}_j\tilde{\sigma}_{ij} = \tilde{p}_i \quad \text{on } \Gamma_1,$$
$$\tilde{u}_i = u_i^0 \quad \text{on } \Gamma_2,$$
$$n\dagger(\tilde{\sigma}_{ij}^{+} - \tilde{\sigma}_{ij}^{-}) = \tilde{p}\dagger \quad \text{on } \Gamma^*. \tag{5.26}$$

That this is indeed true is seen by substituting Eq. (5.25) into Eq. (5.23) and Eqs. (5.5) to (5.6) with $f_i = p_i = 0$, and into the continuity condition $n\dagger(\sigma_{ij}^{+} - \sigma_{ij}^{-}) = 0$. (Summation over repeated indices is implied.)

The special case of this theorem for isotropic ϵ_{ij}'' is known in thermoelasticity as body force analogy[156] due to Duhamel (1838) and Neumann. For deviatoric plastic strains, it was derived in 1931 by Reissner and, in different contexts, by Eschelby (cf. Ref. [156]) and others[138, 145, 150]. To creep of concrete it was first applied in 1964 (cf. Refs. [138, 150]), and simultaneously to creep of metals[156]. For the

replacement of inelastic strains by transverse loads in nonlinear creep of plates, reinforced plates, and composite beams, see Refs. [131, 138, 145, 148–150].

5.5 Approximate Solutions Based on Simplified Linear Creep Laws

For many design purposes, even the solutions based on viscoelasticity of aging materials are too complex. Therefore, simplified methods, embodied in the formulas of current code recommendations, are invariably used in the design of ordinary-type structures in which design experience can be partly substituted for accuracy. These methods either consist of a single elastic analysis or are based on a simplified creep function $J(t, t')$. Normally, they apply only for loads and enforced displacements that are either steady or vary at a rate decaying roughly as $1/(t - t_0)$, t_0 being the instant of introducing the first load or enforced deformation into the structure. Sudden load increments at various times t_0 must be considered separately and the results then superimposed.

A. Effective Modulus Method. This is an old method (cf. Ref. [157]) consisting in a single elastic solution based on the effective modulus $E_{\text{eff}} = 1/J(t, t_0) = E(t_0)/[1 + \phi(t, t_0)]$. Accuracy is usually excellent when aging is negligible as in very old concrete (see comments after Eq. (5.33); for nonaging viscoelasticity this fact was noted and examined in Ref. [158]. In this case, $J(t, t')$ is a function of only $(t - t')$, i.e. creep curves for all t' are identical but mutually horizontally translated. This overestimates creep due to stress changes after t_0 and incorrectly implies, in case of finite $J(\infty, t')$, all creep to be perfectly recoverable after unloading.

B. Age-Adjusted Effective Modulus Method. This method was originated in 1967 by Trost [159], and its rigorous, extended, and general formulation was first given in Ref. [160], on the basis of the following theorem.

THEOREM [160]. *Assume that*

$$\epsilon(t) - \epsilon^0(t) = \epsilon_0 + \epsilon_1 \phi(t, t_0) \tag{5.27}$$

for $t \geq t_0$ *and* $\sigma = 0$ *for* $t < t_0$, *where* ϵ_0 *and* ϵ_1 *are arbitrary constants (such that strain is small). Then*

$$\Delta\sigma(t) = E''(t, t_0)[\Delta\epsilon(t) - \Delta\epsilon''(t)], \tag{5.28}$$

where

$$\Delta\epsilon(t) = \epsilon(t) - \epsilon(t_0), \qquad \Delta\sigma(t) = \sigma(t) - \sigma(t_0), \tag{5.29}$$

$$\Delta\epsilon''(t) = \frac{\sigma(t_0)}{E(t_0)}\phi(t, t_0) + \epsilon^0(t) - \epsilon^0(t_0), \tag{5.30}$$

$$E''(t, t_0) = \frac{E(t_0) - E_R(t, t_0)}{\phi(t, t_0)} = \frac{E(t_0)}{1 + \chi(t, t_0)\phi(t, t_0)}, \tag{5.31}$$

$$\chi(t, t_0) = \frac{1}{1 - E_R(t, t_0)/E(t_0)} - \frac{1}{\phi(t, t_0)}. \tag{5.32}$$

Proof. Equation (5.32) follows from Eq. (5.31). Assume Eqs. (5.28) to (5.31) to be true. Substitution of Eq. (5.31) with Eqs. (5.27), (5.29), and (5.30) [with $\sigma(t_0)/E(t_0) = \epsilon_0$] into Eq. (5.28) yields $\sigma(t) = \sigma(t_0) + [E(t_0) - E_R(t, t_0)](\epsilon_1 - \epsilon_0)$ for $t \geq t_0$. Insertion of this relation with Eq. (5.27) into Eq. (3.1) furnishes

$$(\epsilon_0 - \epsilon_1)\int_{t_0}^{t} J(t, t')\frac{\partial E_R(t', t_0)}{\partial t'}\,dt' = \epsilon_0 + \epsilon_1[E(t_0)J(t, t_0) - 1] - J(t, t_0)\sigma(t_0)$$
$$= \epsilon_0 - \epsilon_1 - (\epsilon_0 - \epsilon_1)E(t_0)J(t, t_0). \tag{5.33}$$

If $\epsilon_0 = \epsilon_1$, this equation is identically satisfied, and if $\epsilon_0 \neq \epsilon_1$, division by $(\epsilon_0 - \epsilon_1)$ yields identity (3.6). Finally, if Eqs. (5.28) to (5.31) were not true, Eq. (3.6) would be contradicted.

Coefficient χ is called aging coefficient and E'' age-adjusted effective modulus because χ adjusts the effective modulus E_{eff} primarily for the aging effect. In absence of aging, $\chi \approx 1$ and $E'' \approx E_{\text{eff}}$. Tables of χ for some typical creep functions were given in Ref. [160]; always $\chi < 1$ and almost always $\chi > 0.5$; χ grows with t as well as t_0.

Importance of the foregoing theorem, by which the calculation of the changes from t_0 to t is reduced to a single elastic analysis according to Eq. (5.28), lies in the fact that χ and E'' are independent of ϵ_0 and ϵ_1, and that strain history (5.27), linear in $\phi(t, t_0)$, closely approximates the exact strain variation corresponding to a linear creep law in most cases. While all other methods give exact solutions only when σ is constant, this method gives an exact solution in infinitely many special cases, in particular the cases of constant σ, constant ϵ (stress relaxation), and the case $\epsilon = \epsilon_1\phi(t, t_0)$ typical of buckling problems or shrinkage-induced stresses.

C. Rate-of-Creep Method. This method ("Dischinger's" method in German, "theory of aging" in Russian), due to Glanville (cf. Ref. [157])

and first widely applied by Dischinger[143], admits simple analytical solutions of many problems (cf. Refs. [83, 84, 138, 151], for example), assuming the creep law in the form

$$\frac{d\epsilon}{d\bar{\phi}} = \frac{1}{E(t)}\frac{d\sigma}{d\bar{\phi}} + \frac{\sigma}{E(t_0)} + \frac{d\epsilon^0}{d\bar{\phi}}, \tag{5.34}$$

or

$$J(t, t') \approx \frac{1}{E(t')} + \frac{\bar{\phi}(t) - \bar{\phi}(t')}{E(t_0)}, \tag{5.35}$$

where $\bar{\phi}(t) = \phi(t, t_0)$. Equation (5.34) corresponds to an age-dependent Maxwell solid[77], and Eq. (5.35) expresses the Whitney's assumption (cf. Ref. [157]) that the creep curves (ϵ versus t) for various t' are identical in shape but mutually translated parallel to the ϵ-axis. Thus, no delayed creep recovery is predicted, and for old concrete negligible creep is obtained, which is false. In relaxation-type problems, prediction of this method represents an upper bound on the stress change from t_0 to t, while the effective modulus method gives a lower bound.

D. Rate-of-Flow Method. This method is based on the creep function

$$J(t, t') \approx \frac{1}{E_d} + \frac{\phi_f(t) - \phi_f(t')}{E(t')}, \qquad \frac{1}{E_d} = \frac{1}{E(t')} + \frac{\phi_d}{E(28)} \tag{5.36}$$

proposed by Prokopovich and Ulickii[161, p. 37] and independently (with a more detailed justification) by England and Illston[21–23]. Coefficient $\phi_f(t)$, analogous to $\bar{\phi}$ in Eq. (5.35), expresses irrecoverable creep or flow, and ϕ_d is a coefficient for delayed elastic (or recoverable) strain which is taken as independent of age t' and (in accordance with item 7, Section 2) depends only on $(t - t')$. Furthermore, Nielsen[162] and Rüsch, and Jungwirth and Hilsdorf (cf. Refs. [157, 167]) proposed to treat the delayed elastic component in terms of the effective modulus, taking ϕ_d as constant ($\phi_d \approx 0.4$ for long-range response). Thus, Eq. (5.36) becomes formally identical to Eq. (5.35), and all formulas based on the rate-of-creep method can be directly applied, replacing E with E_d and $\bar{\phi}$ with ϕ_f. The method is a hybrid of the rate-of-creep and effective modulus methods. Its predictions usually lie between the latter two and are thus closer to the exact solution.

E. Arutyunian's Method and Levi's Method. Arutyunian's creep function[144] corresponds to a single term ($n = 1$) of the Dirichlet series creep function (3.15). Relaxation-type problems then lead to first-order differential equations with variable coefficients for internal force rates or displacement rates[144, 161], and a similar equation relates strain rates and stresses[77, 138]. In most problems with one unknown, integration is possible in terms of the incomplete gamma function, provided E is a constant and $E_u = A + B/t'$[144, 161] or $A + Be^{-t/\tau}$[163], where A, B, and τ are constants. Applications of this method have flourished (particularly in eastern Europe) because, in contrast to the effective modulus and rate-of-creep methods, the proper ratio between the creep of young aging and old nonaging concrete can be introduced. But the exponential shape of the creep curves is far from reality [see Fig. 7(a)]. Also, the calculations are more complex than with any other simplified method in use. Levi's method (cf. Ref. [157]) is a counterpart of Arutyunian's, corresponding to a single term of the Dirichlet series relaxation function (in a certain transformed time variable). It also leads to first-order differential equations and allows analytical integration in simple cases.

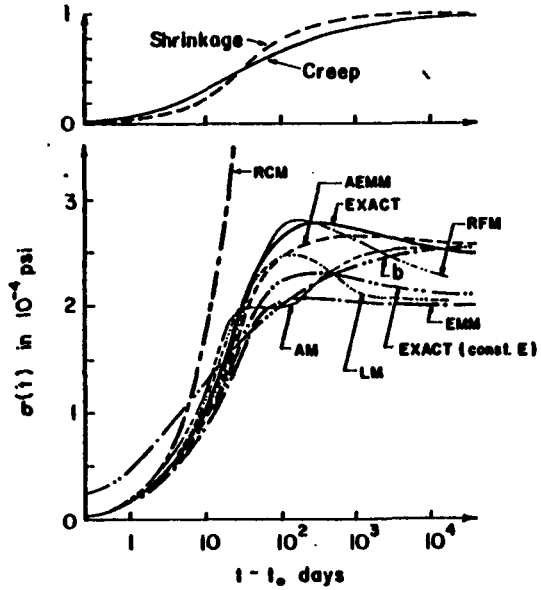

Fig. 27 Development of shrinkage stress at $\epsilon = 0$. Computed for ACI expressions (3.10) to (3.12); solid lines are exact numerical solutions; EMM, AEMM are approximate solutions by effective modulus and age-adjusted effective modulus method; RCM, RFM are by rate-of-creep and rate-of-flow methods; LM, AM are by Levi's and Arutyunian's methods (Subsection 5.5). Top figure shows creep curve $f(t - t')$ from Eq. (3.11) and shrinkage curve $\epsilon_{sh}/\epsilon_{sh}(\infty)$ from Eq. (3.12). (After Bažant, Z. P., and Najjar, L. J., "Comparison of Approximate Linear Methods for Concrete Creep," *J. Struct. Div.*, Proc. Amer. Soc. of Civil Engineers, 99 (1973) 1851–1874.)

Extensive numerical studies of typical practical problems [157] (such as stress relaxation, shrinkage stress, creep buckling deflections, prestress loss in prestressed beams, straining by differential creep due to unequal age, stress redistributions in composite beams, and cracked reinforced beams; Figs. 27–29) indicated that, in comparison with the exact solutions for given $J(t, t')$, the age-adjusted effective modulus method was superior to any other method. Second best was the rate-of-flow method.

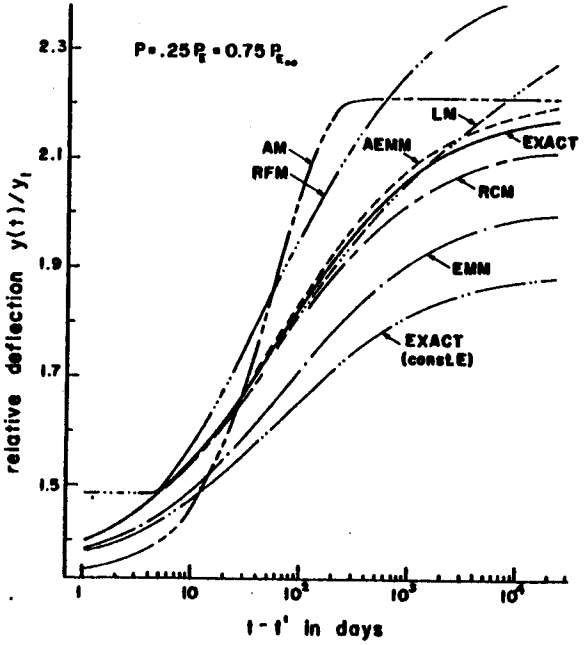

Fig. 28 Creep buckling deflections of a typical slender reinforced concrete column under working loads. Computed for ACI expressions (3.10) to (3.11); same labels as in Fig. 27. For the values of assumed column parameters, see Ref. [157]. (Added in proof: Due to an error, multiply curves exact (const. E) and EMM by $r_0(1 - r_0 + r)$ where r = ordinates as shown, $r_0 = y/y_1$ just after loading, y_1 = ordinate before loading, column shape being sinusoidal.) (After Bažant, Z. P., and Najjar, L. J., "Comparison of Approximate Linear Methods for Concrete Creep," *J. Struct. Div.*, Proc. Amer. Soc. of Civil Engineers, 99 (1973) 1851–1874.)

In favor of the latter, it is sometimes argued that the recovery after sudden complete unloading is fitted better than by superposition of creep curves at constant σ, i.e. $J(t, t')$. This is true, but a complete unloading is rare in practice, and for small or gradual decreases of stress, as in relaxation-type problems, this argument is invalid. Also, it is not desirable to make $J(t, t')$ fit the recovery after complete unloading because the

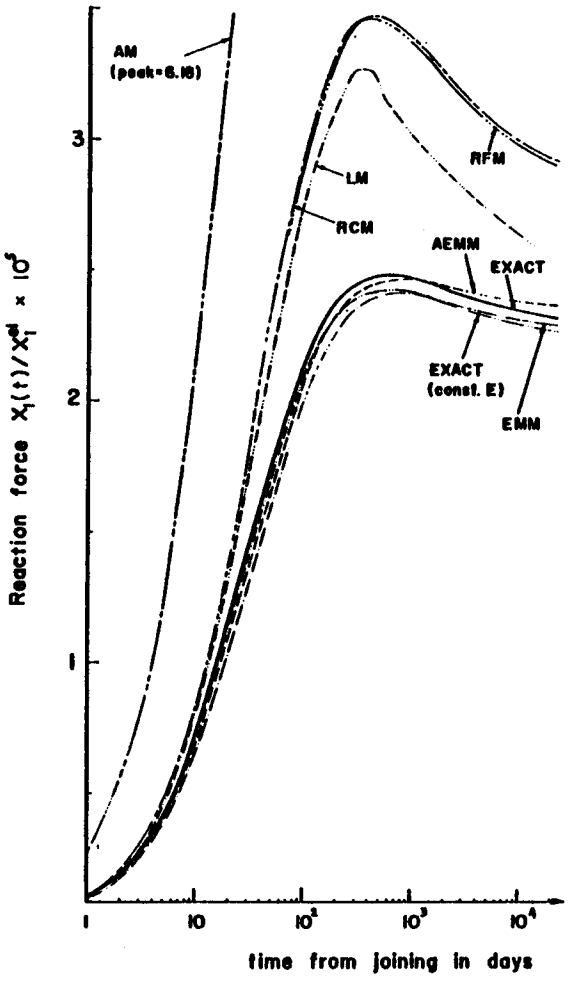

Fig. 29 Shear force X_1 generated by creep in the midspan connection of two concrete cantilevers of different age. Computed for ACI expressions (3.10) to (3.12); same labels as in Fig. 27. For assumed properties of structure, cf. Ref. [157]; X_1^{el} is elastic reaction due to unit displacement. (After Bažant, Z. P., and Najjar, L. J., "Comparison of Approximate Linear Methods for Concrete Creep," *J. Struct. Div.*, Proc. Amer. Soc. of Civil Engineers, 99 (1973) 1851–1874.)

prediction of creep of old concrete is then inevitably sacrificed [157]. Anyhow, it should be remembered that any deviation from the principle of superposition is a nonlinear effect, so that the frequent efforts to correct the deviation by a linear creep law corresponding to a distorted creep function are based on misconception.

6 PRACTICAL PROBLEMS IN DESIGN AND CONCLUSION

Applying the methods of analysis outlined in Section 5, one can analyze most problems encountered in engineering practice. An abundant literature on this subject exists[3, 79, 82, 84, 138, 157, for example]. Here only a brief review of the practical problems will be made.

The most obvious effect of creep to be considered in design is the growth of deflections, which is of concern, e.g., in large-span prestressed concrete bridges. Cases of deflections over one foot in excess of the predicted values have been experienced in some early long-span bridges built in Europe (by segmental cantilevering, with hinges at midspan). This, of course, very adversely affects the serviceability of the structure and may require expensive countermeasures.

In concrete columns, compressed walls, and thin shells, creep magnifies the buckling deflections (Fig. 28) and internal forces due to unavoidable imperfections, and leads to long-time instability under a load several times less than the short-time stability limit. Most building codes, including ACI Code 1971, take creep buckling into account in the form of an approximate effective modulus and distinguish between various ratios of short-time to load-time loads on columns. Similarly, creep buckling is of concern for concrete arches and shells.

In many structures, creep causes extensive redistributions of internal forces and, together with stresses induced by shrinkage (see Ref. [166]) and thermal dilatations, may produce severe cracking and overload of some structural parts (or at least a reduction in the safety against collapse under superimposed short-time load). These redistributions are absent only if the structure is statically determinate or if it is statically indeterminate and homogeneous, that is, the ratio of creep to stress is the same in all points of the structure (cf. Subsection 5.2). This is, of course, not the case if the nonlinearity of creep or the differences in creep properties due to different humidity and temperature in various points of the structure are considered. Even under the assumption of a linear aging viscoelastic material (Section 3), stress redistributions occur, due to the presence of steel reinforcement, which does not creep, the interaction of concrete and steel structural members (as in cable-stayed concrete girders), or the differential creep of parts of significantly different age, as in many structures built with a repeated use of one formwork. In general, creep transfers internal forces from parts creeping more into parts creeping less. A typical example is a bridge span whose halves are cast by cantilever method with the same slip form, one after the other; the younger half tends to deflect more but, because of the connection at midspan, produces a shear force (Fig. 29) relieving its bending moments and augmenting them in the older half. Another important example is the differences in creep and shrinkage shortening of the columns and the shear-wall core in a tall building, resulting from the differences in cross section sizes and reinforcement ratios, and from the differences in environmental conditions between the interior and the exterior of the building. Over a great height, large differences in vertical displacement can accumulate; this strains severely the floor slabs and requires special partition walls that can adapt to the relative movements.

Stress redistributions also occur within all nonhomogeneous cross sections of beams or slabs. In columns, the normal force carried by concrete is gradually transferred upon the steel reinforcement, and its normal stress is further increased by shrinkage of concrete. Similar redistributions of normal forces and bending moments occur within the cross section of steel–concrete composite girders and composite girders consisting of prefabricated prestressed beams covered by a slab cast *in situ* whose concrete is younger and creeps more. Due to creep shortening of the prestressed beam, the prestressing force is partly transferred from the beam on the attached slab, and a camber is produced in the beam. A serious camber may also result from differential creep in composite cross sections, from nonsymmetric shrinkage, and from shrinkage in nonsymmetrically reinforced cross sections or nonsymmetrically drying cross sections. In statically indeterminate structures, free camber is not possible, and secondary internal forces are developed by the camber.

In all prestressed structures, creep and shrinkage cause, of course, a significant loss of prestressing force.

In statically indeterminate structures, creep is beneficial in reducing the forces induced by shrinkage (Fig. 27), or the internal forces due to displacements imposed during the construction by jacks in order to rectify previous undesirable deflections or internal forces in the structure, or the forces due to differential settlements of structure. This reduction is offset when the settlement is gradual rather than instant, as in the case of consolidating clay foundations[164].

When the statical system is changed during construction, e.g., when additional supports or connections are introduced in the structure (Subsection 5.2), creep causes that the internal forces gradually approach those that would exist if the structure were originally built in the new system. A typical example is the construction of a continuous girder from prefabricated simply supported beams by rigidly connecting the beams

above the supports, either with an added top reinforced concrete slab cast *in situ* or with post-tensioned reinforcement running across the support section. In this case, the end cross sections of the girders meeting above the support tend to rotate in opposite directions due to creep of girders, but are prevented to do so by the rigid connection, so that a negative bending moment gradually develops above the support.

The aforementioned problems are tackled by the designers by means of some of the simplified formulations outlined in Subsections 3.2 and 5.5. Such analyses give a crude, though usually sufficient, picture of the deflections and the stress resultants within cross sections of beams or slabs. The values of the resultants then yield, probably with an acceptable error, the necessary amounts of reinforcement and overall cross section dimensions.

However, there should be no illusion that the stresses in concrete computed from the cross section resultants are a good indication of the actual values. To obtain a realistic information on stress distributions within cross sections, it would be necessary to account for the nonuniform drying, shrinkage, and drying creep within the cross section (see Ref. [166]), as well as the nonlinear effects discussed in Section 4, and eventually also temperature history with hydration heat effects.

Such analyses are awaiting successful identification of the material parameters in Section 4 from test data. They probably are of little interest for ordinary building and bridge structures, in which fine cracking of concrete is not of much concern or ample prestress is provided. The situation is, however, different with prestressed concrete pressure vessels for nuclear reactors and secondary reactor containers (and also undersea shells), where cracking is a dominant consideration for serviceability and safety of the structure. Improvement in the prediction of stresses induced by transient and nonuniform temperature fields, and the migration of water within the massive walls of such structures, would undoubtedly improve economy and safety and, what is perhaps even more important, enable exposure of concrete to higher temperatures than the present cautiousness, dictated by ignorance, allows. Therefore, considerable effort is being devoted to these questions at present.

Furthermore, solution to the above questions will be useful for the design of massive blocks of concrete dams, severely stressed by hydration heat effects, and for predicting deflections of slender long-span bridges, in which the serious miscalculations experienced in the past are explicable mostly by asymmetric drying and temperature distributions within the cross sections of the bridge girder.

Although the long-time applied loads that primarily cause creep exhibit narrower statistical distributions than the short-time loads, the environmental conditions, playing an important role in creep and shrinkage, are considerably random. The random nature of material properties is certainly also important. So far, the statistical studies in creep of concrete have been rare[165]. Perhaps, however, the time is not yet ripe for this approach. Before the probabilistic aspects are tackled, the deterministic model of the constitutive equation ought to be reasonably understood, or the statistical parameters would have to account in a large part for ignorance of the deterministic (or average) components in the material behavior.

Acknowledgment. The present paper has been written in connection with a project funded by the U.S. National Science Foundation under Grant GK-26030. The author wishes to express his gratitude to Mr. S. T. Wu, Graduate Research Assistant at Northwestern University, for his help in extracting some of the experimental data from the literature.

REFERENCES

1. Hatt, W. K., "Notes on the Effect of Time Element in Loading Reinforced Concrete Beams," *Proc. ASTM* 7 (1907) 421–433.
2. Williamson, R. B., "Solidification of Portland Cement," in *Progress in Materials Science*, B. Chalmers *et al.* (eds.), Vol. 15, No. 3, Pergamon Press, New York, London (1972).
3. Neville, A. M., and Dilger, W., *Creep of Concrete: Plain, Reinforced, Prestressed*, North-Holland, Amsterdam (1970).
4. Neville, A. M., *Properties of Concrete*, 2nd ed., Wiley, New York (1973).
5. Hanson, J. A., "A 10-Year Study of Creep Properties of Concrete," Concrete Laboratory Report No. Sp-38, U.S. Department of the Interior, Bureau of Reclamation, Denver, Colo. (1953).
6. Harboe, E. M., *et al.*, "A Comparison of the Instantaneous and the Sustained Modulus of Elasticity of Concrete," Concrete Laboratory Report No. C-854, Division of Engineering Laboratories, U.S. Department of the Interior, Bureau of Reclamation, Denver, Colo. (1958).
7. L'Hermite, R., Mamillan, M., and Lefèvre, C., "Nouveaux résultats de recherches sur la déformation et la rupture du béton," *Annales de l'Institut Technique du Bâtiment et des Travaux Publics* 18 (1965) 325–360; see also Int. Conf. on the Structure of Concrete, Cement and Concrete Assoc., London (1968) 423–433.
8. Browne, R. D., and Blundell, R., "The Influence of Loading Age and Temperature on the Long Term Creep Behavior of Concrete in a Sealed, Moisture Stable State," *Materials and Structures* (RILEM) 2 (1969) 133–144.
9. Troxell, G. E., Raphael, J. M., and Davis, R. W., "Long Time Creep and Shrinkage Tests of Plain and Reinforced Concrete," *Proc. ASTM* 58 (1958) 1101–1120.

10. Davies, R. D., "Some Experiments on the Applicability of the Principle of Superposition to the Strain of Concrete Subjected to Changes of Stress, with Particular Reference to Prestressed Concrete," *Mag. Concrete Res.* 9 (1957) 161–172.
11. Ross, A. D., "Creep of Concrete under Variable Stress," *Amer. Concrete Inst. J.* 54 (1958) 739–758.
12. Le Camus, B., "Recherches Expérimentales sur la Déformation du Béton et du Béton Armé, Part II," *Annales, Inst. Techn. du Bâtiment et des Travaux Publics*, Paris (1947).
13. Meyers, B. L., and Slate, F. O., "Creep and Creep Recovery of Plain Concrete as Influenced by Moisture Conditions and Associated Variables," *Mag. Concrete Res.* 22 (1970) 37–8.
14. Roll, F., "Long-Time Creep-Recovery of Highly Stressed Concrete Cylinders," *Amer. Concrete Inst. Spec. Publ. SP-9*, Symposium on Creep, Detroit (1964) 115–128.
15. Freudenthal, A. M., and Roll, F., "Creep and Creep Recovery of Concrete under High Compressive Stress," *Amer. Concrete Inst. J.* 54 (1958) 1111–1142.
16. Aleksandrovskii, S. V., *Analysis of Plain and Reinforced Concrete Structures for Temperature and Moisture Effects (with Account of Creep)* (in Russian), Stroyizdat, Moscow (1966), 443 pp.
17. Ishai, O., "Elastic and Inelastic Behavior of Cement Mortar in Torsion," *Amer. Concrete Inst. Spec. Publ. SP-9*, Symposium on Creep, Detroit (1964) 65–94.
18. Meyer, H. G., "On the Influence of Water Content and of Drying Conditions on Lateral Creep of Plain Concrete," *Materials and Structures* 2 (1969) 125–131.
19. Hannant, D. J., "Strain Behavior of Concrete up to 95°C under Compressive Stresses," *Conf. on Prestressed Concrete Pressure Vessels*, Group C, Paper 17, Institution of Civil Engineers, London (1967) 57–71.
20. Arthanari, S., and Yu, C. W., "Creep of Concrete under Uniaxial and Biaxial Stresses at Elevated Temperatures," *Mag. Concrete Res.* 19 (1967) 149–156.
21. England, G. L., and Illston, J. M., "Methods of Computing Stress in Concrete from a History of Measured Strain," *Civil Engrg. Publ. Works Rev.* (1965) 513–517, 692–694, 846–847.
22. Illston, J. M., "Components of Creep in Maturing Concrete," *Amer. Concrete Inst. J.* 65 (1968) 219–228.
23. Illston, J. M., and Jordaan, I. J., "Creep Prediction for Concrete under Multiaxial Stress," *Amer. Concrete Inst. J.* 69 (1972) 158–164.
24. Aleksandrovskii, S. V., and Popkova, O. M., "Nonlinear Creep Strains of Concrete at Complex Load Histories" (in Russian), *Beton i Zhelezobeton* 16 (1970) 27–32.
25. Kimishima, H., and Kitahara, Y., "Creep and Creep Recovery of Mass Concrete," Tech. Rept. C-64001, Central Research Institute of Electric Power Industry, Tokyo, Sept. 1964.
26. Pirtz, D., "Creep Characteristics of Mass Concrete for Dworshak Dam," Report No. 65-2, Structural Engineering Laboratory, University of California, Berkeley, Oct. 1968.
27. Brettle, H. J., "Increase in Concrete Modulus of Elasticity due to Prestress and Its Effect on Beam Deflections," *Constructional Rev.* (Sydney) 31 (1958) 32–35.
28. Wittmann, F., Einfluss des Feuchtigkeitsgehaltes auf das Kriechen des Zementsteines," *Rheol. Acta* 9 (1970) 282–287.
29. Ruetz, W., "An Hypothesis for the Creep of Hardened Cement Paste and the Influence of Simultaneous Shrinkage," *Int. Conf. on the Structure of Concrete*, held in London, 1965, Cement and Concrete Assoc. (1968) 365–387; see also *Deutscher Ausschuss für Stahlbeton* Heft 183 (1966).

30. Mullen W. G., and Dolch, W. L., "Creep of Portland Cement Paste," *Proc. ASTM* 64 (1964) 1146–1170.
31. Ross, A. D., Illston, J. M., and England, G. L., "Short- and Long-Term Deformations of Concrete as Influenced by its Physical Structure and State," *Int. Conf. on the Structure of Concrete*, held in London, 1965, Cement and Concrete Assoc. (1968) 407–422.
32. Glucklich, J., and Ishai, O., "Creep Mechanism in Cement Mortar," *Amer. Concrete Inst. J.* 59 (1962) 923–948.
33. Cilosani, Z. N., "On the True Mechanism of Creep of Concrete" (in Russian), *Beton i Zhelezobeton* (Moscow) 10 (1964) 75–78.
34. Pickett, G., "The Effect of Change in Moisture Content on the Creep of Concrete under a Sustained Load," *Amer. Concrete Inst. J.* 36 (1942) 333–355; see also "Shrinkage Stresses in Concrete," *Amer. Concrete Inst. J.* 42 (1946) 165–204, 361–400.
35. Feldman, R. F., and Sereda, P. J., "Discussion," *Proc. 5th Int. Symp. on the Chemistry of Cements* (held in Tokyo) 3 (1968) 36–44.
36. L'Hermite, R., "Volume Changes of Concrete," U.S. National Bureau of Standards Monograph 43, *4th Int. Symp. on Chemistry of Cements* (held in Washington, D.C.) 3, Oct. 1960, 659–694.
37. Wittman, F., "Kriechen bei Gleichzeitigem Schwinden des Zementsteins," *Rheol. Acta* 5 (1966) 198–204.
38. Ali, J., and Kesler, C. E., "Creep in Concrete with and Without Exchange of Moisture with the Environment," Univ. of Illinois, Dept. of Theor. Appl. Mech., Report No. 641, Urbana, Dec. 1963.
39. Weil, G., "Influence des Dimensions et des Tensions sur le Retrait et le Fluage de Béton," *RILEM Bull.* No. 3 (1959) 4–14.
40. Hansen, T. C., and Mattock, A. H., "Influence of Size and Shape of Member on the Shrinkage and Creep of Concrete," *Amer. Concrete Inst. J.* 63 (1966) 267–290.
41. Mamillan, M., and Lelan, M., "Le Fluage de Béton," *Annales, Inst. Techn. du Bâtiment et des Travaux Publics* (Supplément) 23 (1970) 7–13 (No. 270), and 21 (1968) 847–850 (No. 246).
42. L'Hermite, R., and Mamillan, M., "Retrait et fluage des bétons," *Annales, Inst. Techn. du Bâtiment et des Travaux Publics* (Supplément) 21 (1968) 1334 (No. 249); and "Nouveaux résultats et récentes études sur le fluage du béton," *Materials and Structures* 2 (1969) 35–41; and Mamillan, M., and Bouineau, A., "Influence de la dimension des éprouvettes sur le retrait," *Annales Inst. Techn. du Bâtiment et des Travaux Publics* (Supplément) 23 (1970) 5–6 (No. 270).
43. Powers, T. C., "Mechanism of Shrinkage and Reversible Creep of Hardened Cement Paste," *Int. Conf. on the Structure of Concrete*, held in London in 1965, Cement and Concrete Assoc., London (1968) 319–344.
44. Hansen, T. C., "Creep and Stress Relaxation in Concrete," *Proc., Swedish Cement and Concrete Res. Inst.*, Royal Inst. of Techn., Stockholm No. 31 (1960).
45. Hannant, D. J., "The Mechanism of Creep of Concrete," *Materials and Structures* (RILEM) 1 (1968) 403–410.
46. Gaede, K., "Versuche über die Festigkeit und die Verformungen von Beton bei Druck-Schwellbeanspruchung," *Deutscher Ausschuss für Stahlbeton* Heft 144, W. Ernst, Berlin (1962).
47. Mehmel, A., and Kern, E., "Elastische und Plastische Stauchungen von Beton infolge Druckschwell-und Standbelastung," *Deutscher Ausschuss für Stahlbeton* Heft 153, W. Ernst, Berlin (1962).

48. Aleksandrovskii, S. V., and Bargii, V. Ya., "Creep of Concrete at Stepwise Alternating Periodic Loads" (in Russian), *Beton i Zhelezobeton* 13 (Dec. 1967) 31–33.
49. Karanfilov, T. S., and Volkov, Yu. S., "Behavior of Reinforced Concrete Structures under Repeated Loads" (in Russian), *Use of Concrete in Mechanical Engineering*, Mashinostroenie, Moscow (1964) 43–80 (cf. also Soviet Code Specification SN 200-62).
50. Gvozdev, A. A., "Creep of Concrete" (survey, in Russian), *Mekhanika Tverdogo Tela*, Proc. of the 2nd Nat. Conf. on Theor. and Appl. Mech., Acad. Sci. USSR, Moscow (1966) 137–152.
51. Wittmann, F., "Kriechverformung des Betons unter Statischer und unter Dynamischer Belastung," *Rheol. Acta* 10 (1971) 422–428.
52. Bažant, Z. P., "Langzeitige Durchbiegungen von Spannbetonbrücken infolge des Schwingkriechens unter Verkehrslasten," *Beton-und Stahlbetonbau* 63 (1968) 282–285.
53. Powers, T. C., "A Discussion of Cement Hydration in Relation to the Curing of Concrete," *Proc. of the Highway Research Board* 27 (1947) 178–188 (PCA Bulletin No. 25).
54. Wittmann, F., "Surface Tension, Shrinkage and Strength of Hardened Cement Paste," *Materials and Structures* (RILEM) 1 (1968) 547–552.
55. Mamillan, M., "Évolution du Fluage et des Propriétés de Béton," *Annales, Inst. Techn. du Bâtiment et des Travaux Publics* 21 (1969) 1033; and 13 (1960) 1017–1052.
56. Browne, R. D., "Properties of Concrete in Reactor Vessels," *Conf. on Prestressed Concrete Reactor Pressure Vessels*, Inst. of Civil Engrg., London (March 1967). Paper 13, 11–13.
57. York, G. P., Kennedy, T. W., and Perry, E. S., "Experimental Investigation of Creep in Concrete Subjected to Multiaxial Compressive Stresses and Elevated Temperatures," Research Report 2864-2, University of Texas, Austin (1970); see also *Amer. Concrete Inst. Spec. Publ. No. 34* (1972) 641–700.
58. McDonald, J. E., "An Experimental Study of Multiaxial Creep in Concrete," *Amer. Concrete Inst. Spec. Publ. No. 34*, Concrete for Nuclear Reactors, Detroit (1972) 732–768.
59. Maréchal, J. C., "Fluage du Béton en Fonction de la Température," *Materials and Structures* (RILEM) 2 (1969) 111–115; see also *Materials and Structures* 3 (1970) 395–406.
60. Bažant, Z. P., and Wu, S. T., "Thermoviscoelasticity of Aging Concrete," *J. Engrg. Mech. Div.*, Proc. Amer. Soc. of Civil Engrs. 100(1974) 575–597; also ASCE Preprint 2110 (1973).
61. Wallo, E. M., Yuan, R. L., Lott, J. L., and Kesler, E. L., "Prediction of Creep in Structural Concrete from Short Time Tests," Sixth Progress Report, Theor. & Appl. Mech. Report No. 658, University of Illinois, Urbana (1965).
62. Fahmi, H. M., Polivka, M., and Bresler, B., "Effect of Sustained and Cyclic Elevated Temperature on Creep and Concrete," *Cement and Concrete Res.* 2 (1972) 591–606.
63. Feldman, R. F., "Mechanism of Creep of Hydrated Portland Cement Paste," *Cement and Concrete Res.* 2 (1972) 521–540.
64. Feldman, R. D., and Sereda, P. J., "A Model for Hydrated Portland Cement Paste as Deduced from Sorption-Length Change and Mechanical Properties," *Materials and Structures* (RILEM) 1 (1968) 509–520.
65. Helmuth, R. A., and Turk, D., "The Reversible and Irreversible Drying Shrinkage of Hardened Portland Cement and Tricalcium Silicate Pastes," *J. Portland Cement Assoc. Res. & Devel. Lab.* 9 (1967) 8–21.

66. Houk, I. E., Orville, E. B., and Houghton, D. L., "Studies of Autogeneous Volume Change in Concrete for Dworshak Dam," *Amer. Concrete Inst. J.* 66 (July 1969) 560–568.
67. Bažant, Z. P., and Najjar, L. J., "Nonlinear Water Diffusion in Nonsaturated Concrete," *Materials and Structures* (RILEM) 5 (1972) 3–20.
68. Bažant, Z. P., "Delayed Thermal Dilatations of Cement Paste and Concrete Due to Mass Transport," *Nuclear Engrg. & Design* 14 (1970) 308–318.
69. Rüsch, H., *et al.*, "Festigkeit und Verformung von unbewehrtem Beton unter konstanter Dauerlast," *Deutscher Ausschuss für Stahlbeton* Heft 198, W. Ernst, Berlin (1968); see also *Amer. Concrete Inst. J.* 57 (1960) 1–28.
70. Hellesland, J., and Green, R., "A Stress and Time Dependent Strength Law for Concrete," *Cement and Concrete Res.* 2 (1972) 261–275.
71. Lauer, R. K., and Slate, F. J., "Autogeneous Healing of Cement Paste," *Amer. Concrete Inst. J.* 52 (1956) 1083–1098.
72. Radjy, F., and Richards, C. W., "Effect of Curing and Heat Treatment History on the Dynamic Response of Cement Paste," *Cement and Concrete Res.* 3 (1973) 7–21.
73. Volterra, V., *Leçons sur les Fonctions de Ligne*, Gauthier-Villars, Paris (1913); and *Theory of Functionals and of Integral and Integrodifferential Equations*, Dover, New York (1959).
74. Boltzmann, Z., "Zur Theorie der Elastischen Nachwirkung," *Sitzber. Akad. Wiss., Wiener Bericht* 70, Wiss. Abh. Vol. I (1874) 275–306; see also *Pogg. Ann. Phys.* 7 (1876) 624.
75. McHenry, D., "A New Aspect of Creep in Concrete and Its Application to Design," *Proc. ASTM* 43 (1943) 1069–1086.
76. Maslov, G. N., "Thermal Stress States in Concrete Masses, with Account of Concrete Creep" (in Russian), *Izvestia Nauchno-Issledovatel'skogo Instituta Gidrotekhniki*, Gosenergoizdat, 28 (1940) 175–188.
77. Bažant, Z. P., "Phenomenological Theories for Creep of Concrete Based on Rheological Models," *Acta Technica ČSAV*, Prague, 11 (1966) 82–109.
78. Christensen, R. M., *Theory of Viscoelasticity*, Academic Press, New York, (1971).
79. American Concrete Institute Comm. 209, Subcom. II, "Prediction of Creep, Shrinkage and Temperature Effects in Concrete Structures," in Designing for Effects of Creep, Shrinkage and Temperature, *Amer. Concrete Inst. Spec. Publ. No. 27*, Detroit (1971) 51–93.
80. Distefano, J. N., and Sackman, J., "Stability Analysis of a Nonlinear or Viscoelastic Column," *ZAMM* 47 (1967) 349–359; see also *Q. Appl. Math.* 24 (1966) 133–141.
81. Distefano, J. N., "Creep Buckling of Slender Columns," *J. Structural Div.*, Proc. Amer. Soc. of Civil Engineers 91 (June 1965) 127–150; see also, *Publ. IABSE* 21 (1961) 37–48; and *Rend., Acc. Naz. Lincei* 27 (Nov. 1959).
82. Guyon, Y., *Constructions en Béton Précontraint*, Eyrolles, Paris (1966).
83. Ulickii, I. I., Chan U. Ya., and Bolyshev, A. V., *Analysis of Reinforced Concrete Structures with Account of Long-Time Processes* (in Russian), Gosstroyizdat, Kiev (1960).
84. Leonhardt, F., *Prestressed Concrete: Design and Construction*, W. Ernst, Berlin (1964) (transl. from German).
85. Wagner, O, "Das Kriechen Unbewehrten Betons," *Deutscher Ausschuss für Stahlbeton* Heft 13, W. Ernst, Berlin (1958).
86. Hardy, G. M., and Riesz, M., "The General Theory of Dirichlet Series," *Cambridge Tracts in Math. & Math. Phys.*, Cambridge Univ. Press, 18 (1915).
87. Lanczos, C., *Applied Analysis*, Prentice-Hall, Englewood Cliffs, N.J. (1964) 272–280.

88. Bažant, Z. P., and Wu, S. T., "Dirichlet Series Creep Function for Aging Concrete," *J. Engrg. Mech. Div.*, Proc. Amer. Soc. of Civil Engineers 99 (1973) 367–387.
89. Bažant, Z. P., and Wu, S. T., "Rate-Type Creep Law of Aging Concrete Based on Maxwell Chain," *Materials and Structures* (RILEM) 7 (1974) 45–60.
90. Cost, T. M., "Approximate Laplace Transform Inversions in Viscoelastic Stress Analysis," *AIAA J.* 2 (Dec. 1964) 2157–2166.
91. Schapery, R. A., "Approximate Methods of Transform Inversion for Viscoelastic Stress Analysis," *Proc. 4th U.S. Nat. Cong. of Appl. Mech.* (held in Berkeley, Calif., June 1962) 2, 1075–1085, ASME.
92. Williams, M. L., "The Structural Analysis of Viscoelastic Materials," *AIAA J.* 2 (1964) 785–808.
93. Ferry, J. D., *Viscoelastic Properties of Polymers*, 2nd ed., Wiley, New York (1970).
94. Distefano, N., "On the Identification Problem in Linear Viscoelasticity," *Zeitschrift für Angewandte Mathematik und Mechanik* 50 (1970) 683–690.
95. Distefano, N., "Quasi-linearization and the Solution of Nonlinear Design Problems in Structures Undergoing Creep," *Int. J. Solids and Structures* 8 (1972) 215–225.
96. Hansen, T. C., "Estimating Stress Relaxation from Creep Data," *Materials Res. Stand.* (ASTM) 4 (1964) 12–14.
97. Klug, P., and Wittmann, F., "The Correlation Between Creep Deformation and Stress Relaxation in Concrete," *Materials and Structures* (RILEM) 3 (1970) 75–80.
98. Biot, M. A., "Variational Principles of Irreversible Thermodynamics with Application to Viscoelasticity," *Phys. Rev.* 97 (1955) 1463–1469.
99. Rice, J. R., "Inelastic Constitutive Relations for Solids: an Internal Variable Theory and its Application to Metal Plasticity," *J. Mech. Phys. Solids* 19 (1971) 433–455.
100. Bažant, Z. P. "Constitutive Equation for Concrete Creep and Shrinkage Based on Thermodynamics of Multiphase Systems," *Materials and Structures* (RILEM) 3 (1970) 3–36; see also *Report 68/1*, Dept. of Civil Engrg., Univ. of Toronto (1968).
101. Roscoe, R., "Mechanical Models for the Representation of Viscoelastic Properties," *Brit. J. Appl. Phys.* 1 (1950) 171–173.
102. Glasstone, S., Laidler, K. J., and Eyring, H., *The Theory of Rate Processes*, McGraw-Hill, New York (1941).
103. Cottrell, A. H., *The Mechanical Properties of Matter*, Wiley, New York (1965).
104. Copeland, L. E., Kantro, D. L., and Verbeck, G., "Chemistry of Hydration of Portland Cement," *Nat. Bur. Stand. Mono. 43*, 4th Int. Symp. on the Chemistry of Cement, held in Washington, D.C. (1960) 429–465.
105. Berwanger, C., "The Modulus of Concrete and the Coefficient of Thermal Expansion below Normal Temperatures," *Amer. Concrete Inst. Spec. Publ. No. 25*, Temperature and Concrete, Detroit (1971) 191–234.
106. Mukaddam, M. A., and Bresler, B., "Behavior of Concrete under Variable Temperature and Loading," *Amer. Concrete Inst. Spec. Publ. No. 34*, Concrete for Nuclear Reactors, Detroit (1972), 771–797.
107. Sackman, J. L., "Creep in Concrete and Concrete Structures," *Proc., The Princeton Univ. Conf. on Solid Mech.* (1963) 15–48.
108. Rashid, Y. R., "Nonlinear Analysis of Two-Dimensional Problems in Concrete Creep," *J. Appl. Mech.* 39 (1972) 475–482.
109. Cruz, C. R., "Elastic Properties of Concrete at High Temperatures," *J. Portland Cement Assoc. Res. & Dev. Lab.* 9 (1967) 37–45.

110. Powers, T. C., "Some Observations on the Interpretation of Creep Data," *RILEM Bull.* No. 33 (Dec. 1966) 381–391.
111. Hrennikof, A., "Shrinkage, Swelling and Creep in Cement," *J. Engrg. Mech. Div.*, Proc. Amer. Soc. Civil Engineers, 85 (July 1959) 111–135.
112. Lynam, C. G., *Growth and Movements in Portland Cement Concrete*, Oxford Univ. Press, London (1934).
113. Freyssinet, E., *Une Révolution dans les Techniques du Béton*, Eyrolles, Paris (1936).
114. Wittmann, F., "Zementsteins Bestimmung Physikalischer Eigenschaften des Zementsteins," *Deutscher Ausschuss für Stahlbeton* Heft 232, W. Ernst, Berlin (1974).
115. Bažant, Z. P., "Thermodynamic Theory of Concrete Deformation at Variable Temperature and Humidity," Report 69–11, Div. of Struct. Engrg. and Struct. Mech., Univ. of Calif., Berkeley, Aug. 1969; see also *Amer. Concrete Inst. Spec. Publ. No. 27* (1971) 411–427.
116. Bažant, Z. P., "Thermodynamics of Interacting Continua with Surfaces and Creep Analysis of Concrete Structures," *Nuclear Engrg. and Design* 20 (1972) 477–505; see also *Cement and Concrete Res.* 2 (1972) 1–16.
117. Creus, G. J., and Onat, E. T., "Mechanics of Porous Adsorbent Materials," *Int. J. Engrg. Sci.* 10 (1972) 649–658.
118. Stouffer, D. C., and Wineman, A. S., "Linear Viscoelastic Materials with Environmental Dependent Properties," *Int. J. Engrg. Sci.* 9 (1971) 193–212.
119. Stouffer, D. C., and Wineman, A. S., "A Constitutive Equation for Linear Aging, Environmental Dependent Materials," *Acta Mechanica* 13 (1972) 31–53.
120. Bowen, R. M., "Toward a Thermodynamics and Mechanics of Mixtures," *Arch. Rat. Mech. Anal.* 24 (1967) 370–403.
121. Flood, E. A. (ed.), *The Solid-Gas Interface*, M. Dekker, New York (1967).
122. Defay, R., Prigogine, I., Bellemans, A., and Everett, D. H., *Surface Tension and Adsorption*, Wiley, New York (1966).
123. Guggenheim, E. A., *Thermodynamics*, 5th ed., Wiley, North-Holland, New York, (1967); see also *Encyclopedia of Physics*, S. Flügge (ed.), Springer, Berlin, Vol. III/2 (1959).
124. de Groot, S. R., and Mazur, P., *Non-Equilibrium Thermodynamics*, North-Holland–Interscience Publ., New York (1962).
125. Bažant, Z. P., and Moschovidis, Z., "Sutface Diffusion Theory for the Drying Creep Effect in Portland Cement Paste and Concrete," *Amer. Ceramic Society J.* 56 (1973) 235–241.
126. Hill, T. L., "Statistical Mechanics of Multimolecular Adsorption (III)," *J. Chem. Phys.* 15 (1947) 767–777.
127. Hanson, J. A., "Effects of Curing and Drying Environments on Splitting Tensile Strength," *Amer. Concrete Inst. J.* 65 (1968) 535–543.
128. Shah, S. P., and Chandra, S., "Critical Stress, Volume Change and Microcracking in Concrete," *Amer. Concrete Inst. J.* 65 (1968) 770–781.
129. Bažant, Z. P., Hemann, J. H., Koller, H., and Najjar, L. J., "A Thin-Walled Cement Paste Cylinder," *Materials and Structures* 6 (1973) 277–281.
130. Aleksandrovskii, S. V., and Kolesnikov, N. S., "Non-Linear Creep of Concrete at Step-Wise Varying Stress," *Beton i Zhelezobeton* 17 (1971) 24–27.
131. Bažant, Z. P., "Numerical Solution of Non-Linear Creep Problems with Application to Plates," *Int. J. Solids & Structures* 7 (1971) 83–97.

132. Mauch, B., and Holley, J. M., "Creep Buckling of Reinforced Concrete Columns," *J. Struc. Div.*, Proc. Amer. Soc. of Civil Engineers, 89 (1963) 451–481.
133. Mozer, J. D., Gerstle, K. H., and Tulin, L. M., "Time-Dependent Behavior of Concrete Beams," *J. Struct. Div.*, Proc. Amer. Soc. of Civil Engineers, 96 (1970) 597–612; see also 99 (1973) 243–258.
134. Cederwall, K., Elfgren, L, and Losberg, A., "Prestressed Concrete Columns Under Long-Time Loading," Prelim. Publ., *IABSE Symp. "Design of Concrete Structures for Creep, Shrinkage and Temperature,"* held in Madrid, publ. in Zürich (1970) 182–189.
135. Ghosh, S. K., and Cohn, M. Z., "Effect of Creep on the Flexural Strength and Deformation of Structural Concrete," Prelim. Publ., *IABSE Symp. "Design of Concrete Structures for Creep . . . ,"* held in Madrid, publ. in Zürich (1970) 207–216.
136. Powers, T. C., and Brownyard, T. C., "Studies of the Physical Properties of Hardened Portland Cement Paste," *Amer. Concrete Inst. J.* 42 (1946) 101–132, 249–336, 469–504; 43 (1947) 549–602, 669–712, 854–880, 933–992.
137. Mandel, J., "Sur les Corps Viscoélastiques Linéaire dont les propriétés Dépendent de l'Age," *Comptes Rendus des Séances de l'Académie des Sciences* 247 (1958) 175–178.
138. Bažant, Z. P., *Creep of Concrete in Structural Analysis* (in Czech), State Publishers of Technical Literature (SNTL), Prague (1966).
139. Bažant, Z. P., "Theory of Creep and Shrinkage of Concrete in Nonhomogeneous Structures and Cross Sections" (in Czech) *Stavebnícky Časopis SAV* 10 (1962) 552–576.
140. Hlaváček, I., and Predeleanu, M., "Sur l'Existence et l'Unicité de la Solutions dans la Théorie du Fluage Linéaire," *Aplikace Matematiky ČSAV*, Prague, 16 (1964) 321.
141. Hlaváček, I., "Variational Principles for Parabolic Equations," *Aplikace Matematiky ČSAV*, Prague, 16 (1964) 287–296.
142. Lubliner, J., and Sackman, J. L., "On Uniqueness in General Linear Viscoelasticity," *Q. Appl. Math.* 25 (1967) 129–138.
143. Dischinger, F., "Untersuchungen über die Knicksicherheit, die Elastische Verformung und das Kriechen des Betons bei Bogenbrücken," *Der Bauingenieur* 18 (1937) 487–520, 539–552, 595–621; see also 20 (1939) 53–63, 286–294, 426–437, 563–572.
144. Arutyunian, N. Kh., *Some Problems in the Theory of Creep* (in Russian), Techteorizdat, Moscow (1952); Engl. transl., Pergamon Press (1966).
145. Bažant, Z. P., "Linear Creep Problems Solved by a Succession of Generalized Thermoelasticity Problems," *Acta Technica ČSAV*, Prague, 12 (1967) 581–594.
146. Bažant, Z. P., "Numerical Determination of Long-Range Stress History from Strain History in Concrete," *Materials and Structures* (RILEM) 5 (1972) 135–141.
147. Cederberg, H., and David, M., "Computation of Creep Effects in Prestressed Concrete Pressure Vessels Using Dynamic Relaxation," *Nuclear Engrg. & Des.* 9 (1969) 439–448.
148. Bažant, Z. P., "Numerical Analysis of Creep of Reinforced Plates," *Acta Technica Hung.* 70 (1971) 415–428.
149. Bažant, Z. P., "Numerical Analysis of Creep of an Indeterminate Composite Beam," *J. Appl. Mech.*, ASME 37 (1970) 1161–1164.
150. Bažant, Z. P., "Approximate Methods for Creep and Shrinkage of Complex Nonhomogeneous Structures" (in Czech), *Stavebnícky Časopis SAV* 12 (1964) 414–431.
151. Bažant, Z. P., "Die Berechnung des Kriechens und Schwindens Nichthomogener Betonkonstruktionen," *Proc. 7th Congress, IABSE* (Int. Assoc. for Bridge and Struct. Engrg.), held in Rio de Janeiro, publ. in Zürich (1964) 887–897.
152. Bažant, Z. P., "Numerically Stable Algorithm with Increasing Time Steps for Integral-Type Aging Creep," *Proc. First Int. Conf. on Struct. Mech. in Reactor Technology*, T. A. Jaeger (ed.), West Berlin, Vol. 4, Part H (1971), 119–127.
153. Taylor, R. L., Pister, K. S., and Goudreau, G. L., "Thermomechanical Analysis of Viscoelastic Solids," *Int. J. Num. Methods in Engrg.* 2 (1970) 45–60.
154. Zienkiewicz, O. C., Watson, M., and King, I. P., "A Numerical Method of Viscoelastic Stress Analysis," *Int. J. Mech. Scl.* 10 (1968) 807–827.
155. Selna, L. G., "A Concrete Creep, Shrinkage and Cracking Law for Frame Structures," *Amer. Concrete Inst. J.* 66 (1969) 847–848; with Supplement No. 66–71.
156. Lin, T. H., *Theory of Inelastic Structures*, Wiley, New York (1968).
157. Bažant, Z. P., and Najjar, L. J., "Comparison of Approximate Linear Methods for Concrete Creep," *J. Struct. Div.*, Proc. Amer. Soc. of Civil Engineers 99 (1973) 1851–1874.
158. Schapery, R. A., "A Method of Viscoelastic Stress Analysis Using Elastic Solutions," *J. Franklin Inst.* 279 (1965) 268–289.
159. Trost, H., "Auswirkungen des Superpositionsprinzips auf Kriech und Relaxationsprobleme bei Beton und Spannbeton," *Beton-und Stahlbetonbau* 62 (1967) 230–238; see also 65 (1970) 155–179.
160. Bažant, Z. P., "Prediction of Concrete Creep Effects Using Age-Adjusted Effective Modulus Method," *Amer. Concrete Inst. J.* 69 (1972) 212–217.
161. Prokopovich, I. E., *Effect of Long-Term Processes Upon Stress and Strain States of Structures* (in Russian), Gosstroyizdat, Moscow (1963).
162. Nielsen, L. F., "Kriechen und Relaxation des Beton," *Beton-und Stahlbetonbau* 65 (1970) 272–275.
163. Bažant, Z. P., "Creep Stability and Buckling Strength of Concrete Columns," *Mag. Concrete Res.* 20 (1968) 85–94.
164. Bažant, Z. P., "Time-Interaction of Statically Indeterminate Structures and Subsoil," *Stavebnícky Časopis SAV* 12 (1964) 542–558.
165. Benjamin, J. R., Cornell, C. A., and Gabrielsen, B. L., "Stochastic Model of Creep Deflections of Reinforced Concrete Beams," *Amer. Concrete Inst. Spec. Publ. No. 12*, Symp. on Flexural Mechanics of Reinforced Concrete, held in Miami, 1964, publ. in Detroit (1965) 557–580.
166. Bažant, Z. P., and Wu, S. T., "Creep and Shrinkage Law for Concrete at Variable Humidity," *J. Engrg. Mech. Div., Proc. Amer. Soc. Civil Engineers* 100 (1974), No. EM6.
167. Rüsch, H., Jungwirth, D., and Hilsdorf, H., "Kritische Sichtung der Verfahren zur Berücksichtigung der Einflüsse von Kriechen," *Beton- und Stahlbetonbau* 68 (1973) 49–60, 76–86, 152–158; with a "Zuschrift" by Z. P. Bažant 69 (1974) 150–151.
168. Coon, M. D., and Evans, R. J., "Incremental Constitutive Laws and Their Associated Failure Criteria with Application to Concrete," *Int. J. Solids and Struct.* 8 (1972) 1169–1183.
169. Valanis, K. C., "A Theory of Viscoplasticity Without Yield Surface," *Arch. Mech. Stos.* 23 (1971) 517–551.
170. Bažant, Z. P., and Asghari, A., "Computation of Age-dependent Relaxation Spectra," *Cement and Concrete Res.* 4 (1974) 567–579; see also "Computation of Kelvin-Chain Retardation Spectra," *Cement and Concrete Res.* 4 (1974) 797–806.
171. Nemat-Nasser, S., "On Nonequilibrium Thermodynamics of Continua," Chapter II of this volume.
172. Bažant, Z. P., "Effect of creep and shrinkage in statically indeterminate concrete structures of nonuniform age" (in Czech), *Inženýrské stavby* (Prague) 9 (1961), 462–432.

8 LIST OF BASIC NOTATIONS

$a_{ww}, a_{ws}, a_{sw}, a_{ss}$ = diffusion coefficients in Eq. (4.8);
C, C_0, C_1 = diffusivity of water in concrete, Eq. (4.40), its reference value and value at $h = 1$;
D = average distance of flow in Eq. (4.17);
E, E_0, E = Young's modulus [Eq. (3.13)], its reference value at time t_0, and operator in Eq. (5.1);
E_r'' = incremental elastic modulus for time step Δt_r in Eq. (5.11);
$E_R(t, t')$ = relaxation modulus [Eq. (3.5)];
$\hat{E}_\mu, E_\mu, E_\infty, E_\mu^s, E_\mu^w$ = moduli for hidden variables in Eqs. (3.15), (3.19), (3.36), and (4.20);
$E_{0_\mu}, \ldots, E_{4_\mu}$ = parameters in Eqs. (3.21a) and (3.21b);
$f(t - t')$ = shape of creep curve in Eq. (3.10);
f_d = area factor for hindered adsorbed layers [Eqs (4.17) and (4.19)];
f_μ = hidden stress equilibrium values, Eq. (4.20);
h, h_e, h_s = relative humidity of water vapor in pores of concrete, environmental humidity, and self-dessication humidity in Eq. (4.38);
$J(t, t'), J^V(t, t'), J^D(t, t')$ = uniaxial, volumetric, and deviatoric creep functions [Eqs. (3.1) and (3.2)];
$\mathbf{J}_w, \mathbf{J}_s$ = fluxes of water and solids in Eq. (4.8);
$\Delta J_{r,q}$ = expression (5.12);
k = $\partial h / \partial w$ = coefficient in Eq. (4.38);
k_a, k_b = slopes of creep curve in Eq. (3.18);
K, K_μ^s, K_μ^w = bulk modulus and the corresponding moduli for hidden stresses in Eq. (4.30);
l_d, L_d = half-thickness of hindered adsorbed layer [Fig. 14(d)] and its boundary length;
$L(t, t')$ = memory function in Eq. (3.8);
M = bending moment or molecular weight of water (18.02 g/mole);
p_i = distributed surface loads of a structure;
p_w, p_s = pressures in water and solids across the hindered adsorbed layer;
R = gas constant = 1.986 cal/°K = 82.06 cm³ × atm (°K × mole)⁻¹;
$\bar{S}_w, \bar{S}_s$ = entropy densities in water and solids in Eq (4.7);

$t; t'$ = time, measured from casting of concrete;
$t_r (r = 1, 2, \ldots)$ = discrete times for step-by-step analysis;
t_0, t_e = instant of first load application and equivalent hydration period in Eq. (4.1);
u_i, u_i^0 = displacement of material points and enforced displacements, Eqs. (5.6) and (5.26);
T, T_0 = absolute temperature and its reference value;
$U_h, U_\mu, U_1, \Delta U$ = activation energies for hydration and creep in Eqs. (4.2) to (4.4) and (4.26);
$\alpha_w', \alpha_w'', \alpha_\mu^s, \alpha_\mu^w$ = thermal dilatation coefficients in Eqs. (4.10) and (4.20);
β, β_T, β_h = relative hydration rates in Eq. (4.1);
$\epsilon, \epsilon^0, \epsilon_{ij}, \boldsymbol{\epsilon}$ = normal strain, stress-independent inelastic strain and strain tensor (linearized);
$\epsilon_\mu, \epsilon_\mu^*$ = hidden strains in Eqs. (3.24), (3.26) (Figs. 10);
$\epsilon_S, \Delta\epsilon_r, \Delta\epsilon_r''$ = instantaneous shrinkage strain in Eqs. (4.19) and (4.20), and strain increments in Eq. (5.11);
η_μ = viscosities associated with hidden variables in Eq. (3.28), (3.29), and (3.36);
κ = $\partial h / \partial T$ = hygrothermic coefficient, Eq. (4.38);
μ_w, μ_s = chemical potentials of water and solids [Eq. (4.7)];
$\nu, \nu(t, t')$ = Poisson's ratio in Eq. (3.3);
π_w, π_s = spreading pressures in water and solids in Eq. (4.7);
τ_μ = relaxation or retardation times [Eq. (3.16)];
$\sigma, \sigma_{ij}, \boldsymbol{\sigma}$ = normal stress and stress tensor;
$\sigma_\mu, \sigma_{s_\mu}, \sigma_{w_\mu}, \sigma_\mu^h$ = hidden stresses in Eqs. (3.28), (3.29), (3.35), (4.20), and their equilibrium value in Eq. (4.24);
$\sigma^V, \sigma^D, \sigma_{s_\mu}^V, \sigma_{s_\mu}^V, \ldots$ = volumetric and deviatoric components of stress and hidden stress tensors, Eq. (4.30);
$\phi(t, t'), \phi_u(t')$ = creep coefficient [Eq. (3.9)] and its conventional "ultimate" value in Eq. (3.10);
$\phi_{ss_\mu}, \ldots, \phi_{ss_\mu}^V, \phi_{ss_\mu}^D, \phi_{ss}^h, \phi_T$ = rate parameters in Eqs. (4.20), (4.32), (4.26);
$\bar{\phi}(t)$ = $\phi(t, t_0)$ [Eqs. (4.35) and (5.34)];
$\chi(t, t_0)$ = aging coefficient in Eq. (5.32);